Journal of Physical and Chemical Reference Data

Elastic Properties of Metals and Alloys, I. Iron, Nickel, and Iron-Nickel Alloys

Cite as: Journal of Physical and Chemical Reference Data **2**, 531 (1973); https://doi.org/10.1063/1.3253127

H. M. Ledbetter, and R. P. Reed

Journal of Physical and Chemical Reference Data **2**, 531 (1973); https://doi.org/10.1063/1.3253127 **2**, 531

Elastic Properties of Metals and Alloys, I. Iron, Nickel, and Iron-Nickel Alloys

H. M. Ledbetter and R. P. Reed

Cryogenics Division, Institute for Basic Standards, National Bureau of Standards, Boulder, Colorado 80302

A comprehensive compilation is given of elastic properties of iron-nickel alloys. When sufficient data exist, preferred values are recommended. This compilation covers, besides pure iron and pure nickel, the entire binary composition range, both b.c.c. and f.c.c. phases. Elastic constants included are: Young's modulus, shear modulus, bulk modulus (reciprocal compressibility), Poisson's ratio, and single-crystal elastic stiffnesses, both second-order and higher-order. Data are compiled for variation of elastic constants with composition, temperature, pressure, magnetic field, mechanical deformation, annealing, and crystallographic transitions. An overview is given from the vantage points of the electron theory of metals, elasticity theory, and crystallographic theory. Also included are discussions of isothermal and adiabatic elastic constants, interrelationships among engineering elastic constants, computation of the latter from single-crystal elastic stiffnesses, and similar topics. Where key data have not been measured, they were generated if possible from existing data using standard formulae. Other gaps, both theoretical and experimental, in the elastic properties of iron-nickel alloys are indicated. A few theoretical results are included where experimental data are nonexistent or scarce. A semantic scheme is proposed for distinguishing elastic constants of solids.

Key words: Bulk modulus; compressibility; elastic constants; Debye temperatures; iron; iron alloys; Lamé constants; nickel; nickel alloys; Poisson's ratio; shear modulus; single-crystal elastic coefficients; Young's modulus.

Contents

List of Tables

List of Figures

Principal Notations

A	elastic anisotropy (after Zener)
A^*	elastic anisotropy (after Chung and Buessem)
B	bulk modulus
c_{ij}, c_{ijkl}	second-order elastic stiffnesses (contracted, full)

c_{ijkl}, c_{ijklmn}	third-order elastic stiffnesses (contracted, full)
c_{11}, c_{12}, c_{44}	three independent elastic stiffnesses for cubic symmetry
C	$=c_{44}$
C'	$=(c_{11}-c_{12})/2$
C_x	specific heat at constant x
E	Young's modulus
F	Helmholtz energy
G	shear modulus
G	Gibbs energy
h	Planck's constant
H	enthalpy
I_i	tensor invariants
k	Boltzmann's constant
l, m, n	Murnaghan's third-order quasi-isotropic elastic constants
M	general elastic modulus
N	Avogadro's number
P	pressure

s_{ij}, s_{ijkl}	elastic compliances (contracted, full)
S	entropy
T	temperature (degrees Kelvin)
u	displacement
v	velocity
v, V	specific volume, volume
α	linear thermal expansion coefficient
β	volume thermal expansion coefficient
γ	shear strain
γ	Grüneisen's constant
δ_{ij}	Kronecker's delta
ϵ	strain
η	strain
θ	Debye characteristic temperature
λ	Lamé constant
λ	magnetostriction constant
μ	Lamé constant $(=G)$
ν	Poisson's ratio
ρ	mass density
σ	stress
τ	shear stress

1. Introduction

In this century, solid-state physics has advanced dramatically. Essential to this advance was accumulation of vast quantities of data describing properties of solids. As much as any set of properties, elastic properties were central in this advance. Similarly, technologies such as metallurgy and ultrasonics have matured only through a necessary knowledge and understanding of elastic properties of solids that provide their basis.

Most solids are crystalline, therefore elastically anisotropic, and are either single crystals or polycrystalline aggregates. Thus, crystalline studies form a large part of solid-state physics, which attempts generally to relate properties of atoms and atom groupings to macroscopic properties of solids at various temperatures, pressures, etc.

While most phenomenological crystal elasticity was developed by late 19th century, systematic studies and practical applications of crystalline elasticity emerged only recently. Uses of crystals in solid-state devices and engineering applications of elastic solids increased substantially since about 1945. Measurement of elastic properties by ultrasonic techniques facilitated these applications.

With the view that elasticity of solids will be increasingly important in both science and technology, a beginning is made here toward a comprehensive compilation and critical review of elastic properties of selected systems that hold high interest for both of these communities. For examples of practical applications of elastic properties one need only consult any standard reference on strength of materials. Perusal of various formulae for describing states of stress such as compression or bending shows that elastic constants are key design parameters. Indeed, few stress-bearing members can be designed adequately in ignorance of the elastic properties of the constitutive material.

Engineering materials that are macroscopically isotropic are completely defined elastically by two parameters. Parameter selection is arbitrary, varying with application. As examples: pressure vessel design requires knowing the bulk modulus, design of rotating shafts requires knowing the rigidity modulus, and design of flexed beams or support columns requires knowing Young's modulus.

For some special scientific purposes it is sufficient to know the elastic properties of a material in some reference state, for example—a pure, annealed, defect-free, single crystal at 0 K and 1 atmosphere. However, for ordinary purposes the elastic properties of a material must be known in other, non-reference, states. Departure from the state of reference usually involves varying one or more of—composition, temperature, pressure, mechanical deformation, magnetic field, or degree of polycrystallinity. Thus, an understanding is sought as to how these variables affect elastic properties. These topics are discussed in sections 10–11 and 13–16.

The purpose of this paper is to present a comprehensive compilation and a critical overview of the elastic properties of alloys of the binary system iron-nickel. These alloys hold much interest for both engineers and scientists, for both metallurgists and geophysicists. Iron-nickel alloys also provide fertile ground for probing relationships between elastic constants and phase transitions, an area of physics and metallurgy now ripe for both theoretical and experimental study. Since both iron and nickel are ferromagnetic, their alloys show a variety of curious magnetic effects, many of which are important technologically; and magnetic effects are frequently coupled to elastic constants, as for example in magnetostriction. Similarly, *Invar*[1] is an alloy of Fe-36Ni[2] where magnetic effects combine with thermal expansion such that virtually no thermal expansivity is exhibited over a wide temperature range, one of the curious exceptions to the almost universal thermal expansion of solids.

Other materials such as *Covar* (thermal expansion coefficient similar to that of glass) and *Permalloy* (exceptionally high magnetic permeability) are based on iron-nickel binary alloys. Metallic meteorites, also scientific curiosities, are iron alloys containing as much as 60 percent nickel. Extensive meteorite metallography has been done to deduce the thermal-mechanical history of meteorites to elucidate the problem of planetary genesis. Finally, the earth's core is generally assumed to be an alloy of iron and nickel, and elastic constants enter many geophysical calculations, notably those dealing with seismic-wave propagation. The many technological applications of Fe-Ni alloys are discussed by Chickazumi [1],[3] Rosenberg [2], and Everhart [3].

This review collects, for the first time, all available data on the elastic properties of iron-nickel alloys. Data are discussed from the viewpoints of the modern theory of metals, elasticity, and crystallography in an attempt to understand, as much as possible, in a unified way the elastic properties of iron-nickel alloys. This is useful because: (1) most of the literature on the subject is purely experimental, and (2) an overview facilitates semi-quantitative extrapolation of existing information to conditions where neither experimental nor theoretical data are available.

Most data are available as engineering elastic constants: Young's modulus, shear modulus, bulk modulus, and Poisson's ratio. Single-crystal data exist also, but less abundantly. Relationships between single-crystal data and engineering data are discussed in section 5. Besides the compositional variation of the elastic constants, data on the effects of temperature, pressure, magnetic field, mechanical deformation, and annealing are also included and discussed. This review is intended to provide a convenient source of information on the elastic properties of iron-nickel alloys and to stimulate further research, both theoretical and experimental. Gaps in the knowledge and understanding of the elastic properties of iron-nickel alloys are delineated.

Since the present article is seen as the first of a series, the discussion herein is more general and more extensive than is necessary for treating only the elastic properties of iron-nickel alloys. Remarks special to iron-nickel are so designated whenever appropriate. Mainly, the elastic properties of metals and alloys are described in general terms. Much of the discussion necessarily applies also to other types of solids such as ionic or covalent crystals. However, readers should make such extrapolations only cautiously.

2. Perspective on Elastic Constants

Invoking three realms of knowledge of solids—pure science, phenomenology, and engineering—elastic parameters of solids are distributed among these realms as shown schematically in figure 1. As far as elastic properties of solids are concerned, objects of interest in these realms are, respectively—discrete atoms or molecules, anisotropic continua, and quasi-isotropic continua.

The α and β can be taken to represent extensions (or contractions) and bendings of valence bonds between atoms in solids; subscript i denotes the various sets of atomic neighbors. The c_{ij}'s represent elastic stiffness coefficients that relate stresses to strains; both stress and strain are specified with respect to a set of axes denoted by indices i and j and usually chosen to coincide with crystallographic axes. E, G, B, and ν denote the Young's modulus, shear modulus, bulk modulus, and Poisson ratio, parameters arising naturally in characterizing, respectively, uniaxial loading, shear loading, hydrostatic loading, and transverse strain under uniaxial loading. (In section 4 all of the elastic constants are defined. In section 5 relationships between single-crystal and polycrystal constants are discussed.)

Many properties of solids are related to elastic coefficients. The most important of these properties is Debye's characteristic temperature θ. Several techniques exist for computing θ from the c_{ij}. In turn, θ relates directly to such properties of solids as heat capacity, intensities of Bragg diffractions, Mössbauer emission, thermal conductivity, electrical resistivity, superconducting transition temperature, etc. Many of these relationships are discussed in section 18.

Elastic coefficients are central in considering defects in solids such as vacancies, interstitials, substitutional impurities, dislocations, twin boundaries, and grain boundaries. Being related to the second spatial derivative of the interatomic potential, elastic coefficients relate intimately to the problem of cohesion in solids, an especially important problem for metals. In this regard, pure-shear elastic coefficients allow for volume effects to be separated from non-volume effects. Many crystalline phenomena—thermal expansion, temperature and pressure derivatives of the second-order elastic coefficients, thermal conductivity of insulators, sound wave attenuation, etc.—are *anharmonic* effects related directly to the existence of third-order, and higher-order, elastic constants. Thus, better understanding, both experimental and theoretical, of elastic constants of solids pays dividends in diverse ways, often unsuspected. (Section 11.3 treats briefly the topic of lattice defects and elastic constants.)

---

[1] Trade names are used to facilitate understanding of work presented; no approval, endorsement, or recommendation by NBS is implied.

[2] Throughout, compositions are expressed as weight percent nickel. Because iron and nickel have similar atomic weights, weight and atomic percentages always differ by less than two percent.

[3] Numerals in brackets indicate literature references at the end of this paper.

3. Terminology

Despite several proposals, there is no generally accepted, rational and consistent terminology for describing the elastic parameters of solids that form the subject of this review. This problem becomes especially acute when semantic distinctions are required among: (1) the general class of all elastic parameters, (2) the sub-class of the parameters used commonly to describe quasi-isotropic or engineering solids, and (3) the sub-class of parameters used to describe anisotropic single crystals. Therefore, a scheme of usage is proposed here that corresponds closely to that usually accepted but makes useful semantic distinctions:

E = Young's modulus	elastic moduli	(polycrystal) engineering elastic constants	elastic constants
G = shear modulus			
B = bulk modulus			
ν = Poisson's ratio			
c_{ij} = elastic stiffnesses	(single-crystal) elastic coefficients		
s_{ij} = elastic compliances			

Adoption of this, or a similar, semantic scheme in the literature of elastic phenomena of solids should allow for a more logical and a more lucid description of the subject than has resulted previously. In much of the existing literature the c_{ij} are referred to simply as "elastic constants". Thus, an alternative to the present proposal would be to substitute "constants" for "coefficients" and perhaps "parameters" for "constants". Also, some authors prefer "technical", "practical", or "bulk" to "engineering".

4. Definitions of Elastic Constants

Elastic materials obey Hooke's law

$$\sigma_{ij}=c_{ijkl}\,\epsilon_{kl}, \tag{4.1}$$

where repeated indices are summed from 1 to 3, σ_{ij} are stress components given by

$$f_i=\sigma_{ij}\,n_j, \tag{4.2}$$

where f_i are the components of a force acting internally on an imaginary plane (with normal $\mathbf{n}$) of a body, and ϵ_{kl} are the (infinitesimal) strain components given by

$$\epsilon_{kl}=\tfrac{1}{2}(\partial u_k/\partial x_l+\partial u_l/\partial x_k), \tag{4.3}$$

and u_k, u_l are components of the displacement.

While Hooke's law emerged experimentally, it can be derived in various ways. For example, Lanczos [4] showed that Hooke's law is the necessary stress-strain relationship when Hamilton's variational principle is invoked.

Equation (4.1) means that the strain response of an elastic material is instantaneous, independent of rate or history. Removal of force restores the original reference configuration; no strain exists in the unstressed state and vice versa. If non-mechanical (electrical, magnetic, thermal, etc.) effects are incorporated, then stress and strain may not vanish simultaneously unless the non-mechanical effects are subtracted from the total stress and strain. Metals approximate Hookean behavior within their elastic limit; plastic deformation frequently begins before non-linear elastic behavior becomes significant.

Except for third-order elastic constants, the elastic constants described herein are either those c_{ijkl} in eq (4.1) or can be derived simply from them.

The c_{ijkl} are components of a fourth-rank tensor and are called the elastic stiffness coefficients. Generally, there are $3^4=81$ such components. However, thermodynamic and symmetry considerations show for all crystal systems that

$$c_{ijkl}=c_{klij}=c_{ijlk}=c_{jikl}\neq c_{ikjl}. \tag{4.4}$$

Complete commutability of indices occurs only when Cauchy's relations, based on central forces between atoms and inversion symmetry, hold. In metals these relations are broken because of the conduction electrons acting through electron-electron and electron-ion interactions.

From eq (4.4) it follows that in general only 21 c_{ijkl} are independent. If Voigt's contracted notation[4] is invoked, then the c_{ijkl} can be represented as a symmetric 6×6 matrix, and Hooke's law becomes

$$\sigma_\alpha=c_{\alpha\beta}\,\epsilon_\beta \tag{4.5}$$

where repeated indices are summed from 1 to 6 and

$$c_{\alpha\beta}=c_{ijkl}$$

$$\sigma_\alpha=\sigma_{ij}$$

$$\epsilon_\beta=\epsilon_{kl},\ \beta=1,2,3$$

$$=2\epsilon_{kl},\ \beta=4,5,6.$$

For cubic symmetry, which is the case for iron, nickel, and all iron-nickel alloys, the 21 $c_{\alpha\beta}$ components reduce to three:

$$c_{11}=c_{22}=c_{33}, \tag{4.6}$$

$$c_{12}=c_{21}=c_{13}=c_{31}=c_{23}=c_{32}, \tag{4.7}$$

and

$$c_{44}=c_{55}=c_{66}; \tag{4.8}$$

---

[4] The Voigt contraction scheme is summarized as follows:

ij, kl:	11	22	33	23, 32	13, 31	12, 21
α, β:	1	2	3	4	5	6

all other $c_{\alpha\beta}$ are zero.

The elastic compliance coefficients s_{ijkl} have the same symmetry as the c_{ijkl} and their relationship is inverse

$$c_{\alpha\beta}s_{\alpha\beta}=\mathbf{I}_{6\times 6} \tag{4.9}$$

where **I** denotes the identity matrix. Formulae for converting $c_{\alpha\beta}$ to $s_{\alpha\beta}$ and vice versa are collected in table 3.

For cubic symmetry, Hooke's law in matrix form is

$$\begin{bmatrix}\sigma_1\\ \sigma_2\\ \sigma_3\\ \sigma_4\\ \sigma_5\\ \sigma_6\end{bmatrix}=\begin{bmatrix}c_{11} & c_{12} & c_{12} & 0 & 0 & 0\\ c_{12} & c_{11} & c_{12} & 0 & 0 & 0\\ c_{12} & c_{12} & c_{11} & 0 & 0 & 0\\ 0 & 0 & 0 & c_{44} & 0 & 0\\ 0 & 0 & 0 & 0 & c_{44} & 0\\ 0 & 0 & 0 & 0 & 0 & c_{44}\end{bmatrix}.\begin{bmatrix}\epsilon_1\\ \epsilon_2\\ \epsilon_3\\ \epsilon_4\\ \epsilon_5\\ \epsilon_6\end{bmatrix} \tag{4.10}$$

The choice of three independent elastic constants is not unique. For example, a useful alternative set advocated by Zener [5] is

$$C=c_{44}, \tag{4.11}$$

$$C'=(c_{11}-c_{12})/2, \tag{4.12}$$

and

$$B=(c_{11}+2c_{12})/3. \tag{4.13}$$

A set arising frequently in ultrasonic experiments is C, C', and

$$C_L=(c_{11}+c_{12}+2c_{44})/2. \tag{4.14}$$

It can be shown that B is the bulk modulus for cubic symmetry. Thus, when a hydrostatic pressure

$$P=-\sigma_1=-\sigma_2=-\sigma_3(\sigma_4=\sigma_5=\sigma_6=0), \tag{4.15}$$

is applied to a cubic crystal the strains are

$$\epsilon_1=\epsilon_2=\epsilon_3=-\Delta V/3V(\epsilon_4=\epsilon_5=\epsilon_6=0), \tag{4.16}$$

and eq (4.1) becomes

$$B=-P/(\Delta V/V). \tag{4.17}$$

For cubic symmetry the compressibility

$$\kappa=-\frac{1}{V}\left(\frac{\partial V}{\partial P}\right) \tag{4.18}$$

is given by

$$\kappa=3(s_{11}+2s_{12})=1/B. \tag{4.19}$$

The constant $C=c_{44}$ relates a shear stress on a {100} plane to the shear strain in any direction in that plane. For a shear stress σ acting along (100)[010] and effecting a shear angle γ

$$\sigma_6=\sigma, \tag{4.20}$$

and

$$\epsilon_6=\gamma. \tag{4.21}$$

All other stress and strain components are zero. Thus, eq (4.1) becomes

$$c_{66}=\sigma/\gamma=c_{44}=C. \tag{4.22}$$

The constant $C'=(c_{11}-c_{12})/2$ relates a shear stress on a {110} plane to a shear strain along $\langle\bar{1}10\rangle$. This is equivalent to the c_{44} case just described, but rotated ± 45° about [001]. In this case the non-vanishing stress components are

$$\sigma_1=-\sigma_2=\sigma \tag{4.23}$$

and the non-vanishing strains are

$$\epsilon_1=-\epsilon_2=\gamma/2 \tag{4.24}$$

so that eq (4.1) becomes in this case

$$(c_{11}-c_{12})/2=\sigma/\gamma=C'=c_{44}\quad\text{rotated}\ \pm 45^\circ\ \text{about}\ [001]. \tag{4.25}$$

For isotropic materials there are only two independent elastic constants. The Lamé constants λ and μ were the first set to be used. For isotropic media, Hooke's law in a reduced matrix form is

$$\begin{bmatrix}\sigma_1\\ \sigma_2\\ \sigma_3\\ \sigma_4\\ \sigma_5\\ \sigma_6\end{bmatrix}=\begin{bmatrix}\lambda+2\mu & \lambda & \lambda & 0 & 0 & 0\\ \lambda & \lambda+2\mu & \lambda & 0 & 0 & 0\\ \lambda & \lambda & \lambda+2\mu & 0 & 0 & 0\\ 0 & 0 & 0 & \mu & 0 & 0\\ 0 & 0 & 0 & 0 & \mu & 0\\ 0 & 0 & 0 & 0 & 0 & \mu\end{bmatrix}\begin{bmatrix}\epsilon_1\\ \epsilon_2\\ \epsilon_3\\ \epsilon_4\\ \epsilon_5\\ \epsilon_6\end{bmatrix} \tag{4.26}$$

Clearly, for isotropic media

$$c_{11}=\lambda+2\mu, \tag{4.27}$$

$$c_{12}=\lambda, \tag{4.28}$$

and

$$c_{44}=\mu. \tag{4.29}$$

Much recent work on isotropic media uses, instead of λ and μ, such constants as the bulk modulus B, Young's modulus E, the shear modulus G, and Poisson's ratio ν. B is defined by eqs (4.13) and (4.17).

Young's modulus is defined as the ratio of uniaxial stress (tensile or compressive) to strain measured along the same axis. Thus, eq (4.1) becomes for stress along [100]

$$E \equiv \frac{\sigma_1}{\epsilon_1} = \frac{1}{s^\circ_{11}}. \tag{4.30}$$

There can be only one shear modulus in the isotropic case, so that

$$G = c^\circ_{44} = \tfrac{1}{2}(c^\circ_{11} - c^\circ_{12}). \tag{4.31}$$

Poisson's ratio is defined as the negative of the ratio of transverse strain to longitudinal strain for the case of uniaxial stress. For stress along [001],

$$\nu = -\epsilon_2/\epsilon_1 = -s^\circ_{12}/s^\circ_{11}. \tag{4.32}$$

Zener [5] introduced an additional parameter, a dimensionless ratio

$$A \equiv C/C' = 2c_{44}/(c_{11} - c_{12}), \tag{4.33}$$

called the elastic anisotropy factor.[5] Clearly, $A = 1$ for isotropy since all shear moduli, including C and C', are equal. Aluminum and tungsten are the only cubic metals with known elastic coefficients where $A \approx 1$. Zener's anisotropy concept has been very useful in discussing b.c.c. lattice instabilities. In fact, Barrett [7] was led by this consideration to discover low-temperature martensitic transformations in both lithium and sodium. Iron-nickel alloys have moderate to high elastic anisotropy. As discussed below, martensitic transitions in iron-nickel alloys can be characterized by a high value of A even though the parent phase is f.c.c. as opposed to b.c.c. for lithium and sodium.

Energetic considerations show that B, E, G (both C and C' for cubic crystals) are all positive. Bounds on ν are 1/2 and -1. No negative values of ν have ever been observed for isotropic media. Typically, ν ranges from 0.25 to 0.45 for metals. Lacking any data, the best guess for metals is $\nu = 1/3$.

Connecting identities among E, G, B, and ν are given in table 1. Other variables included there are Lamé's constants λ and μ, longitudinal and transverse sound velocities v_l and v_t, quasi-isotropic elastic stiffnesses c°_{ij}, and quasi-isotropic elastic compliances s°_{ij}. The sound wave velocities considered herein refer to waves in an infinite medium, that is to the so-called body or volume waves.

The operational definitions of E, B, G, and ν for isotropic media apply also to single crystals. If these measurement operations are applied to single crystals, results depend on the crystal axis $\langle hkl \rangle$ along which the crystal is tested. Elastic constants so obtained are designated E_{hkl}, G_{hkl}, and ν_{hkl} and are related to the c_{ij} and s_{ij} by formulae summarized in table 2 for cubic symmetry. (Note that $B_{hkl} = B$ for all possible hkl.) Thus, by measuring engineering constants on single crystals along three independent directions (100, 110, and 111 are the simplest) c_{ij} and/or s_{ij} can be determined. Before the advent of ultrasonic measurement methods, this method was used extensively to determine c_{ij}; it is still used occasionally.

5. Relationships Among Elastic Coefficients and Engineering Elastic Constants

As described above, cubic crystals are characterized by three elastic coefficients while isotropic and quasi-isotropic solids are characterized elastically by two constants. The relationship between the constants E, G, B, and ν of a quasi-isotropic material and the c_{ij} of a single crystal of the same substance is considered here.

5.1. Isotropic Case ($A = 1$)

The isotropy condition for cubic crystals is

$$c_{11} - c_{12} = 2c_{44} \tag{5.1}$$

When this relationship is satisfied, identities in table 1 hold among various constants for both single crystals and polycrystals.

5.2. Anisotropic Case ($A \neq 1$)

In computing two constants from three, the problem is generally overdetermined. The overdeterminancy was eliminated in the case $A = 1$ by eq (5.1). Many different approaches have been suggested for the anisotropic case. A general review of this subject has apparently not been made, although comparisons of many of the methods were made by Ledbetter [8]. Two of the proposed methods are discussed here since they are important historically, and their basic assumptions establish upper and lower limits for the correct result. A compromise averaging method is then discussed that gives good results with quite simple formulae.

The problem is one of averaging a tensor property over all possible spatial orientations, that is,

$$\langle c_{ij} \rangle = \frac{1}{2\pi} \int_{\varphi=0}^{\pi} \int_{\theta=0}^{\pi} f(\varphi,\theta) \quad \sin\theta \, d\theta \, d\varphi \tag{5.2}$$

where $f(\phi,\theta)$ contains the directional dependence of the c_{ij}. Many schemes have been proposed for solving eq (5.2) or its equivalent, but these have not been reviewed critically.

---

[5] There is no unique definition of crystalline elastic anisotropy. For example, Chung and Buessem [6] proposed an improved form, although slightly more complicated. Their factor A^* is zero for isotropy, gives better relative magnitudes of elastic anisotropies than does A, and is especially useful in interpreting $A < 1$ cases, which occur frequently for non-metals and also for metals such as vanadium and chromium.

Voigt [9] assumed constant strain and averaged the c_{ij} with the result

$$G_V = \tfrac{1}{5}\,(c_{11} - c_{12} + 3c_{44}). \tag{5.3}$$

Reuss [10], on the other hand, assumed constant stress and averaged the s_{ij} with the result

$$G_R = \frac{5}{4(s_{11} - s_{12}) + 3s_{44}}. \tag{5.4}$$

For both cases, the bulk modulus is given by eq (4.13). Thus, all engineering elastic constants can be determined from G and B by using equations in table 1. Hill [11] showed on thermodynamic grounds that eqs (5.3) and (5.4) represent upper and lower limits on the shear modulus and proposed either an arithmetic or a geometric average, that is,

$$G_{H_A} = \tfrac{1}{2}\,(G_V + G_R), \tag{5.5}$$

or

$$G_{H_G} = (G_V G_R)^{1/2}, \tag{5.6}$$

where subscripts V and R refer to Voigt's and Reuss's approximations. Hill's method, owing to both its simplicity and its reliability, is used widely and was used here. While Hill's average has no theoretical or physical basis, it agrees closely (particularly for low elastic anisotropy) with averages that have such bases. As discussed by Landau and Lifshitz [12], the problem of averaging the c_{ij} to obtain E, G, ν, etc. cannot be solved uniquely.

6. Measurement Methods and Errors

6.1. Measurement Methods

The subject of measuring elastic constants has been reviewed extensively by several authors, [13]–[22]. Thus, only those experimental aspects essential to understanding and interpreting the data herein will be described briefly.

Direct, indirect, and derived methods are distinguished first. Direct methods are based on definitions of elastic constants. For example, measuring Young's modulus directly requires measuring simultaneously stress and strain along a uniaxial loading direction. Indirect methods are based on calculations using other measured elastic constants as input. Thus, an indirect measurement of Young's modulus could be made by measuring B and ν and using the formula $E = 3B/(1-2\nu)$. A derived method involves a physical relationship between an elastic constant and some nonelastic parameters, the latter being measured and the elastic constant then being calculated. For example, Young's modulus is a simple and well-known function of longitudinal and transverse sound-wave velocities and mass density. Both direct and indirect methods measure elastic constants while derived methods measure nonelastic parameters.

Secondly, static and dynamic methods are distinguished. Static methods are characterized by time-independent or, at least, slowly-varying (quasi-static) applied stresses. Slow deformation rates ensure heat exchange with surroundings. Thus, static methods are constant temperature, or isothermal. Dynamic methods are characterized by time-dependent, rapidly-varying stresses that preclude heat transfer between a specimen and its environment. Thus, dynamic methods are isentropic or adiabatic. Static methods have been important historically, but have been largely pre-empted by dynamic methods. (Distinctions between isothermal and adiabatic elastic constants are discussed in section 7.) Emergence of high-frequency (ultrasonic) experimental methods has been accompanied naturally by smaller specimen sizes, about one centimeter. For efficiency and accuracy in the case of single crystals, specimens are cut and oriented on specific crystallographic planes.

Thirdly, relaxed and unrelaxed moduli are distinguished. Usually, measuring an elastic constant involves imposing a vibrational frequency on a specimen. Relaxation processes due to interstitial impurities, dislocations, grain boundaries, residual stresses, etc. can occur within the specimen. A measurement frequency lower than the natural frequency of the relaxation events measures a relaxed elastic constant. Conversely, a measurement frequency exceeding the relaxation frequency measures *unrelaxed* elastic properties. If super-imposed and relaxation frequencies are about equal, then considerable internal friction or energy dissipation results, and measured elastic constants fall somewhere between relaxed and unrelaxed values. Differences between relaxed and unrelaxed constants are usually less than a few percent.

Relative merits of various experimental methods for specific materials, conditions, and elastic constants are discussed in references [13]–[22].

Aside from magnetic effects, which are discussed below, there are two additional problems in measuring elastic properties of iron-nickel alloys.

First, impurities. Effects of substitutional impurities can be estimated from the work of Speich, et al. [23] who determined the variation of E and G for Fe due to alloying elements. Carbon is the principal interstitial impurity, and small concentrations have negligible effect on elastic properties of iron-nickel alloys. Whether large concentrations of carbon increase [24] or decrease [25] elastic stiffnesses is still unresolved. Most theory predicts an increase. But most experiments reveal a decrease due to carbon [25].

Secondly, b.c.c. phases that contain twins as a result of the f.c.c. to b.c.c. transition may show spuriously low elastic stiffnesses due to a twin-boundary contribution to the strain. This problem becomes acute near ~35Ni where the martensite is heavily twinned, but it can be overcome by using high-frequency measurement methods.

6.2. Measurement Errors

The emergence of dynamic methods, particularly ultrasonic techniques in the megahertz region, has allowed such high precision that elastic constants are now among the most accurately measurable properties of solids. Static methods are limited mainly by the imprecision of measuring stress and strain, and extensive calibrations are usually required. Dynamic methods employ relatively small stresses and strains, namely those produced by a piezoelectric transducer. Whereas static methods claim accuracies of about one percent, dynamic methods can detect relative elastic modulus changes as small as 10^{-8} (see Holder [26]). Absolute values of elastic moduli are restricted primarily by transducer-specimen bond corrections, phase-shift corrections (see McSkimin [27]), non-flatness and misorientation of specimen faces (see Waterman [28]), and transducer misorientation. Careful specimen preparation and proper experimental techniques can result in absolute errors being as small as 10^{-4}.

Chronological variations of the engineering elastic constants of iron are shown in figure 2. While more recent values are more self-consistent, none of the older values can be excluded on the basis of deviations from the mean.

7. Isothermal and Adiabatic Elastic Constants

Distinctions between isothermal and adiabatic elastic constants are discussed here. (These constants are denoted herein by subscripts T and S denoting constant temperature and constant entropy, respectively.) The distinction arises naturally from measurement methods. Slow or static loading gives isothermal constants while rapid or dynamic loading gives adiabatic constants. For most engineering purposes, differences between the two cases are negligible, being a few percent or less. However, for detailed comparisons between elastic constants, this difference becomes important. Using thermodynamic relations generalized to include elastic strain energy it can be shown that [29]

$$s_{ijkl_S} - s_{ijkl_T} = -\alpha_{ij}\alpha_{kl}T/C_\sigma \tag{7.1}$$

where s_{ijkl} = elastic compliances; α_{ij}, α_{kl} = thermal expansion coefficients; T = temperature, and C_σ = heat capacity per unit volume at constant stress σ. Since solids have, almost invariably, positive thermal expansion coefficients, adiabatic compliances are smaller than isothermal compliances. Differences were computed for a few cases by Hearmon [29].

A similar relationship exists between the isothermal and adiabatic stiffnesses, c_{ijkl}. Thus, after Mason [30],

$$c_{ijkl_S} - c_{ijkl_T} = \lambda_{ij}\lambda_{kl}T/C_\epsilon \tag{7.2}$$

where λ_{ij}, λ_{kl} = the temperature coefficients of stress at constant strain, and C_ϵ = heat capacity per unit volume at constant strain.

For cubic symmetry

$$\alpha_{11} = \alpha_{22} = \alpha_{33} = \alpha, \tag{7.3}$$

$$\alpha_{12} = \alpha_{13} = \alpha_{23} = 0, \tag{7.4}$$

$$\lambda_{11} = \lambda_{22} = \lambda_{33} = \lambda, \tag{7.5}$$

and

$$\lambda_{12} = \lambda_{13} = \lambda_{33} = 0; \tag{7.6}$$

thus

$$\lambda = 3\alpha B_T, \tag{7.7}$$

so that in the cubic case, in compact notation:

$$s_{11_S} - s_{11_T} = s_{12_S} - s_{12_T} = -\frac{\alpha^2 T}{C_P}, \tag{7.8}$$

$$s_{44_S} - s_{44_T} = 0, \tag{7.9}$$

$$c_{11_S} - c_{11_T} = c_{12_S} - c_{12_T} = B_S - B_T = 9\alpha^2 B_T^2 T/C_V, \tag{7.10}$$

and

$$c_{44_S} - c_{44_T} = 0. \tag{7.11}$$

For completeness, relationships between isothermal and adiabatic engineering elastic constants are given also:

$$E_S = \frac{E_T}{1 - E_T\,(T\beta^2/9C_P)} \approx E_T + (E_T)^2\frac{T\beta^2}{9C_P}, \tag{7.12}$$

$$\frac{1}{B_S} = \frac{1}{B_T} - \frac{9\beta^2\,TV}{C_P}, \tag{7.13}$$

$$\nu_S = \frac{\nu_T + E_T\,(T\beta^2/9C_P)}{1 - E_T\,(T\beta^2/9C_P)} \approx \nu_T + (1 + \nu_T)\,E_T\frac{T\beta^2}{9C_P}, \tag{7.14}$$

and

$$G_S = G_T, \tag{7.15}$$

where T = temperature, β = volume thermal expansion coefficient, V = volume, and C_P = heat capacity per unit volume at constant pressure. Derivations of these relationships were given by Landau and Lifshitz [31] and Bhatia [32], for example. Approximations in eqs (7.12) and (7.14) assume that $ET\beta^2/C_P$ is small. Isothermal and adiabatic shear moduli are equivalent since shear at constant volume, and entropy, leaves temperature unaffected.

Finally, the relationship of the isothermal and adiabatic moduli to the thermodynamics of elastic deformation is indicated. The first law of thermodynamics is, including an elastic energy term,

$$dU = TdS + \sigma_i d\epsilon_i. \tag{7.16}$$

The increment of Helmholtz free energy $F = U - TS$ is

$$dF = -SdT + \sigma_i d\epsilon_i, \tag{7.17}$$

so that the stress tensor is given by

$$\sigma_i = (\partial U/\partial\epsilon_i)_S = (\partial F/\partial\epsilon_i)_T, \tag{7.18}$$

for the isothermal and adiabatic cases, respectively. And finally,

$$c_{ik_x} \equiv (\partial\sigma_i/\partial\epsilon_k)_{x,\epsilon}, \tag{7.19}$$

where ϵ denotes constancy of all strains except ϵ_k so that

$$c_{ik_S} = (\partial^2 U/\partial\epsilon_i\partial\epsilon_k)_{S,\epsilon}, \tag{7.20}$$

and

$$c_{ik_T} = (\partial^2 F/\partial\epsilon_i\partial\epsilon_k)_{T,\epsilon}. \tag{7.21}$$

8. Elements Iron and Nickel

The purpose here is to collect data for both Fe and Ni that relate to their elastic properties and to the elastic properties of their alloys. Table 4 summarizes the data.

Both elements are transition metals (incomplete 3*d* electronic shells) and occur in the first long period of Mendeleev's table, separated in that row only by Co. As shown in table 4, Fe and Ni are quite similar in most of their properties. As discussed below, this similarity is reflected in many aspects of the elastic properties of Fe-Ni alloys.

Properties of solids that are determined largely by orbital electrons must vary periodically with atomic number according to Mendeleev's table of elements. This subject is an important part of the phenomenology and science of solids. However, since this review treats only two elements that are closely related in both the periodic table and in their basic properties, periodic variation of elastic and related properties will not be discussed here in any detail. Interested readers should see Mack [33], Dorn and Tietz [34], Vereshchagin and Lichter [35], Ryabinin [36], Köster and Franz [37], and Gschneider [38].

9. Iron-Nickel Phase Diagram

Since elastic properties of alloys are related intimately to the corresponding constitution diagram, some cursory considerations of Fe-Ni phase equilibria are appropriate. One of the first proposals for an Fe-Ni phase diagram was made on the basis of meteorite metallography [39]. A currently accepted phase diagram is shown in figure 3, adapted from Hansen and Anderko [40], Elliott [41], and Shunk [42]. This diagram is relatively simple, reflecting similar atomic sizes, melting points, heats of fusion, etc. of Fe and Ni. Hume-Rothery's criteria [43] for solid solubility are favorable: atomic size difference is small, electronegativities and valences are identical. Difference in crystal structures at room and lower temperatures precludes complete solid solubility. Complete mutual miscibility does occur at higher temperatures where both crystal structures are f.c.c.

Nickel is f.c.c. at all temperatures and is complicated only by a paramagnetic-to-ferromagnetic transition, the Curie temperature being 627 K. Iron has two allotropic phase transitions: b.c.c. (α)-to-f.c.c. (γ) at 1183 K, and f.c.c. (γ)-to-b.c.c. (δ) at 1663 K. Also, Fe undergoes a paramagnetic-to-ferromagnetic transition at 1043 K. The lower allotropic transition in iron is unusual since a b.c.c. phase becomes stable at lower temperatures. Because of vibrational entropies, b.c.c. phases are stable usually at higher temperatures. The upper allotropic transition γ-to-δ is also unusual. As first explained by Seitz [44], f.c.c. γ would be expected to be stable up to its melting point since its Debye temperature is lower than that of the b.c.c. phase. Debye temperatures are measures of lattice vibrational energies. According to Seitz, the γ-to-δ transition occurs because the electronic energy becomes large, on the order of kT. This happens because the electronic specific heat, which increases linearly with T, becomes relatively large due to partly filled *d* shells; the *d* shells have a high density of states; therefore a large number of electrons are available at the top of the unfilled band to absorb thermal energy.

Polymorphic transitions of iron were interpreted differently by Zener [5]. He ascribed the upper transition δ-to-γ to a low value of $C' = (c_{11} - c_{12})/2$, the $\{110\}_\delta$ $\langle\bar{1}10\rangle_\delta$ shear modulus. Absence of elastic data of any kind for δ Fe precludes experimental confirmation of this proposal. He ascribed the lower transition γ-to-α to a spontaneous magnetization (ferromagnetism) of b.c.c. Fe. The difference between the Curie temperature and the allotropic transition temperature was ascribed to a local correlation of electron spins, ferromagnetism being a long-range correlation.

The γ-to-α transition that occurs on cooling has martensitic character in the range of about 18 to 34 Ni and "massive" character for compositions up to about 18 Ni [45]. Some evidence suggests that very rapid cooling of γ prevents a diffusion mechanism and gives a martensitic transformation in alloys of lower Ni content, even Fe [46].

Curie temperatures representing paramagnetic-to-ferromagnetic transitions are shown in figure 3 as dotted lines; data were taken from the recent compilation of

Connolly and Copenhaver [47]. Possible relevance of Curie temperatures to structural transitions was discussed by Davies and Magee [48].

An order-disorder transition occurs in the $FeNi_3$ region, the critical temperature at stoichiometry being about 776 K. Some evidence also exists that order-disorder transitions occur near the stoichiometric compositions Fe_3Ni and FeNi [49]. Because of strong similarities between Fe and Ni atoms, occurrence of Fe-Ni superlattices is surprising and not understood completely, though magnetic interactions between atoms are surely important.

Thermodynamic equilibrium in Fe-Ni alloys is not established readily, and the final form of the equilibrium diagram has probably not yet emerged. For present purposes, metastable states corresponding to continuous heating and cooling are more important than the equilibrium states since man-made Fe-Ni alloys are metastable. In figure 3 the two long-short dashed curves are so-called realization curves representing boundaries of the α and γ phases for Fe-rich alloys. Thus, in practice the b.c.c. phase exists at room temperature up to about 30 Ni, beyond the 10 Ni predicted by "equilibrium" phase boundaries.

Recent experimental and theoretical work on meteorites has suggested modifications of existing Fe-Ni phase diagrams; for example, see Goldstein and Ogilvie [50] and Kaufman and Ringwood [51].

For further details on Fe-Ni phase equilibria readers can consult refs. [40, 41, and 42].

10. Compositional Dependence of Elastic Constants

Compositional variation data, including iron and nickel, are given in figures 4–8 and in tables 5–19. Many earlier data (pre-1945) are based on poorly characterized materials, and data variation is due probably to non-identical specimens and test conditions. Trace impurities influence elastic constants through an impurity-dislocation interaction; dislocations contribute an additional strain upon stress application. Similarly, small residual stresses affect measured elastic constants. Thus, measurements made on low-impurity, well-annealed specimens are much preferred. Both residual stresses and dislocation density are reduced by annealing. As discussed in section 11, presences of some types of defects are useful for minimizing dislocation effects.

Changes in elastic constants due to alloying are usually considered to consist of three parts: (1) change in valency or electron/atom ratio; (2) change in interatomic spacing, and (3) change in interatomic potential. A fourth contribution—change in band structure energy—is complicated, not generally understood, and is treated usually either by simple approximations or by neglecting it.

For Fe-Ni alloys valence is invariant if d electrons are neglected; both elements have two 4s electrons. As shown by Reed and Schramm [52], lattice parameters of both Fe and Ni are reduced only slightly by alloying; thus, the lattice paramenter effect is small and possibly negligible. The interatomic potential may change significantly; this effect has apparently never been estimated. An estimation could be made by assuming a Born-Mayer, or similar, ion-core repulsive potential and evaluating the Born-Mayer parameters from the c_{ij}. Similarly, contributions from 3d and 4s band structure energies are undoubtedly important but apparently have never been evaluated. Thus, the theory of alloying effects on the elastic properties of transition metals is presently inadequate for treating the problem even qualitatively. Since both valence and lattice parameter effects are negligible, the Fe-Ni system provides an opportunity for studying effects of band structure and/or effects of changing interatomic potential on elastic properties.

An alternative model by Zener [53] explains lowering of elastic moduli by alloying such as shown in figures 5 and 6. Zener's model is based on residual strain energy arising from the atomic size difference of solvent and solute atoms. Since relative sizes also affect the mutual solubility of species, the effect is related crudely to the limits of maximum solubility; a lower solubility giving a larger effect on the modulus per unit solute. It can be shown simply that strain energy associated with uniaxial tension is largely shear-strain energy rather than dilatation-strain energy. For the shear modulus Zener was able to relate the composition coefficient to the temperature coefficient. Thus,

$$1/G(dG/dx)=4/Nk(\delta r/r)^2(dG/dT), \qquad (10.1)$$

where x = compositional variable, N = Avogadro's number, k = Boltzmann's constant, r = radius of solvent atom, and δr = radius difference between solvent and solute atoms. As shown in section 13, (dG/dT) is usually negative so that (dG/dx) is negative also. Since behaviors of E and G are usually parallel, compositional dependence of E is also accounted for, albeit crudely. Magnetic effects are involved in the minima of elastic stiffnesses near 30 Ni; these effects are discussed in section 15.

Poisson's ratio ν is a poorly characterized elastic constant, both experimentally and theoretically. Especially, the effect of alloy composition on ν cannot be predicted a priori. Observed variations of ν with composition for Fe-Ni alloys are shown for both b.c.c. and f.c.c. phases in figure 8. While data are sparse, certain trends seem to be established. The b.c.c. data, obtained by indirect methods, increase monotonically with increasing Ni content, extrapolating to $\nu=1/2$ at about 40 Ni, indicating that b.c.c. Fe-Ni is unstable at higher Ni contents. The large magnitude of $d\nu/dx$ for the b.c.c. phase is surprising, and reflects a significant change in the interatomic interaction as Ni is alloyed with Fe. This may be the largest change in ν now known for any primary solid solution and reflects undoubtedly the transition-metal aspect (unfilled 3d electronic shell) of the two species. For comparison, ν is constant within experimental error for alloys of Cu, 0–38 percent Zn [37].

For the f.c.c. phase (the open symbols in figure 8), ν changes in a more complicated manner with composition, having a maximum at about 40 Ni. Köster and Franz [37] interpreted the compositional variation of ν for the f.c.c. phase in terms of magnetostriction, which is discussed in section 15.

Decreases in E and G with increasing Ni content shown in figures 5 and 6 are relatively large, about 1 percent modulus change per atomic percent of solute up to ~35 Ni. Drastic changes of E and/or G with alloying are typical of systems that have limited mutual solid solubility and that tend to form intermetallic phases. Strong compositional variations in Fe-Ni alloys are unexpected because Fe and Ni have similar properties. Magnetic effects are probably important. This subject is ripe for theoretical study. Additional references on alloy effects were given by Speich, Schwoeble, and Leslie [23].

Studies of effects of alloying on elastic constants in systems other than iron-nickel were summarized by Hearmon [54]. Some additional studies include:

Cu, Ag+many solutes	Hopkin, Pursey, Markham [55]
Cu-Al	Cain, Thomas [56]
Cu-Al, Cu-Sn	Moment [57]
Mg-Ag, -Sn, -In	Eros, Smith [58]
Fe-Al	Leamy, Gibson, Kayser [59]
Ni-Co	Leamy, Warlimont [60]
Ni-Cu	Sakurai, et al. [61]
Pd-Rh, Pd-Ag	Walker, et al. [62]
Cu. Ag. Au+B-metals	Köster [63]

Friedel [64] correlated deviations from Vegard's law with difference in compressibilities of solute and solvent. (Vegard's law states that, in substitional alloys, lattice parameters are related linearly to concentration.) As discussed by Mott [65], Friedel [66] extended these considerations to elastic constants. His correlations are most appropriate when atomic volume changes rapidly with composition but Fermi energy is constant. Oriani [67] criticized some aspects of the elastic approach. Muñoz [68] showed that if $\delta r/r$ exceeds about 1 percent then second-order terms become important but that second-order theory breaks down if $\delta r/r$ exceeds about 7 percent.

11. Effects of Mechanical Deformation, Annealing, Recovery, and Lattice Defects

Crystals and crystal aggregates described above were assumed tacitly to be perfect except for substitutional impurities. thermal vibrations. free surfaces. and (in the case of aggregates) grain boundaries. In this section the small but important effect on elastic constants due to various lattice defects is discussed, both implicitly in terms of macroscopic mechanical states and explicitly in terms of defect contributions per se.

11.1. Mechanical Deformation

Since mechanical loading beyond the elastic limit causes plastic deformation and increases a solid's volume, one expects a lowering of elastic stiffnesses by cold-working. Few data exist for testing this hypothesis for Fe-Ni alloys. Most available experimental data are given in figures 9 and 10 for iron, figures 11 and 12 for nickel, and in figure 13 for their alloys. Properties of deformed metals are difficult to understand because of preferred orientations that may be introduced by working, that is, a mechanically induced anisotropy whose degree and nature are usually unknown. For example, such anisotropy may account for the non-parallel behavior of E and G of Ni with plastic deformation as shown in figures 11 and 12. Usually, highly anisotropic mechanical states arise from severe plastic deformation.

Effects of mechanical deformation on elastic properties are difficult problems both experimentally and theoretically. As discussed below, full understanding is inaccessible since it depends on detailed interactions among various species of lattice defects that are deformation induced. These interactions vary with material and depend on composition, crystal structure, mechanical and thermal histories, etc., that is, on any variable which affects the character and/or number of deformation-induced defects. An obviously important variable is method of deformation; whether loading is tensile, compressive, hydrostatic, torsional, slow, impulsive, etc. In short, the relationship between plastic deformation and elastic properties is complicated and will remain so. Additional well-characterized experimental data would illumine the subject somewhat. Interested readers may find some solace in Zener's [69] study where the latent energy of cold-work is related to the lattice expansion accompanying lattice distortion.

A good example of effects of preferred orientations on elastic properties is shown in figure 8 where the upper curve gives the compositional variation of ν for 44 percent cold-worked alloys. In several cases, values of ν exceeding $^1/_2$ were found. As described in section 4, $^1/_2$ is the upper limit for an isotropic aggregate. Thus, ν can provide a fairly sensitive index for presence of strong preferred orientations. The problem of correcting elasticity measurements for slightly anisotropic aggregates was discussed in detail by Bradfield and Pursey [70] and by Pursey and Cox [71].

Effects on elastic constants due to mechanical deformation can be correlated to a certain extent with effects due to radiation damage since both methods introduce large numbers of lattice *point* defects. Many fundamental studies, both experimental and theoretical, have been made on radiation damage effects. For a review see Seitz and Koehler [72]. Additional data on deformation and elastic constants are included in figures 14, 18, 19, 26, 30, and 32.

11.2. Annealing

When deformed materials are heated, lattice defects and distortions induced by cold-work are eliminated; that is, lattices recover to unstrained and unstressed states. If both amount of cold-work and annealing temperature are sufficiently high, recrystallization occurs; a new set of strain-free grains grows from the deformed matrix material. Preferred orientations can arise also from recrystallization and subsequent grain growth. Thus, interpretation of the elasticity of a recrystallized material can also be complicated by an anisotropic aspect or annealing texture just as in the case of a material with a deformation texture. Some annealing data for nickel are given in figure 14. For nickel, the Young's modulus for a heavily deformed specimen is close to that of the magnetically saturated state; and higher annealing temperatures produce lower moduli. As also shown in figure 14, rapid cooling from the annealing temperature to room temperature (quenching) tends to increase the modulus, presumably because of stresses induced by temperature gradients during quenching.

11.3. Lattice Defects

Since both deformation and annealing processes must be described ultimately by creation and annihilation of lattice defects, effects on elastic constants due to four types of lattice imperfections—vacancies, interstitials, dislocations, and grain boundaries—will be discussed briefly. Effects due to presence of lattice defects are expected to be especially strong in systems where core-core repulsion energies contribute significantly to elastic constants, for example in noble and in transition metals. Of various energy terms that contribute to elastic constants (see section 17), exchange repulsion terms are probably most affected by displacements of atoms from equilibrium positions.

Since creation of vacancies decreases mass density, one expects vacancies to lower elastic stiffnesses. Theoretical verification of this was obtained by Bruggeman [73] and by Mackenzie [74], and by Dienes [75] who used the Fuchs [76] extended Wigner-Seitz approach with a Morse potential for sodium and a Born-Mayer potential for copper.

In the presence of thermal or static defects, Schoknecht and Simmons [77] showed that

$$VB_T^{-1} \equiv \left(\frac{\partial V(P,T)}{\partial P}\right)_T = V^\circ B^{\circ -1}_T - \sum_{i,j}\left[n_j\left(\frac{\partial v_{ij}(P,T)}{\partial P}\right)_T + v_{ij}\left(\frac{\partial n_j}{\partial P}\right)_T\right], \qquad (11.1)$$

where $v_{ij} = (\partial g_{ij}/\partial P)_T$ is the free volume of formation of the defect j, g_{ij} = partial Gibbs energy of defect, n_j = number of defects of species j, and superscript ° denotes the defect-free case. For thermal monovacancies eq (11.1) becomes

$$B_T^{-1} - B^{\circ -1}_T \approx \frac{nV^2}{NkTv_a}, \qquad (11.2)$$

since $(\partial V(P,\ T)/\partial P)_T$ is small; v_a = atomic volume. Thus, the bulk modulus B is decreased by thermal vacancies.

Conversely, interstitials increase mass density, and higher elastic stiffnesses are expected. Theoretical calculations by Bruggeman [73] and by Dienes [75] also predict this effect. Considering copper and sodium, Dienes showed that a 1 percent vacancy concentration decreases all of the elastic stiffnesses by about 1 percent, while a 1 percent interstitial concentration increases all elastic stiffnesses by about 10 percent. The large difference between effects of vacancies and interstitials is related directly to relaxation of lattices around defects. Dienes found for copper that the percent change in interatomic distance upon relaxation was 2 and 9 percent for vacancies and interstitials, respectively. Dienes also concluded that interatomic relaxation is much larger in a b.c.c. (more open) crystal structure than in an f.c.c. (close-packed) crystal structure. Melngailis [78] considered how Frenkel defects (vacancy-interstitial pairs) affect elastic properties of copper and concluded that an elastic softening results. This is consistent with the observation that Frenkel defects decrease mass density. Point defects can alter elastic stiffnesses by another mechanism, dislocation pinning. This phenomenon is discussed next.

In discussing effects of dislocations on elastic constants, two types of dislocations are distinguished—those which move freely upon stress application and those which are immobile or pinned. That dislocations should lower elastic stiffnesses was noted apparently first by Eshelby [79]. Subsequently the problem was treated theoretically by Koehler and DeWit [80] for the case of pinned dislocations in f.c.c. crystals. Elastic stiffnesses are altered because reversible dislocation motions contribute a reversible elastic strain component to the total strain. Thus, total strain is increased for a given stress and observed elastic stiffnesses are lower. Koehler and DeWit found approximately that

$$\Delta E/E = -K\rho L^2, \qquad (11.3)$$

where E = Young's modulus, K = constant, ρ = dislocation density, and L = average dislocation loop length. For annealed copper they concluded that pinned dislocations contribute only a few percent to elastic constants, but that for slightly deformed materials (where dislocation densities are much higher) the contribution to elastic constants can be 10 percent or higher. Because of dilatational components in their strain fields, edge dislocations are about ten times as effective as screw dislocations (which have only a shear strain field) in decreasing elastic stiffnesses. Granato and Lücke [81] gave a detailed vibrating string model for pinned dislocations where damping is related to elastic modulus change; this work was initiated by Koehler [82].

A related subject—anisotropic dislocation theory—has become within recent years a flourishing area of solid-state physics with many intriguing applications for single-crystal elastic data. Interested readers should see chapter 13 of the text by Hirth and Lothe [83].

If thermal oscillations (phonons) are considered crystalline defects, then phonon contributions to elastic stiffness can be computed from statistical thermodynamics. Holder [84] did such a calculation for the bulk modulus with the result for large T that

$$\frac{\Delta B}{B}=\frac{3NkT}{BV}\left\{-\gamma\frac{B}{V}-V\frac{\partial}{\partial V}\left(\frac{\gamma}{V}\right)\right\} \tag{11.4}$$

where B = modulus, N = Avogadro's number, k = Boltzmann's constant, V=volume, T=temperature, and γ=Grüneisen's constant. According to Holder, substitution of appropriate experimental values into eq (11.4) predicts approximately the observed thermal variation of the bulk modulus. Extension of this, or a similar, approach to dB/dT would be quite useful.

Grain boundaries can affect elastic constants at higher temperatures when a static or slowly-varying load is applied such that stress relaxation occurs across grain boundaries [5]. At higher temperatures, the viscous aspect of grain boundaries becomes more important, grain-boundary sliding occurs as a Le Chatelier accommodation, and the elastic moduli are effectively lowered. This effect is often seen as a departure from linear temperature dependence and varies with the stress frequency.

12. Higher-Order Elastic Coefficients

Deviations from Hooke's law (stress is proportional linearly to strain) require the concept of elastic coefficients higher than second-order. These coefficients arise naturally from a Taylor expansion of the elastic internal energy about the unstrained or reference state. Thus,

$$U=U_0+a(x-x_0)^2+b(x-x_0)^3+c(x-x_0)^4+\ldots, \tag{12.1}$$

and the nth order elastic constant is the nth derivative of the energy evaluated at the reference spacing. For example

$$(\partial^2U/\partial(x-x_0)^2)_{x=x_0}$$
$$=2a=\text{second-order elastic coefficient} \tag{12.2}$$

$$(\partial^3U/\partial(x-x_0)^3)_{x=x_0}$$
$$=6b=\text{third-order elastic coefficient} \tag{12.3}$$

and so on.

Identifying elastic stiffnesses with coefficients in a series expansion of energy in terms of strains was first discussed in detail by Birch [85]. More recently, Brugger [86] gave definitions of nth order isothermal and adiabatic elastic coefficients:

$$c^S_{ijkl\ldots}=\rho_0(\partial^nU/\partial\eta_{ij}\partial\eta_{kl}\ldots)_S, \tag{12.4}$$

$$c^T_{ijkl\ldots}=\rho_0(\partial^nF/\partial\eta_{ij}\partial\eta_{kl}\ldots)_T, \tag{12.5}$$

$$s^S_{ijkl\ldots}=\rho_0(\partial^nH/\partial t_{ij}\partial t_{kl}\ldots)_S, \tag{12.6}$$

and

$$s^T_{ijkl\ldots}=\rho_0(\partial^nG/\partial t_{ij}\partial t_{kl}\ldots)_T, \tag{12.7}$$

where

$$\eta_{ij}=[(\partial x_k/\partial a_i)(\partial x_k/\partial a_j)-\delta_{ij}]/2, \tag{12.8}$$

are Lagrangian strain components. F=Helmholtz elastic energy, S=entropy, H=enthalpy, G=Gibbs elastic energy, T=temperature, a_i and x_i are Cartesian components of a material particle in unstrained and strained states, and ρ_0=mass density of undeformed state. The t_{ij} represent thermodynamic tensions conjugate to the variables η_{ij}; for example

$$t_{ij}=\rho_0(\partial F/\eta_{ij})_T=\rho_0(\partial U/\eta_{ij})_S. \tag{12.9}$$

Currently there is much activity, both theoretical and experimental, on third-order elastic constants of metals. Fourth-order and higher-order elastic constants have been explored only slightly.

The primary significance of third-order elastic coefficients is that they relate directly to anharmonic properties of lattices such as thermal expansion, thermal conductivity, differences between adiabatic and isothermal elastic constants, and temperature and pressure coefficients of elastic constants. Anharmonic crystal properties were discussed by Leibfried and Ludwig [87].

Anharmonic properties of solids can be described conveniently by invoking Grüneisen's γ. Brugger [88] gave a generalized isothermal Grüneisen parameter

$$\gamma_i^{kl}\equiv-\frac{1}{\omega_i}\left(\frac{\partial\omega_i}{\partial\eta_{kl}}\right)_{\eta=0}, \tag{12.10}$$

where ω_i=angular frequency of ith normal mode. By differentiating the wave equation Brugger related this parameter to second-order and third-order elastic stiffnesses c_{klmn} and c_{klmnop}:

$$\gamma_i^{kl}(\mathbf{n})=-(\tfrac{1}{2}w_i)[2w_iu_ku_l+(c_{klmn}+c_{klmnop}u_ou_p)n_mn_n] \tag{12.11}$$

where

$$w_i = c_{klmn} n_k n_m u_l u_n, \ \mathbf{n} = \text{propagation vector},$$

and $\mathbf{u}$ = polarization vector.

Grüneisen's parameter figures prominently in equations of state for solids. For example

$$P + dU/dV = \gamma E_{\text{vibr}}/V \tag{12.12}$$

is the Mie-Grüneisen equation of state, which is a special case (all γ_i are equal) of the more general form

$$P + dU/dV = \frac{1}{V} \sum_i \gamma_i \left\{ h\nu_i/2 + \frac{h\nu_i}{\exp(h\nu_i/kT) - 1} \right\} \tag{12.13}$$

that follows simply from the thermodynamic partition function for an array of oscillators.

Grüneisen's model succeeds for two reasons. First, while the γ_i are not equal the assumption describes macroscopic thermodynamic properties fairly well. Secondly, while γ depends on volume the dependence is slight; thus, treating γ as a constant, independent of temperature, leads to theoretical predictions that are largely verified by observation. Section 18 discusses a few anharmonic properties. Interested readers should see Grüneisen [89] and Slater [90] for further discussion of γ and its applications to theory of solids.

For tetrahedral cubic symmetry (point groups $T = 23$, $T_h = m3$) there are eight independent third-order elastic coefficients as shown by Birch [85], Fumi [91], and Hearmon [92].

$$c_{111} = c_{222} = c_{333}, \tag{12.14}$$

$$c_{112} = c_{133} = c_{223}, \tag{12.15}$$

$$c_{113} = c_{122} = c_{233}, \tag{12.16}$$

$$c_{123},$$

$$c_{144} = c_{255} = c_{366}, \tag{12.17}$$

$$c_{155} = c_{266} = c_{344}, \tag{12.18}$$

$$c_{166} = c_{244} = c_{355}, \tag{12.19}$$

and

$$c_{456}.$$

All other coefficients are zero.

For octahedral cubic symmetry (point groups $T_d = \bar{4}3m$, $O = 432$, and $O_h = m3m$) there are two additional relationships:

$$c_{112} = c_{113}, \tag{12.20}$$

and

$$c_{155} = c_{166}, \tag{12.21}$$

and therefore only six independent third-order elastic coefficients. Both b.c.c. and f.c.c. crystal structures have O_h point symmetry.

The Cauchy (central-force) conditions for cubic third-order elastic constants are:

$$c_{112} = c_{166}, \tag{12.22}$$

and

$$c_{144} = c_{123} = c_{456}. \tag{12.23}$$

Thus, cubic Cauchy crystals have three independent third-order elastic constants. Like second-order constants, Cauchy conditions for third-order constants are not expected to hold in metals because of free-electron effects. However, for Cu, Ag, and Au, Hiki and Granato [93] showed that Cauchy conditions are more closely followed for third-order than for second-order constants. This is because ion-ion overlap forces. which are central forces, contribute more strongly to higher-order elastic constants. Similar considerations should apply also to the transition metals.

For isotropy, there are three relationships among third-order constants corresponding to eq (5.1) for second-order constants:

$$c_{112} = c_{123} + 2c_{144}, \tag{12.24}$$

$$c_{166} = c_{144} + 2c_{456}, \tag{12.25}$$

and

$$c_{111} = c_{123} + 6c_{144} + 8c_{456}. \tag{12.26}$$

Thus, for isotropic crystals there are three independent third-order elastic constants.

Available c_{ijk} data for iron and nickel are collected in tables 20 and 21. No third-order elastic constants have been measured or calculated for Fe-Ni alloys.

Elastic coefficients are invaluable for testing the validity of model interatomic potentials. Such tests are quite sensitive since second- and third-order elastic coefficients relate to second and third derivatives of the potential. These coefficients describe changes not only with respect to various shear deformation, but also with respect to volume deformations. Such detailed comparisons have borne out, for example, the validity of pseudopotentials as applied to the simple metals, [94]–[97]. In many cases, a knowledge of the experimentally determined coefficients gives directly information on the interatomic forces. For example, if Cauchy relations are satisfied one expects a central-force type model to successfully predict the elastic coefficients. Hiki and Granato [93] observed that the third-order elastic coefficients of Cu, Ag, and Au followed the Cauchy relations much more closely than did the second-order elastic coefficients. From this observation they concluded that short-range central forces, in this case arising from *d*-shell overlap, become increasingly more important as one considers higher-order derivatives of the total energy. As shown in tables 5 and 6, second-order Cauchy relationships are violated for both iron and nickel, as expected. However, the deviations are small, about 20 percent. The data in table 21 show that for nickel the deviations from third-order Cauchy relationships are quite small, and also that the deviation from the condition for first-nearest-neighbor interactions is very small. The situation for iron is more ambiguous, and additional experimental third-order data would be very valuable.

Several proposals have been made for averaging the c_{ijk} to obtain the quasi-isotropic coefficients c°_{ijk}. Most of the considerations discussed in section 5 for obtaining c°_{ij} apply also to the c°_{ijk} case. Hamilton and Parrott [98] pointed out that the difference between Voigt's and Reuss's averages are even more important for the c_{ijk} than for the c_{ij}. Whether a Hill-type average is also appropriate for the c_{ijk} has not yet been established. The problem of averaging c_{ijk} is ripe for both theoretical and experimental study. Interested readers should see Barsch [99], Nran'yan [100], Cousins [101], and Chang [102].

Some authors have reported quasi-isotropic third-order elastic constants as Lamé coefficients ν_1, ν_2, and ν_3 or as Murnaghan's constants l, m, and n. These are related to the c°_{ijk} as follows:

$$c^{\circ}_{123}=\nu_1=l, \tag{12.27}$$

$$c^{\circ}_{144}=\nu_2=m, \tag{12.28}$$

$$c^{\circ}_{456}=\nu_3=n, \tag{12.29}$$

$$c^{\circ}_{112}=\nu_1+2\nu_2, \tag{12.30}$$

$$c^{\circ}_{166}=\nu_2+2\nu_3, \tag{12.31}$$

and

$$c^{\circ}_{111}=\nu_1+6\nu_2+8\nu_3. \tag{12.32}$$

13. Temperature Dependence of Elastic Constants

Temperature (and as discussed in section 14, also pressure) variations of elastic constants are an important part of the subject of equations of state of solids. If equations of state were known precisely, then elastic constants and their temperature and pressure coefficients could be calculated immediately. Large parts of both theoretical and experimental solid-state physics would then be obviated. In fact, equations of state of solids are known only crudely, and such parameters as $\partial c_{ij}/\partial T$ and $\partial c_{ij}/\partial P$ are measured and used to test and to improve the equations.

The problem of temperature dependence of elastic constants of solids was first considered carefully by Born and co-workers [103]. Zener [104] discussed the problem in terms of an oscillator model of solids. Discussion here is purely thermodynamic and therefore more general.

It is easy to show that temperature coefficients of elastic stiffnesses, or any linear combination of elastic stiffnesses, should approach zero as T approaches zero. Invoking Nernst's heat theorem that the entropy S of all crystalline solids approaches zero as T approaches zero, then

$$\lim (\partial S/\partial x_i)_T=0, \tag{13.1}$$

where x_i is any usual thermodynamic variable that preserves crystallinity. Physically this means that the entropy change in an isothermal physical process goes to zero as T approaches zero, that is all crystalline states of a solid have zero entropy at zero temperature. Also,

$$\lim_{T\to 0} (\partial^2 S/\partial x_i \partial x_j)_T=\lim_{T\to 0} [\partial/\partial x_i(\partial S/\partial x_j)]_T=0. \tag{13.2}$$

If x_i and x_j are strains ϵ_i and ϵ_j and if a Maxwell relation in elasticity variables

$$(\partial\sigma_k/\partial T)_\epsilon=(\partial S/\partial\epsilon_j)_T, \tag{13.3}$$

is invoked, then

$$\lim_{T\to 0} [\partial/\partial\epsilon_i(\partial\sigma_k/\partial T)_\epsilon]=\lim_{T\to 0} [\partial/\partial T(\partial\sigma_k/\partial\epsilon_i)_\epsilon]=0, \tag{13.4}$$

and

$$\lim_{T\to 0} [\partial/\partial T(c_{ki})]=0, \tag{13.5}$$

since

$$c_{ki}\equiv(\partial\sigma_k/\partial\epsilon_i)_{T,\epsilon}. \tag{13.6}$$

Thus, elastic stiffnesses c_{ij} approach constant values with vanishing slope when plotted versus temperature as T approaches zero. This feature must be considered when extrapolating elastic data at cryogenic temperatures.

Temperature dependence of elastic stiffness at higher temperatures cannot be demonstrated so simply since the effect is anharmonic. Like thermal expansion, it relates to higher-order elastic coefficients, which were described in section 12. Any discussion of higher-order or anharmonic effects is simplified by introducing Grüneisen's parameter

$$\gamma=-(V/\nu_i)(d\nu_i/dV)=-d\ln\nu_i/d\ln V \tag{13.7}$$

where V= volume of the crystal and ν_i= frequency of ith normal vibrational mode. Grüneisen's γ is actually a tensor property, but its isotropic form is sufficient for many purposes. In the quasi-harmonic model, γ does not depend explicitly on temperature [105]. And it is related directly to various thermodynamic properties, for example [106],

$$\gamma=\beta V B_T/C_v \tag{13.8}$$

where β= volume thermal expansion coefficient, V= volume, B_T= isothermal bulk modulus and C_v= specific heat at constant volume. Thus, γ can be determined from a set of macroscopic thermodynamic parameters. For metals γ has a range of 1 to 3 and is usually about 2 [107]. This limited range of γ is expected since by integration of eq (13.7)

$$\nu_i \propto V^{-\gamma}, \tag{13.9}$$

that is the volume dependence of vibrational frequencies is weak and is roughly similar for all materials. If an Einstein oscillator model of solids is invoked, then

$$\nu_i = \nu = k\theta/h \tag{13.10}$$

where θ= characteristic temperature, k= Boltzmann's constant and h =Planck's constant. Substitution into eq (13.7) gives

$$\gamma = -d\ln\theta/d\ln V = -(V/\theta)(d\theta/dV). \tag{13.11}$$

Invoking the well-known relationship

$$C_p - C_v = TV\beta^2 B, \tag{13.12}$$

for quasi-isotropic solids, combining this with eq (13.8) and rearranging terms,

$$C_p/C_v = 1 + \gamma T\beta = 1 + \gamma T(dV/dT)_P/V. \tag{13.13}$$

Substituting from eq (13.11)

$$C_p/C_v = 1 - T(d\theta/dT)_P/\theta. \tag{13.14}$$

Thus, since $C_p > C_v$, the characteristic temperature decreases with increasing temperature. The characteristic temperature θ can be related to the elastic moduli, e.g., E, by invoking relationships introduced originally by Madelung [108] and by Einstein [109],

$$\theta = KE^{1/2}f(\nu), \tag{13.15}$$

where $f(\nu)$ depends upon Poisson's ratio. Assuming that $\nu \neq \nu(T)$, which is only crudely true, then

$$d\theta/\theta = (1/2)dE/E, \tag{13.16}$$

and

$$(1/E)(dE/dT)_P = (2/T)(1 - C_p/C_v). \tag{13.17}$$

Thus, in this model elastic stiffnesses behave exactly as the characteristic temperature; their coefficients are negative.

Since elastic coefficients c_{ij} are given by the second spatial derivative of the elastic potential energy, one expects a priori a slow decrease of c_{ij} with increasing temperature due to the interatomic potential becoming more shallow as atomic vibration amplitudes increase.

In fact, it has been shown experimentally [54] for a wide variety of materials that dc_{ij}/dT is zero at $T=0\,K$, is constant and negative at high temperatures ($T > \theta$), and changes rapidly at low temperatures. The exact low temperature dependence of c_{ij} remains an unsettled problem; several suggestions have been made on either theoretical or empirical grounds for the low-temperature dependence of c_{ij}. These include

$$c_{ij}(T) = c_{ij}(0)[1 - KT^4], \tag{13.18}$$

$$c_{ij}(T) = c_{ij}(0) - AT\exp(-T_0/T), \tag{13.19}$$

and

$$c_{ij}(T) = c_{ij}(0) - B/[\exp(C/T) - 1]. \tag{13.20}$$

All these functions fit selected data quite well, indicating that the exact form of the interpolation from $T > \theta$ to $T=0$ is unimportant for most purposes.

Since no fourth-order elastic stiffness have yet been measured, it is attractive to attempt a derivation of fourth-order constants from the temperature derivatives of second-order constants. Hiki, Thomas, and Granato [110] derived expressions among dc_{ij}/dT, c_{ijk} and c_{ijkl} in the high-temperature limit of a continuum model. This approach to the c_{ijkl} has been made for β Cu-Zn [111], NaCl [112], and the noble metals [93] and was discussed by Holder and Granato [113].

Temperature variation data are given mainly in figures 15–32 and also in 33–6 and 38. The only really anomalous temperature data are shown in figure 17 where for Fe-Ni alloys containing about 30 percent Ni, most elastic stiffnesses have *positive* temperature coefficients over a wide temperature range. Positive coefficients, while unusual, occur also in other systems; for example Mo(c_{12}), Pd(c_{11}, c_{12}, c_{44}), and Th(c_{12}) [54]. However, no single theory accounts for occurrences of positive coefficients; separate explanations must be sought for anomalies in individual cases. In the case of Fe ~30 Ni alloys, apparently no explanation has been proposed in the literature. Usual magnetic effects can be disregarded since Curie temperatures (see figure 3) lie well below temperature regions where anomalies occur. It is interesting to note that alloys in this composition range show also curious "invar" effects and phase transition effects. Both these aspects are discussed below.

For additional discussion on the temperature variation of elastic constants, readers should see refs. [87] and [114]–[116].

At low temperatures where the internal energy is given approximately by

$$U = U_0 + aT^2 + bT^4, \tag{13.21}$$

it follows that a general elastic stiffness M is

$$M(T) = \frac{\partial^2 U}{\partial\epsilon^2} = M(0) + \frac{\partial^2 a}{\partial\epsilon^2}T^2 + \frac{\partial^2 b}{\partial\epsilon^2}T^4 + \beta V\frac{\partial M(0)}{\partial V}T \tag{13.22}$$

where ϵ= appropriate strain, β= volume expansion coefficient, and the linear term allows for thermal expansion. Alers [22] described the validity of eq (13.22) for several metals and pointed out that for transition metals the quadratic term, which arises from the electron gas, dominates the quartic term that arises from lattice vibrations.

Sutherland [117] suggested eighty years ago that reduced shear modulus $G(T)/G(0)$ plotted versus reduced temperature T/T_m gave a universal curve for all metals and that G becomes zero at $T=T_m$. While Sutherland's correlation of reduced G's remains valid and valuable, it is now known that G need not vanish at the melting point [118].

In figures 18 and 23 anomalous increases both in E and G are shown that result from crystallographic phase transitions. Generally, elastic properties are discontinuous through first-order phase transitions. This topic is discussed in section 16.

In absence of a saturating magnetic field, ferromagnetic materials may show anomalous elastic behavior as a function of temperature due to motion of magnetic domains upon stress application. As shown in figures 14 and 19, mobility of ferromagnetic domain walls leads to an effective elastic softening because domain walls can contribute an additional strain. When materials are heated through the ferromagnetic-to-paramagnetic transition, then they usually behave normally since in the paramagnetic state there are no magnetic domain walls that can move under applied stress. Applying a strong magnetic field to the ferromagnetic state has a similar effect; domain walls take positions that are most favorable for minimizing the total energy of the system, and they are effectively immobile until the magnetic field is removed. These topics are discussed further in section 15.

Apparently, no theory has been proposed to explain the variation of ν with T. For many purposes this variation can be ignored since it is small for most solids. As discussed by Slater [119], $d\nu/dT$ should be positive since the upper limit of $\nu=1/2$ corresponds to a liquid, and heating metals increases their volume and their behavior becomes more liquid-like. Köster and Franz [37] discussed some experimental and a few analytical aspects of $d\nu/dT$. As shown in figures 30 and 31, $d\nu/dT$ is positive and small for both iron and nickel.

14. Pressure Dependence of Elastic Constants

Most existing data for the pressure variation of the elastic constants are for the bulk modulus (reciprocal compressibility). This is because compressibility can be determined directly as a volume change under pressure as shown by eq (4.18). Extensive data for metallic elements were acquired in the pioneering experiments of Bridgman [120].[6] Following Bridgman, compressibility data are expressed frequently in the form

$$V=V_0(1-aP+bP^2), \tag{14.1}$$

where both coefficients a and b depend on temperature. The compressibility is

$$B^{-1}=-(1/V)(\partial V/\partial P)=(a-2bP)/(1-aP+bP^2). \tag{14.2}$$

Coefficient a is the initial (zero-pressure) isothermal compressibility, and b is related to the pressure derivative of the isothermal bulk modulus by the relationship

$$b=(1/2B_0^2)(1+\partial B/\partial P)_{P=0}. \tag{14.3}$$

The first expressions for the pressure dependence of the elastic stiffnesses were given by Birch [85]:

$$c_{11}(P)=c_{11}(0)+\phi(2c_{11}+2c_{12}+6c_{111}^*+4c_{112}^*), \tag{14.4}$$

$$c_{12}(P)=c_{12}(0)+\phi(-c_{11}-c_{12}+c_{123}^*+4c_{112}^*), \tag{14.5}$$

and

$$c_{44}(P)=c_{44}(0)+\phi(c_{11}+2c_{12}+c_{44}+\tfrac{1}{2}c_{144}^*+c_{166}^*, \tag{14.6}$$

where ϕ is defined by

$$V/V_0=(1+2\phi)^{3/2} \tag{14.7}$$

with V_0= original volume and V= volume at pressure P. Conversion of P to ϕ is accomplished by eqs (14.1) and (14.7). The third-order coefficients appearing in eqs (14.4)–(14.6) are related to the third-order coefficients defined by Brugger [86] as follows:

$$c_{111}^*=c_{111}/6, \tag{14.8}$$

$$c_{112}^*=c_{112}/2, \tag{14.9}$$

$$c_{123}^*=c_{123}, \tag{14.10}$$

$$c_{144}^*=2c_{144}, \tag{14.11}$$

and

$$c_{166}^*=2c_{166}. \tag{14.12}$$

It follows that the pressure derivatives of the second-order elastic coefficients may be written as

$$-(\partial c_{11}/\partial P)_{P=0}=(2c_{11}+2c_{12}+c_{111}+2c_{112})/3B, \tag{14.13}$$

---

[6] Much confusion exists concerning Bridgman's compressibility values because the compressibility standard, iron, was re-evaluated. Different corrections have been used, and old and new values are sometimes not distinguished. Gschneider [38] discussed this problem in detail, and his recommendations are adopted here.

$$-(\partial c_{12}/\partial P)_{P=0}=(-c_{11}-c_{12}+c_{123}+2c_{112})/3B, \tag{14.14}$$

$$-(\partial c_{44}/\partial P)_{P=0}=(c_{11}+2c_{12}+c_{44}+c_{144}+2c_{166})/3B, \tag{14.15}$$

and

$$-(\partial B/\partial P)_{P=0}=(c_{111}+6c_{112}+2c_{123})/9B, \tag{14.16}$$

where the bulk modulus B is

$$B=\tfrac{1}{3}(c_{11}+2c_{12}). \tag{14.17}$$

By using the finite strain theory of Murnaghan [121] and Birch [85], Ghate [122] derived theoretical expressions for the pressure dependence of second-, third-, and fourth-order elastic constants. For the second-order case, he obtained the general form

$$c_{ij}(P)=c_{ij}(0)+A\eta+B\eta^2 \tag{14.18}$$

where η is the Lagrangian strain and the parameters A and B are linear combinations of c_{ij} and c_{ijk}. Ghate's second-order equations are identical to Birch's when the third-order elastic coefficients are defined identically.

It is interesting to note that no expressions comparable to eqs (14.13)–(14.16) have yet been derived for the temperature derivatives in terms of higher-order elastic coefficients, even from simple models.

Both the temperature and pressure dependence of the elastic constants can be deduced qualitatively very simply by assuming a linear anharmonic oscillator model. In the harmonic approximation the energy per atom is

$$U=U_0+\tfrac{1}{2}k(x-x_0)^2, \tag{14.19}$$

where U_0=energy in unstrained (reference) state, k="spring" constant, and x_0=position of atom corresponding to U_0. In the simplest anharmonic model, a single asymmetric term appears. Thus,

$$U=U_0+\tfrac{1}{2}k(x-x_0)^2-\tfrac{1}{6}l(x-x_0)^3, \tag{14.20}$$

is the energy when a particle is displaced from x_0 to x. (The negative sign of the cubic term assures positive thermal expansion coefficients.)

The second-order elastic constant is

$$c_2\equiv(\partial^2U/\partial(x-x_0)^2)=k-l(x-x_0). \tag{14.21}$$

Thus, when the linear chain is compressed (e.g., by increasing the pressure) $x<x_0$ and c_2 is increased. Similarly, when the chain is expanded (e.g., by increasing the temperature) $x>x_0$ and c_2 is decreased. In this model, both temperature and pressure effects are simply related to changes in x, the linear lattice parameter.

The influence of pressure on the elastic constants of Fe-Ni alloys is shown in tables 14, 15, and 22.

15. Magnetic Field Dependence of Elastic Constants

Since magnetic interactions between atoms contribute to the total energy of a ferromagnet, there must be a corresponding contribution to the elastic constants, which are second derivatives of the total energy with respect to appropriate strains. Direct observation of this contribution would elucidate the nature of the magnetic exchange energy, particularly its derivatives with respect to atomic spacing. However, except in the presence of a saturating magnetic field, this contribution is overridden by effects due to magnetic domain boundaries.

In the domain theory of ferromagnets the demagnetized state corresponds to an array of domains, each of which is permanently magnetized to saturation. The domains are oriented randomly so that a specimen has no net magnetization. Net magnetization is achieved by applying an external magnetic field so that magnetization vectors within domains tend to align with the external field.

Magnetic effects on elastic constants were first observed in 1902 by Honda [123] who termed the phenomenon the "ΔE effect"; ΔE refers to the difference in Young's modulus E_0-E_d between saturated and demagnetized states. In the demagnetized state, elementary magnetic domains can change their magnetization direction under applied stress and grow at the expense of neighboring domains that have different orientations that are energetically unfavorable in the applied stress field. Growth consists of motion of domain boundaries (Bloch walls). At magnetic saturation domain walls are immobile, and a "true" or maximum value of E is obtained.

Stress plays a role similar to magnetic field in determining a specimen's magnetization. In effect, stress alters magnetization, which alters a ferromagnet's elastic constants. If domain redistribution does not occur, then different elastic constants are observed. Domain redistribution is prevented, for example, by superimposing a saturating magnetic field or by a high magnetic anisotropy energy.

The following brief analysis follows closely that given by Lee [124].

Assuming that the total strain ϵ_t consists of nonmagnetic and magnetic parts, Kornetski [125] showed empirically that

$$\epsilon_t=\epsilon_0+\epsilon_m=\sigma(1/E_0+1/E_1+E_2), \tag{15.1}$$

where numerical subscripts indicate derivatives of $1/E$ with respect to stress. In the demagnetized state

$$1/E_d=1/E_0+1/E_1. \tag{15.2}$$

And at saturation $\epsilon_m = 0$ so that $E = E_0$. From eq (15.1) it follows that $E = \sigma/\epsilon$ first decreases, passes through a minimum, and then approaches E_0 as stress is increased. Figure 19.17 in Chickazumi [1] shows this behavior; see also figures 13.123 and 13.124 in Bozorth [126].

As shown in figures 18 and 19, the ΔE effect for annealed Ni is several percent and for Fe less than one percent. For alloys, as shown in figures 34 and 37, the effect is strongly composition dependent.

Clearly, the ΔE effect should be related to the magnetostriction constant, λ, the strain due to magnetic saturation. Chickazumi [1] has given relationships of the form

$$(\Delta E/E^2)_{hkl} \sim \lambda_{hkl} \qquad (15.3)$$

and for Fe-Ni a plot of λ versus composition (his fig. 19.14). The ΔE effects shown in figures 34 and 37 correlate remarkably well with the variations of λ with composition, being zero at about 28 and 82 nickel and with maxima at about 40 and 100 nickel.

Taking $\Delta B = 0$, it can be shown from table 1 that the change in the shear modulus is related to the change in the Young's modulus by the relationship

$$\Delta G/G = (3G/E)\,\Delta E/E. \qquad (15.4)$$

This effect is shown in figures 34 and 35. Clearly, the bulk modulus is unaffected by magnetic fields since hydrostatic pressures do not cause domain boundary movements.

The importance of the ΔE effect is well-illustrated by the *Elinvar* alloys (Fe ~ 35 Ni ~ 10 Cr) where the decrease in E due to increased temperature is largely compensated for by a smaller $\Delta E/E$ effect with increasing temperature. Thus, to a good approximation E is independent of T for *Elinvar* alloys below their Curie temperatures.

16. Effects of Crystallographic Transitions on Elastic Constants

When metals or alloys undergo crystallographic transitions, their elastic constants change for several possible reasons: (1) change of lattice type, (2) change of specific volume, (3) change of electronic or Brillouin zone structure, (4) change of relative positions of atoms in the unit cell (even when lattice type is invariant, for example, hexagonal-to-hexagonal with a change in c/a ratio). In most cases, there is also a non-physical effect, namely a change of co-ordinate axes. The effect can be eliminated by a suitable co-ordinate transformation or alternatively by considering force constants, for example—the spring constant between atoms in closest-packed directions in both phases. In short, any parameter that affects vibrational spectra must also influence elastic constants. No a priori basis exists for predicting effects of phase transitions on elastic constants. Each case must be considered individually since both energetics and mechanisms of solid-solid transitions vary widely.

If a phase transition can be characterized completely by lattice considerations, then clearly the lower temperature phase must be elastically harder than the high temperature phase since it must have a higher Debye characteristic temperature in order to be the phase of lowest free energy at lower temperatures. As shown in figures 18, 23, 26, and 38, in Fe-Ni alloys, with one exception at low Ni contents, low temperature phases are elastically softer. Thus, in this system strong electronic effects are undoubtedly involved in the f.c.c.-to-b.c.c. phase transition. Volume increase during the f.c.c.-to-b.c.c. transition may also account partially for the observed elastic softening.

Phase transitions characteristically show a marked increase in damping in the region of the transition temperature. Thus, materials should deform readily in the temperature regions of their phase transitions since deformation mechanisms are augmented by damping mechanisms. In fact, some superplastic phenomena are due directly to phase-transition softening. Spurious elastic measurements can be obtained near a phase change, and such data should be interpreted carefully.

It is attractive to consider a simple explanation for crystallographic transitions, namely, mechanical and therefore also thermodynamic instability of lattices. In 1940, Born [127] derived mechanical, thermodynamic stability conditions that apply to all cubic crystals regardless of unit-cell size and regardless of the type of interatomic forces. These conditions follow from the requirement that elastic strain energy

$$U_e = c_{ij}\epsilon_i\epsilon_j/2, \qquad (16.1)$$

is positive-definite. that is

$$U_e \geqslant 0. \qquad (16.2)$$

In other words, any elastic strain or combination of strains must *increase* elastic energy. Stability conditions can be derived readily by considering the matrix array of elastic coefficients for a cubic crystal, eq (4.10), and requiring that each principal minor of this matrix is positive. After some algebra, it results that

$$c_{11} > 0, \qquad (16.3)$$

$$c_{11} > |c_{12}| \text{ or } (c_{11} - c_{12}) > 0, \qquad (16.4)$$

$$(c_{11} + 2c_{12}) > 0, \qquad (16.5)$$

and

$$c_{44} > 0. \qquad (16.6)$$

If any of these conditions are violated, then crystals are unstable with respect to long-wavelength phonons and a transition to another crystal structure or to a liquid phase must occur. Of course, such transitions may occur for other reasons since phase equilibria are determined by *relative* stabilities of competing structures and eqs (16.3)–(16.6) describe conditions of absolute instabilities. These conditions may be summarized by saying that c_{11}, the bulk modulus $(c_{11}+2c_{12})/3$, and the two shear moduli $(c_{11}-c_{12})/2$ and c_{44} must all be positive.

Since elastic stiffnesses for cubic crystals are found experimentally to be always positive, eq (16.4) is usually the strongest stability constraint.

The following assumptions are implicit in deducing eqs (16.3)–(16.6):

(a) Lattices undergo homogeneous deformations. According to Born and Huang [128] this means that only long-wavelength vibrational modes are important.

(b) Elastic strain energy density is expanded only to second-order terms in deformation parameters.

Equations (16.3)–(16.6) also imply inequalities for the wave velocities, which are related to the c_{ij} by the Christoffel equations (see eq (18.3)).

By assuming a Mie-Grüneisen form of interatomic potential

$$\varphi(r)=-\frac{a}{r^m}+\frac{b}{r^n}, \qquad (16.7)$$

where $n>m$ for a minimum energy to exist, and $m>3$ for cohesive energy to be finite, Born [127] proved that

(a) simple cubic lattices are never stable;

(b) face centered lattices are always stable;

(c) body-centered lattices are unstable except for small exponents m and n in the force law.

For an interatomic potential given by eq (16.7), the concept of mechanical instability applies only to b.c.c. lattices. Zener [129] extended the concept of mechanical instability to include ideas on shear anisotropy and vibrational entropy. While Zener's ideas were proposed originally to explain instability of higher-temperature b.c.c. phases on cooling, they can be applied to any phase instability on cooling or heating. (For example, as shown by Fisher and Renken [130], the hexagonal-to-b.c.c. transitions in Ti, Zr, and Hf seem to show an unusual temperature dependence of vibrational entropy near the transformation temperatures.) Despite success claimed for Zener's criteria, they are not universal. Many phase transformations occur without shear constants becoming small or elastic anisotropies becoming large. Conversely, some systems with small shear constants and/or high elastic anisotropies exhibit no phase transitions.

Thus, while Zener's criteria are useful for testing for possible occurrences of phase transitions, they are neither necessary nor sufficient. (As discussed above, the *limit* of vanishing $c_{11}-c_{12}$ *is* sufficient reason for a phase transition to occur.)

Iron-nickel alloys in the region of 28 to 35 Ni all undergo diffusionless-shear (martensitic) transformations. In all cases as the transformation temperatures are approached, C' decreases while C is relatively unchanged. Thus, the elastic anisotropy increases with decreasing temperatures above the transformation temperature. Furthermore, data in table 7 show that the elastic anistropy of f.c.c. Fe-Ni alloys is maximum at about 35 Ni, which corresponds roughly to the $\alpha-\gamma$ realization phase boundary shown in figure 3.

Recently, for Fe-Ni and Fe-Ni-C alloys, Diesburg [131] correlated the temperature coefficients of the c_{ij} with the morphologies of the martensite phase. Since, as discussed in section 13, the dc_{ij}/dT are related to higher-order elastic coefficients, the desirability is indicated of measuring higher-order elastic coefficients to elucidate the problem of phase instabilities. Higher-order stability conditions corresponding to eqs (16.3)–(16.6) have apparently never been published.

17. Theoretical Calculation of Elastic Constants

Theory of elastic properties of solids is part of the theory of cohesion; see Jaswon [132] and Seitz [133]. Besides elastic properties, cohesion theories usually predict also: lattice parameters or specific volumes, cohesive energies, pressure-volume relationships, and, at their most ambitious, energy differences between allotropic forms. Thus, elastic properties relate fundamentally to solid-state theory and therefore also to other parameters associated with theory. (See also section 18.)

Transition metals, which have incomplete d shells and which include both iron and nickel, pose particularly difficult problems for most theories of cohesion. It is known that even filled d shells, such as in noble metals, can contribute significantly to cohesion. When d shells are incomplete the contribution is even larger since incomplete shells contribute to bonding in solids because the average energy of the solid's energy band differs substantially from the atomic energy level. In simplest models, filled energy bands contribute nothing to cohesion.

17.1. Fundamental Models

Elastic stiffnesses of monovalent metals have been calculated successfully by methods of Fuchs [76] and Fröhlich [134]. The former gives shear constants $(c_{11}-c_{12})/2$ and c_{44} while the latter gives the bulk modulus $(c_{11}+2c_{12})/3$. Fuchs considered three principal contributions to shear constants: (1) electrostatic energy of positive ions in a negative, charge-compensating electron gas, (2) exchange energy due to ion-core overlap and repulsion, and (3) Fermi or kinetic energy of the valence electrons. A minor contribution also considered by Fuchs was the van der Waals or dipole-dipole energy.

Recently, so-called pseudopotential methods have proven quite useful for calculating several properties of "simple" metals [135]. These methods replace, for computational purposes, the rapidly and strongly oscillating potential near the ion-core with a smooth, slowly-varying effective potential. With respect to elastic constants, this method has been fairly successful for simple metals. But, to date, no pseudopotential calculation of elastic constants has been made for transition metals (incomplete *d* shells). It would be very valuable to extend pseudopotential theory to this case, which includes both iron and nickel.

Johnson [136] constructed an interatomic potential for iron based on experimentally observed elastic constants. That is, in effect, the reverse problem; but it is useful to consider the results because they decompose the elastic constants into various contributing energies. The Fermi energy contribution was neglected and only electrostatic and ionic terms were considered. By computing the electrostatic contribution it was deduced by difference that the ionic term makes the dominant contribution to iron's elastic constants. This reflects the large ion-core size of iron compared to its interatomic spacing.

To determine the applicability of a Morse potential to studies of atomic properties of crystals, Girifalco and Weizer [137] calculated second-order elastic coefficients for several cubic metals including iron and nickel. Morse's potential for a pair of atoms is

$$\varphi(r_{ij}) = D[e^{-2\alpha(r_{ij}-r_0)} - 2e^{-\alpha(r_{ij}-r_0)}] \qquad (17.1)$$

where r_{ij} = center-to-center spacing of ion pair, r_0 = equilibrium separation of two ions. $\varphi(r_0) = -D$ = dissociation energy, and α is an adjustable "hardness" parameter evaluated from the compressibility.

These results are in only fair agreement with observation considering how the three Morse parameters were evaluated. $B = (c_{11} + 2c_{12})/3$ was input, and an elaborate (1000 neighboring atoms) lattice sum was performed. And, of course, the fundamental defect of a Morse, or similar, interatomic potential is that it permits only central pair-wise interactions, neglecting non-central and many-body forces. Central forces demand in the cubic case that $c_{12} = c_{44}$, and this condition is rarely observed experimentally. Lincoln, Koliwad and Ghate [138] used a Morse potential to calculate third-order elastic constants of several cubic metals and some of their results disagree strongly with experiment. Iron and nickel were not included in their calculations. Third-order elastic stiffnesses as well as the pressure coefficients of the second-order elastic stiffnesses were recently calculated by Mathur and Sharma [139] using a Morse potential; their results are given in tables 20 and 21. All of these results should be considered cautiously since Milstein [140] recently criticized application of Morse potentials to b.c.c. crystals since such potentials cannot predict values of c_{ij} in the b.c.c. case that are within stability limits imposed by Born's criteria (see section 16). Use of a Morse potential for f.c.c. metals was recently criticized on experimental grounds [141].

Ducastelle [142] studied theoretically the elastic coefficients of transition metals assuming the total energy to consist of a *d* band contribution (using a tight binding approximation) and a Born-Mayer repulsion term. His model accounted for the variation in c_{ij} along a transition series for f.c.c. and h.c.p. crystal structures. Failure to account for the b.c.c. case was attributed to *d* band details not included in his model. For both Fe and Ni, his calculated c_{ij} agreed surprisingly well with observation.

Lieberman [143] recently carried out a self-consistent-field band calculation for zero temperature and pressure with a potential incorporating both exchange and correlation contributions. For iron a good result was obtained for the bulk modulus.

Rosenstock and Blanken [144] considered interatomic forces in several cubic solids, including nickel, on the basis of experimentally observed dispersion of lattice vibrations.

Zwikker [145] showed for metals that the bulk modulus is given by

$$B = \frac{mn}{9} \cdot \frac{I}{V} \qquad (17.2)$$

where I = ionization energy, V = volume, and m, n = exponential factors in the Mie-Grüneisen potential energy, eq (16.7). Values of m and n were tabulated by Fürth. However, application of a Mie-Grüneisen potential to metals is quite approximate since it does not contain non-central forces.

17.2. Hard-Sphere Model

Much metallurgy and crystal physics can be understood, albeit crudely, by considering a hard-sphere model of solids. In this model, atoms are represented as incompressible spheres in contact along close-packed lattice directions, $\langle 111\rangle_{\text{b.c.c.}}$ and $\langle 110\rangle_{\text{f.c.c.}}$. This model assumes implicitly that only ion-ion repulsion energies contribute to elastic constants. This approximation is reasonably good for both noble metals and transition metals. Table 23 gives *relative* elastic constants for both b.c.c. and f.c.c. crystals based on a hard-sphere model; B was set arbitrarily to unity. Considering the model's crudeness, predicted relative quantities correlate surprisingly well with observation in many aspects. For example:

(1) $c_{11} \gtrsim c_{12} \gtrsim c_{44}$,

(2) $B \sim E$,

(3) $G \sim 3/8E$,

(4) high A for b.c.c. case, and

(5) low $\{110\}\langle\bar{1}10\rangle$ shear resistance for b.c.c. case.

Additional aspects of hard-sphere models were discussed by Mott [146].

18. Relationship of Elastic Constants to Other Physical Parameters

The purpose here is to indicate briefly how elastic properties of crystals relate to a wide variety of solid-state phenomena, many of which might appear to be independent of elasticity. While some of the relationships described here are empirical and not understood altogether, they have proven useful in interpreting behavior of solids.

Elastic properties of solids are related intimately to atomic vibrational, or phonon, spectra. Vibrational spectra link elastic properties with most other phenomena that are discussed here.

Frequency distributions of atomic vibrations in crystals have intrigued scientists since Debye's parabolic approximation to the problem was proposed in 1912. Despite intense efforts, theorists have failed to either devise an exact mathematical solution for frequency spectra or to explain why Debye's crude model is effective; obviously, for many purposes the exact shape of frequency distributions is relatively unimportant. Thus, many lattice vibrational problems in many branches of solid-state physics are discussed meaningfully in terms of Debye's theta.

While the main purpose of this section is to relate elastic properties to other solid-state phenomena, this can be done most conveniently by invoking Debye's θ. Thus, for present purposes θ should be considered an elastic stiffness parameter.

The Debye thetas calculated by several authors from their elastic data are given in table 24.

Sound Velocities

Sound waves in solids differ from sound waves in gases or liquids in two vital ways. First, solids transmit transverse or shear waves as well as longitudinal or dilatational waves. Secondly, sound waves in solids are polarized, and in the anisotropic case polarization vectors are not simply related (orthogonal) to the propagation vector.

Debye's θ is linearly related to a mean sound velocity v_m, that is

$$\theta = K v_m, \tag{18.1}$$

where $K = (h/k)(3/4\pi v_a)^{1/3}$, where h = Planck's constant, k = Boltzmann's constant, and v_a = atomic volume.

For single crystals, v_m is obtained from elastic constants by the integration over all space

$$3v_m^{-3} = \int \sum_{\alpha=1,2,3} v_\alpha^{-3}\, d\Omega/4\pi, \tag{18.2}$$

where v_1 = quasi-longitudinal wave velocity, v_2 and v_3 = quasi-transverse wave velocities, $d\Omega$ = increment of solid angle, and 4π = normalization factor. Velocities v_α are roots of Christoffel's equations

$$\det\,(c_{ijkl}x_jx_k - \rho v^2 \delta_{il}) = 0, \tag{18.3}$$

which follow from the equations of motion of plane, monochromatic waves where ρ = mass density, c_{ijkl} = fourth-rank elastic stiffness tensor, x_i = components of unit wave vector relative to cubic axes, and δ_{il} = Kronecker delta.

For polycrystals these equations simplify to

$$\rho v_l^2 = B + 4G/3, \tag{18.4}$$

and

$$\rho v_t^2 = G, \tag{18.5}$$

where v_l = longitudinal wave velocity and v_t = transverse wave velocity. The mean velocity is obtained by averaging over v^{-3}, that is

$$3v_m^{-3} = v_l^{-3} + 2v_t^{-3}. \tag{18.6}$$

As shown in table 1, v_l and v_t can be computed from any two polycrystalline elastic constants together with the mass density.

Some authors prefer to regard v_l as the velocity of sound in solids while others prefer v_m; either concept is valid in context.

For further discussion of these relationships the reader should consult Blackman [147], for example.

Sound velocities for Fe, Ni, and Fe-Ni alloys have been computed from elastic coefficients by Anderson [148] and by Simmons and Wang [149].

Specific Heats

Historically, lattice specific heats have been most frequently used to determine the Debye temperature θ_s. Debye [150] showed that

$$C_v = 9Nk\left(\frac{T}{\theta_s}\right)^3 \int_0^{\theta_s/T} \frac{z^4 e^z dz}{(e^z-1)^2}, \tag{18.7}$$

where C_v = specific heat at constant volume, N = Avogadro's number, k = Boltzmann's constant, T = absolute temperature. Electronic contributions to C_v, which are linear in T, must be separated from measured values of C_v. Measurements of θ by specific heats have been summarized by DeSorbo [151] and by Holm [152]. The relationship between θ_s and θ_{elastic} was discussed by Alers and Neighbors [153] and by Alers [154]. From existing data, errors in θ_e are smaller than those in θ_s.

Many authors [155]–[157] have discussed the equivalence of θ_s and θ_{elastic} at $T = 0$.

Entropies

Vibrational entropies S can be calculated from Boltzmann's relationship

$$S = k \ln w, \tag{18.8}$$

where w = randomness. For a system of three-dimensional oscillators Lumsden [158] showed for a Debye frequency spectrum that

$$S=Nk\left[4-3\ln\frac{\theta}{T}+\frac{3}{40}\left(\frac{\theta}{T}\right)^2-\frac{3}{2240}\left(\frac{\theta}{T}\right)^4+\ldots\right]. \tag{18.9}$$

Again, S calculated by eq (18.9) contains only vibrational terms; electronic and other non-vibrational terms must be determined separately.

All other usual thermodynamic quantities can be calculated from θ by invoking the thermodynamic partition function, as discussed by Fowler and Guggenheim [159], for example.

Zero Point Energy

Behavior of many substances at low temperatures is influenced by zero point energy, which arises as a quantum effect; the energy of a linear oscillator in its ground state of energy at $T=0$ K is $h\nu/2$ where ν is the vibrational frequency of the oscillator. Integration over a Debye spectrum gives for zero point energy

$$E_0=\frac{9}{8}Nh\nu_{\max}=\frac{9}{8}R\theta \tag{18.10}$$

since $h\nu_{\max}=k\theta$. Details concerning eq (18.10) were given by Domb and Salter [160].

Thermal Conductivity

While thermal conductivity occurs by many mechanisms and the theories of these are difficult and disputed, θ is a pervasive parameter for describing these mechanisms. For example, Klemens [161] discussed a relationship due to Leibfried and Schloemann for lattice thermal conductivity of non-metals at high temperatures, $T > \theta$:

$$K \approx \text{constant}\ \frac{\theta^3}{\gamma^2 T}, \tag{18.11}$$

where γ = Grüneisen parameter. A similar expression was derived on a different basis by Dugdale and MacDonald [162]. While γ^2 is relatively constant from one material to another, θ^3 changes considerably. By comparing theoretical and observed values of KT at room temperatures, Klemens established the approximate validity of the θ^3 dependence of K.

Electrical Resistivity

The most convenient point of departure here is Bloch and Grüneisen's relationship that describes for many metals the temperature variation of their electrical resistivity ρ over a wide temperature range:

$$\rho(T)=\frac{C}{A}\,\frac{T^5}{\theta_r^6}\int_0^{\theta_r/T}\frac{z\,dz}{(e^z-1)(1-e^{-z})}, \tag{18.12}$$

where C = constant, A = atomic weight, and θ_r = characteristic temperature for lattice resistivity.

Since in Bloch's theory only longitudinal lattice vibrations affect ρ, no agreement between θ_r and θ would be expected; in Debye's theory there are two transverse vibrational modes for each longitudinal mode. Since $\theta_l > \theta_t$, it would be expected that $\theta_r > \theta$. However, Grüneisen showed that $\theta_r \approx \theta$ for a large number of cases. Blackman [163] considered the problem by calculating θ_l both by averaging wave velocities as v^{-3}, as is conventional, and as v^{-5}, as is suggested by eq (18.12); no correlations between these thetas and θ_r were found. A recent experimental study by Cullen [164] for Cu-Au alloys showed that θ_l (from elastic coefficients) exceeds θ_r but that θ_l and θ_r have the same compositional dependence, which differs from that of θ. This implies that transverse phonons contribute to θ_r in a way not now known.

The general problem of θ_r was discussed at length by Kelly and MacDonald [165] and by Meaden [166] who gave a compilation of θ_r values.

Bragg Intensities

As shown early in this century by Debye and by Waller, change in intensities of Bragg scattering of x-rays by crystals with increasing temperature due to change of the atomic structure factor is given by

$$I(T)=Ie^{-2M}. \tag{18.13}$$

The Debye-Waller factor $2M$ is simply related to Debye's theta:

$$2M=\frac{12h^2}{mk\theta_M}\,\frac{\sin^2\phi}{\lambda^2}\left(\frac{D(x)}{x}+\frac{1}{4}\right), \tag{18.14}$$

where h = Planck's constant, k = Boltzmann's constant, m = mass of atom, ϕ = Bragg angle, λ = x-ray wavelength, and $D(x)$ = Debye function where $x=\theta/T$, T being absolute temperature. The factor 1/4 allows for zero point energy.

As shown by Zener and Bilinsky [167] θ_M in eq (18.14) is obtained by the average

$$3\theta_M^{-2}=\theta_l^{-2}+2\theta_t^{-2}, \tag{18.15}$$

rather than the usual average

$$3\theta^{-3}=\theta_l^{-3}+2\theta_t^{-3}. \tag{18.16}$$

Thus, θ_M is always slightly larger than θ by a few percent.

This topic was discussed extensively by Lonsdale [168], by James [169], and by Herbstein [170].

For both Fe and Ni, Singh and Sharma [171] recently reported Debye-Waller factors computed from elastic stiffnesses.

Vibration Amplitudes

This subject relates closely to the preceding section in that the Debye-Waller factor can be expressed as

$$2M = \frac{16\pi^2 \sin^2 \phi}{3\lambda^2} \langle u^2 \rangle, \tag{18.17}$$

where $\langle u^2 \rangle$ = mean square atomic vibrational amplitude parallel to diffracting plane. Thus, one has

$$\langle u^2 \rangle = \frac{3h^2 T}{\pi^2 m k \theta_M^2} \left(D(x) + \frac{x}{4} \right). \tag{18.18}$$

Lonsdale [168] tabulated $\langle u^2 \rangle$ values for many elements. She emphasized that vibration amplitudes are anisotropic even for cubic symmetry and that vibrational anisotropy can be calculated from elastic coefficients.

For Fe-Ni alloys, $\langle u^2 \rangle$ were computed from E and G by Tanji and Shirakawa [172] and by Tanji [173] to interpret thermal expansion, electrical resistivity, and abnormal volume expansion of *Invar* alloys. For Fe and Ni, $\langle u^2 \rangle$ were recently computed from elastic stiffnesses by Singh and Sharma [171].

Melting

As discussed in section 16, if a material is heated and elastic constants change with temperature such that any of Born's stability criteria are violated, then a phase change must occur—either to another solid phase or to a liquid. Of course, phase changes can occur for other reasons—generally a lowering of free energy. Lindemann [174] believed that melting occurred when atomic vibration amplitudes reached critical magnitudes. This topic was developed extensively by Pines [175] who showed that

$$\theta \approx C \left(\frac{kT_m}{AV_0^{2/3}} \right)^{1/2}, \tag{18.19}$$

where C = constant, A = atomic weight, k = Boltzmann's constant, T_m = absolute melting temperature, and V_0 = atomic volume. Pines concluded that melting occurs when the root-mean-square atomic displacement becomes roughly $r_0/8$ where $2r_0$ = interatomic spacing.

Thermal Expansivity

As is well known, thermal expansion is an anharmonic effect inconsistent with Debye's model of solids. However, Grüneisen showed for most temperatures that volume expansivity β is proportional to specific heat C_p, and at low temperatures

$$\gamma = \frac{\beta B}{\rho C_v}, \tag{18.20}$$

where C_v = specific heat at constant volume, ρ = mass density, B = bulk modulus, and γ = Grüneisen constant with a value of about 2 for all solids. Clearly then at low temperatures

$$\theta^3 \approx K \frac{\gamma \rho}{\beta B}, \tag{18.21}$$

where K = constant. This equation is also important because it allows computation of θ from a single elastic constant plus thermal data. Manipulation of thermodynamic equalities yields many alternative expressions for θ, related generally to Grüneisen's equation of state

$$\gamma = \frac{V}{C_v} \left(\frac{\partial P}{\partial T} \right)_V = - \frac{V \left(\frac{\partial V}{\partial T} \right)_P}{C_p \left(\frac{\partial V}{\partial P} \right)_S} = - \frac{V \left(\frac{\partial V}{\partial T} \right)_P}{C_v \left(\frac{\partial V}{\partial P} \right)_T}. \tag{18.22}$$

Atomic Diffusivity

Diffusion coefficients for metallic self-diffusion or for substitutional diffusion of different metals are well known to be given by Arrheniuss's empirical relationship

$$D = A \exp\,(-\Delta H/RT), \tag{18.23}$$

where A and ΔH are temperature-independent constants, R = universal gas constant, and T = temperature.

Assuming a vacancy mechanism for diffusion, then

$$\Delta H = \Delta H_f + \Delta H_m, \tag{18.24}$$

where ΔH_f = formation energy of a vacancy and ΔH_m = motion energy of a vacancy. Realizing from thermodynamics that

$$\Delta G = \Delta H - T\Delta S, \tag{18.25}$$

where G = Gibbs free energy and S = entropy, then elastic constants are related to diffusion coefficients through a model given by Zener [176] and independently by LeClaire [177], which shows that

$$\Delta G_m \approx KE, \tag{18.26}$$

where E = Young's modulus appropriate to ΔH_m, and K has units of volume. Substitution into eq (18.23) gives after rearrangement

$$\ln D + KE/RT = \ln D_0 - \Delta G_f/RT, \tag{18.27}$$

where

$$\ln D_0 = \ln A - \Delta S_f/R - \Delta S_m/R.$$

Since in single crystals E varies with direction, its choice is not unique. Reasonable choices are E_{111} for b.c.c. lattices and E_{110} for f.c.c. lattices. Along with its directionality, the temperature dependence of E_{ijk} must also be considered.

Mechanical Plasticity

Some empirical and semi-empirical relationships between elastic and plastic properties of solids were suggested by Pugh [178]. While this topic is now only embryonic, it is discussed briefly here because it has high potential importance but has received little emphasis in the scientific literature.

That elastic-plastic relationships should exist is expected from microplastic theories where most all dislocation equations contain explicitly various elastic constants.

Advantages of such relationships include: (1) relating plasticity more intimately to interatomic forces; (2) possibility of correlating plastic properties with other parameters via elastic properties, for example with atomic number, melting temperatures, or Debye thetas; and (3) a higher degree of correlation among plastic properties themselves.

Some relationships suggested by Pugh include: (1) for $T < T_m/3$ resistance to plastic deformation is proportional to Gb, where G = shear modulus and b = magnitude of Burgers vector; (2) fracture strength is proportional to Ba, where B = bulk modulus and a = lattice parameter; (3) range of plasticity is proportional to B/G, so that a high value of B/G indicates malleability and a low value indicates brittleness.

Besides Pugh, interested readers should see also Crutchley and Reid [179].

Diatomic Molecular Vibration Frequencies

Relationships between interatomic force constants determined from ultrasonic wave velocities in solids and force constants determined spectroscopically from gas molecules might appear at first to be vague and complicated. However, rough empirical relationships between θ_{solid} and θ_{gas} were demonstrated by Baughan [180]; and Waser and Pauling [181] demonstrated the relevance of Badger's rule to solids. Badger [182] discovered for diatomic gases that $k \sim d^{-3}$ where k = force constant and d = interatomic distance. Recent work by Haussuhl [183] and by Gilman [184] suggests that $k \sim d^{-4}$ is a better correlation for most solids, a dependence first predicted theoretically by Fuchs [76].

These studies suggest strong correspondences between vibrational properties of atoms in solid and gaseous forms. Since better and more complete experimental data now exist, both elastic and spectroscopic, a re-examination of the problem would be appropriate to determine its synergistic aspects. Both iron and nickel were included in the studies of Baughan, and Waser and Pauling.

Other Properties

Elastic Debye temperatures correlate with many other solid-state phenomena that are not discussed here, for example—theoretical strength, Mössbauer emission, superconducting transition temperatures, infra-red reststrahlen, diffuse x-ray scattering, and neutron scattering. For discussion of some of these phenomena with respect to θ and/or elastic constants the reader should see Partington [185], Cartz [186], Neshpor [187], and Herbstein [170] as examples.

19. Concluding Remarks

As evidenced by over 200 references to the experimental literature, elastic properties of iron, nickel, and iron-nickel alloys have been much studied with the result that most are now well characterized.

Despite this intensity of effort, a few of the elastic properties have been studied experimentally only cursorily, and the general subject would be strengthened by further studies. These properties include: (1) temperature dependence of the bulk modulus of nickel, (2) pressure dependence of properties other than single-crystal coefficients or the bulk modulus, and (3) explicit dependence of properties on magnetic field.

Other properties have not yet been studied experimentally; these include: (1) pressure derivatives of alloys, (2) third-order elastic stiffnesses of alloys, and (3) fourth-order elastic stiffnesses of both iron and nickel.

From existing single-crystal data it would be useful to derive averaged elastic constants and sound velocities.

Ripe problems for theoretical study include: (1) relationship of elastic constants to phase transitions, particularly martensitic transitions, (2) effects of ferromagnetism on elastic properties, (3) contributions of d electrons to bonding and to elasticity, (4) thermal dependence of elastic properties, and (5) the existence and role of atomic ordering on elasticity.

Since iron-nickel alloys are of much interest both scientifically and technologically, one might expect many of these areas to be studied intensively within the next few years.

Dr. G. Speich of the U.S. Steel Corp., and Drs. G. Hausch and H. Warlimont of the Max-Planck Institut für Metallforschung graciously supplied preprint versions of their work.

Dr. E. R. Naimon of NBS contributed greatly to the final stages of constructing the manuscript.

This work was supported in part by the NBS Office of Standard Reference Data. Dr. R. S. Marvin of OSRD made many valuable comments on the manuscript.

20. References for Text

[1] Chickazumi, S., Physics of Magnetism (Wiley, New York, 1964).

[2] Rosenberg, S. J., Nickel and Its Alloys, Nat. Bur. Stand. (U.S.), Monogr. 106, 156 pages (May 1968).

[3] Everhart, J. L., Engineering Properties of Nickel and Nickel Alloys (Plenum, New York, 1971).

[4] Lanczos, C., The Variational Properties of Mechanics (Univ. of Toronto Press, Toronto, 1970) p. 376.

[5] Zener, C., Elasticity and Anelasticity of Metals (Univ. of Chicago Press, Chicago, Illinois, 1948).

[6] Chung, D. H., and Buessem, W. R., The elastic anisotropy of crystals, J. Appl. Phys. **38**, 2010 (1967).

[7] Barrett, C. S., A low temperature transformation in lithium, Phys. Rev. **72**, 245 (1947).

[8] Ledbetter, H. M., Estimation of Debye temperatures by averaging elastic coefficients, J. Appl. Phys. **44**, 1451 (1973).

[9] Voigt, W., Ueber die Beziehung zwischen den beiden Elasticität sconstanten isotroper Körper, Ann. Physik (Leipzig) **38**, 573 (1889).

[10] Reuss, A., Berechnung der Fliessgrenze von Mischkristallen auf Grund der Plastizitätsbedingung für Einkristalle, Z. Angew. Math. Phys. **9**, 49 (1929).

[11] Hill, R., The elastic behavior of a crystalline aggregate, Proc. Phys. Soc. London **A65**, 349 (1952).

[12] Landau, L. D., and Lifshitz, E. M., Theory of Elasticity (Pergamon, London, 1959) p. 40.

[13] Read, T. A., Wert, C. A., and Metzger M., in Methods of Experimental Physics, vol. 6A, K. Lark-Horovitz and V. A. Johnson (eds.), (Academic, New York, 1959).

[14] Fuller, E. R., Jr., Granato, A. V., Holder, J., and Naimon, E. R., Ultrasonic studies of the properties of solids, in Methods of Experimental Physics, R. V. Coleman (ed.), (Academic, New York), forthcoming.

[15] Truell, R., Elbaum, C., and Chick, B. B., Ultrasonic Methods in Solid State Physics (Academic, New York, 1969).

[16] Beyer, R. T., and Letcher, S. V., Physical Ultrasonics (Academic, New York, 1969).

[17] Mason, W. P., Physical Acoustics and the Properties of Solids (Van Nostrand, New York, 1958).

[18] Truell, R., and Elbaum, C., High frequency ultrasonic stress waves in solids, in Handbuch der Physik, vol. XII, S. Flügge (ed.), (Springer-Verlag, Berlin, 1962).

[19] Dignum, R., Brief review of ultrasonic attenuation with some emphasis on work at ultrahigh frequency. Amer. J. Phys. **32**, 507 (1964).

[20] Huntington, H. B., The elastic constants of crystals, in Solid State Physics, vol. 7, F. Seitz and D. Turnbull (eds.), (Academic, New York, 1958).

[21] Armstrong, P. E., Measurements of elastic constants, in Techniques of Metals Research—Volume V—Measurement of Mechanical Properties Part 2, R. F. Bunshah (ed.), (Interscience, New York, 1971).

[22] Alers, G. A., The measurement of very small sound velocity changes and their use in the study of solids, in Physical Acoustics, vol. IV-A, W. P. Mason (ed.), (Academic, New York, 1966).

[23] Speich, G. R., Schwoeble, A. J., and Leslie, W. C., Elastic constants of binary Fe-base alloys, Met. Trans. **3**, 2031 (1972).

[24] Dey, B. N., Gilman, J. J., and Nehrenberg, A. E., The elastic stiffnesses of Fe-Ni-C martensites, Phil. Mag. **24**, 1257 (1971).

[25] Speich, G. R., and Leslie, W. C., Elastic constants of martensite, Met. Trans. **4**, 1873 (1973).

[26] Holder, J., Improvements on pulse superposition velocity measurements, Rev. Sci. Instrum. **41**, 1355 (1970).

[27] McSkimin, H. J., Pulse superposition method for measuring ultrasonic wave velocities in solids, J. Acoust. Soc. Amer. **33**, 12 (1961).

[28] Waterman, P. C., Orientation dependence of elastic waves in single crystals, Phys. Rev. **113**, 1240 (1959).

[29] Hearmon, R. F. S., An Introduction to Applied Anisotropic Elasticity (Oxford U. P., London, 1961) p. 15.

[30] Mason, W. P., Piezoelectric Crystals and their Application to Ultrasonics (Van Nostrand, Princeton, N.J., 1950) p. 29.

[31] Reference [12], p. 17.

[32] Bhatia, A. B., Ultrasonic Absorption (Oxford U. P., London, 1967) p. 40.

[33] Mack, D. J., Young's modulus—its metallurgical aspects, Trans. AIME **166**, 68 (1946).

[34] Dorn, J. E., and Tietz, T. E., The modulus of elasticity—a review of metallurgical factors, Metal Progr. **58**, 81 (1950).

[35] Vereschagin, L. F., and Lichter, A. I., Dependence of the compressibility of elements on the atomic number, Dokl. Akad. Nauk SSSR **86**, 745 (1952). English translation available in NTIS report AD 290677.

[36] Ryabinin, Yu. N., Influence of pressure on periodic properties of elements, Dokl. Akad. Nauk SSSR **104**, 721 (1955). English translation available in NTIS report AD 290676.

[37] Köster, W., and Franz, H., Poisson's ratio for metals and alloys, Met. Rev. **6**, 1 (1961).

[38] Gschneider, K., Physical properties and interrelationships of metallic and semimetallic elements, in Solid State Physics, vol. 16, F. Seitz and D. Turnbull (eds.), (Academic, New York, 1964).

[39] Osmond, F., and Cartaud, G., Rev. Met. (Paris) **1**, 69 (1904). Reported in reference [55].

[40] Hansen, M., and Anderko, K., Constitution of Binary Alloys (McGraw-Hill, New York, 1958).

[41] Elliott, R. P., Constitution of Binary Alloys, First Supplement (McGraw-Hill, New York, 1965) p. 442.

[42] Shunk, F. A., Constitution of Binary Alloys, Second Supplement (McGraw-Hill, New York, 1969) p. 335.

[43] Hume-Rothery, W. and Raynor, G. V., The Structure of Metals and Alloys (Inst. of Metals, London, 1956).

[44] Seitz, F., The Modern Theory of Solids (McGraw-Hill, New York, 1940) p. 487.

[45] Gilbert, A., and Owen, W. S., Diffusionless transformation in iron-nickel, iron-chromium and iron-silicon alloys, Acta Met. **10**, 45 (1962).

[46] Wayman, C. M., and Altstetter, C. J., Martensite in zone-refined iron, Acta Met. **10**, 992 (1962).

[47] Connolly, T. F., and Copenhaver, E. D., Bibliography of magnetic materials and tabulation of magnetic transition temperatures, ORNL Report RMIC-7, Rev. 2 (1970).

[48] Davies, R. G., and Magee, C. L., Austenite ferromagnetism and martensite morphology, Met. Trans. **1**, 2927 (1970).

[49] Reference [42], p. 336.

[50] Goldstein, J. I., and Ogilvie, R. E., A re-evaluation of the iron-rich portion of the Fe-Ni system, Trans. Met. Soc. AIME **233**, 2083 (1965).

[51] Kaufman, L., and Ringwood, A. E., High pressure equilibria in the iron-nickel system and the structure of metallic meteorites, Acta Met. **9**, 941 (1961).

[52] Reed, R. P., and Schramm, R. E., Lattice parameters of martensite and austenite in Fe-Ni alloys, J. Appl. Phys. **40**, 3453 (1969).

[53] Zener, C., Relation between residual strain energy and elastic moduli, Acta Crystallogr. **2**, 163 (1949).

[54] Hearmon, R. F. S., The elastic constants of non-piezoelectric crystals, in Landolt-Börnstein New Series; Vol. 1; Elastic, Piezoelectric, Piezooptic and Electrooptic Constants of Crystals; K.-H. Hellwege and A. M. Hellwege (eds.), (Springer-Verlag, Berlin, 1966).

[55] Hopkin, L. M. T., Pursey, H., and Markham, M. F., Precise measurements of the elastic constants of copper and silver base alloys, Z. Metallk. **61**, 535 (1970).

[56] Cain, L. S., and Thomas, J. F., Jr., Elastic constants of α-phase Cu-Al alloys, Phys. Rev. **B4**, 4245 (1971).

[57] Moment, R., Elastic stiffnesses of copper-tin and copper-aluminum alloy single crystals, J. Appl. Phys. **43**, 4419 (1972).

[58] Eros, S., and Smith, C. S., Low-temperature elastic constants of magnesium alloys, Acta Met. **9**, 14 (1961).

[59] Leamy, H. J., Gibson, E. D., and Kayser, F. X., The elastic stiffness coefficients of iron-aluminum alloys—I—experimental results and thermodynamic analysis, Acta Met. **15**, 1827 (1967).

[60] Leamy, H. J., and Warlimont, H., The elastic behaviour of Ni-Co alloys, Phys. Status Solidi **37**, 523 (1970).

[61] Sakuri, J., Mitsuhiro, F., Nakamura, Y., and Takaki, H., Elastic

constants of Ni-Fe and Ni-Cu alloys, J. Phys. Soc. Jap. **19**, 308 (1964).

[62] Walker, E., Ortelli, J., and Peter, M., Elastic constants of monocrystalline alloys of Pd-Rh and Pd-Ag between 4.2 °K and 300 °K, Phys. Lett. **31A**, 240 (1970).

[63] Köster, W., On the influence of B-metals on the elastic modulus of copper, silver, and gold, Trans. Jap. Inst. Metals **12**, 139 (1971).

[64] Friedel, J., Deviations from Vegard's law, Phil. Mag. **46**, 514 (1955).

[65] Mott, N. F., The cohesive forces in metals and alloys, Rep. Progr. Phys. **25**, 218 (1962).

[66] Friedel, J., Nuovo Cim. (Suppl.) Ispra Conf. on Radiation Damage, reported in ref. [65].

[67] Oriani, R. A., Thermodynamics of liquid Ag-Au and Au-Cu alloys and the question of strain energy in solid solutions, Acta Met. **4**, 15 (1956).

[68] Muñoz, R., On the elastic model for the deviations from Vegard's law, Phil. Mag. **14**, 1105 (1966).

[69] Zener, C., Theory of lattice expansion introduced by cold-work, Trans. AIME **147**, 361 (1942).

[70] Bradfield, G., and Pursey, H., The role of preferred orientation in elasticity investigations, Phil. Mag. **44**, 437 (1953).

[71] Pursey, H., and Cox, H. L., The correction of elasticity measurements on slightly anisotropic materials, Phil. Mag. **45**, 295 (1954).

[72] Seitz, F., and Koehler, J. S., Displacement of atoms during irradiation, in Solid State Physics, vol. 2, F. Seitz and D. Turnbull (eds.) (Academic, New York, 1956).

[73] Bruggeman, D. A. G., Ann. Phys. (Leipzig) **29**, 160 (1937).

[74] Mackenzie, J. K., The elastic constants of a solid containing spherical holes, Proc. Phys. Soc. London **B63**, 2 (1950).

[75] Dienes, G. J., A theoretical estimate of the effect of radiation on the elastic constants of simple metals, Phys. Rev. **86**, 228 (1952).

[76] Fuchs, K., A quantum mechanical calculation of the elastic constants of monovalent metals, Proc. Roy. Soc. London **A153**, 622 (1936).

[77] Schoknecht, W. E., and Simmons, R. O., Thermal vacancies and thermal expansion, in Thermal Expansion—1971 (Am. Inst. Physics, New York, 1972).

[78] Melngailis, G., A model for the change in elastic modulus of a solid caused by point defects, Phys. Status Solidi **16**, 247 (1966).

[79] Eshelby, J. D., Dislocations as a cause of mechanical damping in metals, Proc. Roy. Soc. London **A197**, 396 (1949).

[80] Koehler, J. S., and DeWit, G., Influence of elastic anisotropy on the dislocation contribution to the elastic constants, Phys. Rev. **116**, 1121 (1959).

[81] Granato, A. V., and Lücke, K., Theory of mechanical damping due to dislocations, J. Appl. Phys. **27**, 583 (1956).

[82] Koehler, J. S., The influence of dislocations and impurities on the damping and the elastic constants of metal single crystals, in Imperfections in Nearly Perfect Crystals (Wiley, New York, 1952).

[83] Hirth, J. D., and Lothe, J., Theory of Dislocations (McGraw-Hill, New York, 1968).

[84] Holder, J., Thermodynamic properties of crystals containing imperfections, thesis, Univ. of Illinois at Urbana-Champaign (1968).

[85] Birch, F., Finite elastic strain of cubic crystals, Phys. Rev. **71**, 809 (1947).

[86] Brugger, K., Thermodynamic definition of higher order elastic coefficients, Phys. Rev. **133**, A1611 (1964).

[87] Leibfried, C., and Ludwig, W., Theory of anharmonic effects in crystals, in Solid State Physics, vol. 12, F. Seitz and D. Turnbull (eds.), (Academic, New York, 1961).

[88] Brugger, K., Generalized Grüneisen parameters in the anisotropic Debye model, Phys. Rev. **137**, A1826 (1965).

[89] Grüneisen, E., Ann. Phys. (Leipzig) **26**, 393 (1908).

[90] Slater, J. C., Introduction to Chemical Physics (McGraw-Hill, New York, 1939).

[91] Fumi, F. G., Third-order elastic constants of crystals, Phys. Rev. **83**, 1274 (1951).

[92] Hearmon, R. F. S., 'Third-order' elastic coefficients, Acta Crystallogr. **6**, 331 (1953).

[93] Hiki, Y., and Granato, A. V., Anharmonicity in noble metals; higher order elastic constants, Phys, Rev. **144**, 411 (1966).

[94] Suzuki, T., Granato, A. V. and Thomas, J. F., Jr., Second- and third-order elastic constants of alkali metals, Phys, Rev. **175**, (1968).

[95] Suzuki, T., Second- and third-order elastic constants of aluminum and lead, Phys. Rev. **B3**, 4007 (1971).

[96] Naimon, E. R., Suzuki, T., and Granato, A. V., Third-order elastic constants of magnesium. II. Theoretical, Phys. Rev. **B4**, 4297 (1971).

[97] Cousins, C. S. G., The use of elastic shear constants to test the validity of model potential theories, J. Phys. C **2**, 765 (1969).

[98] Hamilton, R. A. H., and Parrott, J. E., The third-order elastic constants of quasi-isotropic materials, J. Phys. **C1**, 829 (1968).

[99] Barsch, G. R., Relation between third-order elastic constants of single crystals and polycrystals, J. Appl. Phys. **39**, 3780 (1968).

[100] Nrañyan, A. A., Third-order elastic constants of a polycrystalline aggregate consisting of cubic single crystals, Sov. Phys.-Crystallogr. **15**, 68 (1970).

[101] Cousins, C. S. G., A note on the estimation of the third-order elastic constants of quasi-isotropic materials, J. Phys. C **1**, 835 (1968).

[102] Chang, R., Relationships between the nonlinear elastic constants of monocrystalline and polycrystalline solids of cubic symmetry, Appl. Phys. Lett. **11**, 305 (1967).

[103] See, for example, Born, M., and Huang, K., Dynamical theory of Crystal Lattices (Oxford U. P., London, 1954).

[104] Ref. [5], p. 24 ff.

[105] Ref. [87], p. 277 ff.

[106] Ref. [90], eq (4.16) in chapter 13.

[107] Ref. [38], table 24.

[108] Madelung, E., Nachr. Kgl. Ges. Wiss. Goettingen (1909) and (1910); Z. Physik **11**, 898 (1910).

[109] Einstein, A., A relation between elastic constants and specific heat for solids with monatomic molecules, Ann. Phys. (Leipzig) **34**, 170 (1911). In German.

[110] Hiki, Y., Thomas, J. F., Jr., and Granato, A. V., Anharmonicity in noble metals: some thermal properties, Phys. Rev. **153**, 764 (1967).

[111] Swartz, K. D., Anharmonicity in NaCl and beta brass, thesis, Univ. of Illinois at Urbana-Champaign (1966).

[112] Swartz, K. D., Anharmonicity in sodium chloride, J. Acoust. Soc. Amer. **41**, 1083 (1967).

[113] Holder, J., and Granato, A. V., Thermodynamic properties of solids containing defects, Phys. Rev. **182**, 729 (1969).

[114] Huntington, H. B., The elastic constants of crystals, in Solid State Physics, vol. 7, F. Seitz and D. Turnbull (eds.), (Academic, New York, 1958).

[115] Varshni, Y. P., Temperature dependence of the elastic constants, Phys. Rev. **2**, 3952 (1970).

[116] Lakkad, S. C., Temperature dependence of the elastic constants, J. Appl. Phys. **42**, 4277 (1971).

[117] Sutherland, W., A kinetic theory of solids with an experimental introduction, Phil. Mag. **32**, 31 (1891).

[118] Siegel, S., and Cummerow, R., On the elasticity of crystals J. Chem. Phys. **8**, 847 (1940).

[119] Ref. [90] p. 240.

[120] Bridgman, P. W., The Physics of High Pressure (Bell, London, 1952).

[121] Murnaghan, F. D., Finite deformation of an elastic solid, Amer. J. Math. **59**, 235 (1937).

[122] Ghate, P. B., Effect of hydrostatic pressure on the elastic behavior of cubic crystals, Phys. Status Solidi **14**, 325 (1966).

[123] Honda, K., Shimizu, S., and Kusakabe, S., Change of the elastic modulus of ferromagnetic materials during magnetization, Phys. Z. **3**, 380 (1902). In German.

[124] Lee, E. W., Magnetostriction and magnetomechanical effects, Rep. Progr. Phys. **18**, 184 (1955).

[125] Kornetski, M., Connection between Young's modulus and damping of ferromagnetic materials, Wiss. Veroeff. Siemens-Werken **17**, 48 (1938).

[126] Bozorth, R. M., Ferromagnetism (Van Nostrand, Princeton, N. J., 1951) pp. 684–99.

[127] Born, M., On the stability of crystal lattices. I, Proc. Cambridge Phil. Soc. **36**, 160 (1940).

[128] Ref. [103], p. 140 ff.

[129] Ref. [5], p. 22.

[130] Fisher, E. S., and Renken, C. J., Single-crystal elastic moduli and the hcp → bcc transformation in Ti, Zr, and Hf, Phys. Rev. **135**, A482 (1964).

[131] Diesburg, D. E., Elastic constants of Fe-Ni-C alloys, thesis, Iowa State Univ. (1971).

[132] Jaswon, M. A., The Theory of Cohesion (Pergamon, London, 1954).

[133] Seitz, F., The Modern Theory of Solids (McGraw-Hill, New York, 1940).

[134] Frölich, H., A quantum mechanical discussion of the cohesive forces and thermal expansion coefficients of the alkali metals, Proc. Roy. Soc. London **A158**, 97 (1937).

[135] Harrison, W. A., Pseudopotentials in the Theory of Metals (Benjamin, New York, 1966).

[136] Johnson, R. A., Interstitials and vacancies in α iron, Phys. Rev. **134**, A1329 (1964).

[137] Girifalco, L. A., and Weizer, V. G., Application of the Morse potential function to cubic metals, Phys. Rev. **114**, 687 (1959).

[138] Lincoln, R. C., Koliwad, K. M. and Ghate, P. B., Morse-potential evaluation of second- and third-order elastic constants of some cubic metals, Phys. Rev. **157**, 463 (1967).

[139] Mathur, S. S., and Sharma, Y. D., Third-order elastic constants of body centered cubic crystals, Phys. Status Solidi **39**, K39 (1970).

[140] Milstein, F., Theoretical strength of a perfect crystal, Phys. Rev. **3**, 1130 (1971).

[141] Routbort, J. L., Reid, C. N., Fisher, E. S., and Dever, D. J., High-temperature elastic constants and the phase stability of silicon-iron, Acta Met. **19**, 1307 (1971).

[142] Ducastelle, F., Modules élastiques des métaux de transition, J. Phys. (Paris) **31**, 1055 (1970).

[143] Lieberman, D. A., New potential function for atomic and solid-state calculations, Phys. Rev. **2**, 244 (1970).

[144] Rosenstock, H. B. and Blanken, G., Interatomic forces in various solids, Phys. Rev. **145**, 546 (1966).

[145] Zwikker, C., Physical Properties of Solid Materials (Pergamon, London, 1954) p. 94.

[146] Mott, N. F., Recent advances in the electron theory of metals, in Progress in Metal Physics, vol. 3, B. Chalmers (ed.), (Pergamon, Oxford, 1952) p. 93.

[147] Blackman, M., The specific heat of solids, in Handbuch der Physik, vol. VII–1 (Springer-Verlag, Berlin, 1955).

[148] Anderson, O. L., Determination and some uses of isotropic elastic constants of polycrystalline aggregates using single-crystal data, in Physical Acoustics, vol. III–B, W. P. Mason (ed.), (Academic, New York, 1965).

[149] Simmons, G., and Wang, H., Single Crystal Elastic Constants and Calculated Aggregate Properties: A Handbook (M.I.T. Press, Cambridge, Mass., 1971).

[150] Debye, P., Theory of specific heats, Ann. Phys. (Leipzig) **39**, 789 (1912). In German.

[151] DeSorbo, W., The effect of lattice anisotropy on low-temperature specific heat, Acta Met. **2**, 274 (1954).

[152] Holm, M. W., Debye characteristic temperatures-table and bibliography, AEC Res. & Dev. Report, IDO-16399 (1957).

[152] Holm, M. W., Debye characteristic temperatures-table and determined from elastic constants and calorimetry, Rev. Mod. Phys. **31**, 675 (1959).

[154] Alers, G. A., Use of sound velocity measurements in determining the Debye temperature of solids, in Physical Acoustics, vol. III–B, W. P. Mason (ed.), (Academic, New York, 1965).

[155] Barron, T. H. K., and Klein, M. L., Thermal and elastic properties of crystals at low temperatures, Phys. Rev. **127**, 1997 (1962).

[156] Feldman, J. L., The relation between θ (elastic) and θ (calorimetric) near $T = 0$ °K, Proc. Phys. Soc. London **84**, 361 (1964).

[157] Overton, W. C., Jr., Experimental evidence for a difference between thermal and elastic Debye thetas of a crystal near 0 °K, Phys. Lett. **37A**, 287 (1971).

[158] Lumsden, J., Thermodynamics of Alloys (Inst. of Metals, London, 1952) p. 88.

[159] Fowler, R., and Guggenheim, E. A., *Statistical thermodynamics* (Cambridge U. P., London, 1960).

[160] Domb, C., and Salter, L., The zero point energy and θ values of metals, Phil. Mag. **43**, 1083 (1952).

[161] Klemens, P. G., Thermal conductivity and lattice vibrational modes, in Solid State Physics, vol. 7, F. Seitz and D. Turnbull (eds.), (Academic, New York, 1958) pp. 46–7.

[162] Dugdale, J. S., and MacDonald, D. K. C., Lattice thermal conductivity, Phys. Rev. **98**, 1751 (1955).

[163] Blackman, M., On θ values in the resistance of metals, Proc. Phys. Soc. London **64**, 681 (1951).

[164] Cullen, W. H., Jr., Debye temperatures of copper-rich, Cu-Au alloys, Ames Lab., Iowa, Report IS-T478 (1971).

[165] Kelly, F. M., and MacDonald, D. K. C., On θ values in metals, Can. J. Phys. **31**, 147 (1953).

[166] Meaden, G. T., Electrical Resistance of Metals (Plenum, New York, 1965).

[167] Zener, C., and Bilinsky, S., Theory of the effect of temperature on the reflection of x-rays by crystals, Phys. Rev. **50**, 101 (1936).

[168] Lonsdale, K., Vibration amplitudes of atoms in cubic crystals, Acta Crystallogr. **1**, 142 (1948).

[169] James, R. W., The Optical Principles of the Diffraction of x-rays (Bell, London, 1954).

[170] Herbstein, F. H., Methods of measuring Debye temperatures and comparison of results for some cubic crystals, Adv. Phys. **10**, 313 (1961).

[171] Singh, N., and Sharma, P. K., Debye-Waller factors of cubic metals, Phys. Rev. **3**, 1141 (1971).

[172] Tanji, Y., and Shirakawa, Y., Thermal expansion coefficient of Fe-Ni (fcc) alloys, J. Jap. Inst. Metals Sendai **34**, 228 (1970). In Japanese.

[173] Tanji, Y., Debye temperature and lattice deviation of Fe-Ni (fcc) alloys, J. Phys. Soc. Jap. **30**, 133 (1971).

[174] Lindemann, F. A., Phys. Z. **11**, 609 (1910).

[175] Pines, D., Elementary Excitations in Solids (Benjamin, New York, 1963) pp. 34–7.

[176] Zener, C., Theory of D_0 for atomic diffusion in metals, J. Appl. Phys. **22**, 372 (1951).

[177] LeClaire, A. D., Theory of D_0 in the Arrhenius equation for self-diffusion in cubic metals, Acta Met. **1**, 438 (1953).

[178] Pugh, S. F., Relations between the elastic moduli and the plastic properties of polycrystalline pure metals, Phil. Mag. **45**, 823 (1954).

[179] Crutchley, D. E., and Reid, C. N., in Sixth Plansee Seminar on High Temperature Materials (Reutte, Tyroe, 1968). Reported in ref. [141].

[180] Baughan, E. C., Vibration frequencies in diatomic molecules and in solid metals, Trans. Faraday Soc. **48**, 121 (1952).

[181] Waser, J., and Pauling, L., Compressibilities, force constants,

and interatomic distances of the elements in the solid state, J. Chem. Phys. **18**, 747 (1950).

[182] Badger, R. M., A relation between internuclear distances and bond force constants, J. Chem. Phys. **2**, 128 (1934).

[183] Haussuhl, S., Das elastische Verhalten von Flusspat und strukturverwandten Kristallen, Phys. Status Solidi **3**, 1072 (1963).

[184] Gilman, J. J., Micromechanics of Flow in Solids (McGraw-Hill, New York, 1969) pp. 29–41.

[185] Partington, J. R., An Advanced Treatise of Physical Chemistry—Volume 3—The Properties of Solids (Longmans, Green and Co. London, 1952), pp. 357–72.

[186] Cartz, L., Thermal vibrations of atoms in cubic crystals II: the amplitude of atomic vibrations, Proc. Roy. Soc. London **B68**, 957 (1955).

[187] Neshpor, V. S., On relations between certain thermal characteristics of solids, Fiz. Metal. Metalloved. **7**, 559 (1959). English translation in Phys. Metals Metallogr. (USSR) **7**, 79 (1969).

21. Bibliography of Reviews and Compilations

Alexandrov, K. S., and Ryzhova, T. V., The elastic properties of crystals, Sov. Phys.-Crystallogr. **6**, 228 (1961).

Allard, S. (ed.), International Tables of Selected Constants, vol. 16, Metals: Thermal and Mechanical Data (Pergamon, Oxford, 1969).

Anderson, O. L., Determination and some uses of isotropic elastic constants of polycrystalline aggregates using single-crystal data, in Physical Acoustics, vol. III-B, W. P. Mason (ed.), (Academic, New York, 1965).

Bechmann, R., and Hearmon, R. F. S., The third-order elastic constants, in Landolt-Börnstein New Series, vol. 2, K.-H. Hellwege and A. M. Hellwege (eds.), (Springer-Verlag, Berlin, 1969).

Becker, R., and Döring, W., Die Temperaturabhangigkeit des Elastizitätsmoduls, in Ferromagnetismus (Springer-Verlag, Berlin, 1939).

Bhagavantam, S., Elastic properties of single crystals and polycrystalline aggregates, Proc. Ind. Acad. Sci. **41**, 72 (1955).

Birch, F., Compressibility; elastic constants, in Handbook of Physical Constants, S. P. Clark, Jr. (ed.), (The Geological Society of America, New York, 1966).

Boas, W., and Mackenzie, J. K., Anisotropy in metals, in Progress in Metal Physics, B. Chalmers (ed.), (Pergamon, New York, 1950).

Bollenrath, F., Hauk, V., and Müller, E. H., Zur Berechnung der vielkristallinen Elastizitätskonstanten aus den Werten der ein Kristalle, Z. Metallk. **58**, 76 (1967).

Bridgman, P. W., The Physics of High Pressure (Bell, London, 1949).

Bridgman, P. W., Recent work in the field of high pressures, Rev. Mod. Phys. **18**, 1 (1946).

Buch, A., The Mechanical Properties of Pure Metals (Scientific-Technical Publ., Warsaw, 1968).

Chevenard, P., Recherches expérimentales sur les alliages de fer, de nickel it de chrome, Trav. Mem. Bur. Int. Poids Mes. **17**, 142 (1927).

Clark, S. P., Jr. (ed.), Handbook of Physical Constants (Geological Society of America, New York, 1966).

Dorn, J. E., The modulus of elasticity—a review of metallurgical factors, Metal Progr. **58**, 81 (1950).

Fedorov, F. L., Theory of Elastic Waves in Crystals (Plenum Press, New York, 1968).

Gschneider, K. A., Jr., Physical properties and interrelationships of metallic and semimetallic elements, in Solid State Physics, vol. 16, F. Seitz and D. Turnbull (eds.), (Academic, New York, 1964).

Guillaume, C.-H., Recherches metrologiques sur les aciers au nickel, Trav. Mem. Bur. Int. Poids Mes. **17**, 1 (1927).

Hearmon, R. F. S., An Introduction to Applied Anisotropic Elasticity (Oxford U. P., London, 1961).

Hearmon, R. F. S., The elastic constants of anisotropic materials, Rev. Mod. Phys. **18**, 409 (1946).

Hearmon, R. F. S., The elastic constants of anisotropic materials, II, Adv. Phys. **5**, 323 (1956).

Hearmon, R. F. S., The elastic constants of non-piezoelectric crystals, in Landolt-Börnstein New Series, vol. 1, Elastic, Piezoelectric, Piezooptic, and Electrooptic Constants of Crystals, K.-H. Hellwege and A. M. Hellwege (eds.), (Springer-Verlag, Berlin, 1966); updated in vol. 2 (1969) of same series.

Huntington, H. B., The elastic constants of crystals, in Solid State Physics vol. 7, F. Seitz and D. Turnbull, (eds.), (Academic, New York, 1958).

Jones, H., Structural and elastic properties of metals, Physica **15**, 13 (1949).

Köster, W., and Franz, H., Poisson's ratio for metals and alloys, Met. Rev. **6**, 1 (1961).

March, J. S., Alloys of Iron and Nickel. I. Special Purpose Alloys (McGraw-Hill, New York, 1938) pp. 107–34.

Mason, W. P., Physical Acoustics and the Properties of Solids (Van Nostrand, Princeton, N.J., 1958).

Mason, W. P., and Thurston, R. N., (eds.), Physical Acoustics, Principles and Methods (Academic, New York, 1964-present). This annual series contains many important articles on solid elasticity.

Mason, W. P., Piezoelectric Crystals and their Application to Ultrasonics (Van Nostrand, New York, 1950).

McCain, W. S., and Maringer, R. E., Mechanical and physical properties of invar and invar-type alloys, DMIC Memo. 207, Battelle Mem. Inst., Columbus, Ohio (1965).

Pomerance, H., Bibliography of second and third order elastic constants, ORNL–RMIC–9, Oak Ridge Natl. Lab., Tenn. (1968).

Samsonov, G. V., Handbook of Physicochemical Properties of the Elements (IFI/Plenum, New York, 1968).

Schram, K. H., Daten zur Schallgeschwindigkeit in reinen Metallen, Z. Metallk. **53**, 729 (1962).

Simmons, G., Hashin bounds for aggregates of cubic crystals, J. Grad. Res. Cent. **36**, 1 (1967).

Simmons, G., Single crystal elastic constants and calculated aggregates properties, J. Grad. Res. Cent. **34**, 1 (1965).

Simmons, G., and Wang, H., Single Crystal Elastic Constants and Calculated Aggregate Properties: A Handbook (The M.I.T. Press, Cambridge, Mass., 1971).

Sundara Rao, R. V. G., Vedam, K., and Krishnan, R. S., Elastic constants, in Progress in Crystal Physics, vol. I, R. S. Krishnan (ed.), (S. Viswanathan, Central Art Press, Chetput, Madras, India, 1958).

Zener, C., Elasticity and Anelasticity of Metals (Univ. of Chicago Press, Chicago, 1948).

22. Older References

22.1. Iron, Young's Modulus

Wertheim, Pogg. Ann. Erg. **E2**, 1 (1848).

Kupffer, A., Mem. Imp. Acad. St. Petersburg (VI series), **6**, 393 (1857).

Kohlrausch and Loomis, Pogg. Ann. **141**, 481 (1870).

Streintz, H., Uber die Anderung der Elastizitat und der Large eines vom galvanischem Strome durchflorsenen Drahtes, Pogg. Ann. **150**, 368 (1873).

Pisati, G., Sulla elasticita dei metalli a diverse temperature, Nuovo Cimento **1**, 181 (1877); **2**, 137 (1877); **4**, 152 (1878); **5**, 34, 135, 145 (1879).

Kiewiet, H., Wiedermann's Ann. **29**, 617 (1886).

Noyes, Phys. Rev. **2**, 277 (1895); **3**, 432 (1896).

Shakespeare, Phil. Mag. **47**, 539 (1899).

Thomas, P. A., Dissertation, Jena (1899); quoted in Keulegan, Houseman (1933).

Gray, Blyth, and Dunlop, Proc. Roy. Soc. London **67**, 180 (1900).

Gray, T., Effect of hardening on the rigidity of steel, Science **16**, 337 (1902).

Walker, Proc. Roy. Soc. Edinburgh **27**, 343 (1907); **28**, 652 (1908); **31**, 186 (1910).

Harrison, Proc. Phys. Soc. London, **27**, 8 (1914).

Dodge, Phys. Rev. **5**, 373 (1915).
Dadourian, H. M., Phil. Mag. **42**, 442 (1921).

22.2. Iron, Shear Modulus

Napiersky, Pogg. Ann. Erg. **3**, 351 (1853).
Kupffer, Mem. Imp. Acad. St. Petersburg **6**, 397 (1857).
Kohlrausch and Loomis, Pogg. Ann. 141, 481 (1870); Am. J. Sci. **50**, (1870).
Pisati, Nuovo Cimento, Ser III, **1**, 181 (1877); **2**, 137 (1877); **4**, 152 (1888); **5**, **34**, 135, 145 (1879).
Tomlinson, Proc. Roy Soc. London **40**, 343 (1886).
Katzenelsohn, Beibl. Ann. **12**, 307 (1888).
Gray, Blyth, and Dunlop, Proc. Roy. Soc. London **67**, 180 (1900).

22.3. Iron, Poisson Ratio

Bauschinger, J., Der Zivilingenier **25**, 81 (1879).
Katzenelson, N., Inn. Diss., Berlin (1887).
Amagat, E. H., Ann. Chim. Phys. **22**, 119 (1891)
Bock, A., Weid. Ann. **52**, 609 (1894).
Stromeyer, C. E., Proc. Roy. Soc. London **55**, 373 (1894).
Cardani, P., Z. Physik **4**, 449 (1903).

22.4. Nickel, Young's Modulus

Lessing, A., Uber die Elastizitat einiger Kupfer-Nickel-legierungen, Dissertation, Univ. Berlin (1900).
Guillaume, C-E., Recherches sun le Nickel et Ses Alliages, Archives Sci. Phys. Nat., sec. 4, **5**, 255 (1898).

22.5. Nickel, Shear Modulus

See references in section 22.2.

22.6. Iron-Nickel Alloys, Young's Modulus

Barus, C., Amer. J. **34**, 175 (1887); Phys. Rev. **13**, 257 (1901).
Mercadier, E., Sur la determination des constants et du coefficient d'elasticite de l'acier-nickel, C. R. Acad. Sci. **113**, 33 (1891).
Howard, J. E., Nickel Steel from Springfield Armory, Tests of Metals of Metals (U.S. Arsenal, Watertown, Mass., No. 4816, 4817, 1893) p. 237.
Howard, J. E.. Nickel Steel from Springfield Armory, Tests of Metals (U.S. Arsenal, Watertown, Mass., Nos. 5520, 5521, 1896) pp. 60, 431.
Day, Electrician **39**, 480 (1897).
Howard, J. E., Nickel steel rifle barrels, Tests of Metals (U.S. Arsenal Watertown, Mass., 1898) pp. 391, 690.
Howard, J. E., Nickel steel, Tests of Metals, (U.S. Arsenal, Watertown, Mass. 1898) p. 679.
Rudeloff, M., Funfter Bericht des Sonderausschusses fur Eisen legierungen, Verh. Ver. Beford. Gewerb. **77**, 327 (1898).
Stevens, J. S., and Dorsey, H. G., Phys. Rev. **9**, 116 (1899).
Stevens, J. S., Phys. Rev. **10**, 111 (1900).
Honda, K., and Shimizu, S., J. Sc. Coll. **16**, Art. 12, 13 (1902).

23. Notes on Tables

The following shorthand notations are used in the tables:

$f(A)$ = function of aging,

$f(CR)$ = function of cooling rate,

$f(D)$ = function of plastic deformation,

$f(GS)$ = function of grain size,
$f(H)$ = function of magnetic field,

$f(O)$ = function of atomic ordering,

$f(P)$ = function of pressure,

$f(Ph)$ = function of phase (transition),

$f(R)$ = function of recovery,

$f(S)$ = function of stress,

$f(T)$ = function of temperature,

$f(X)$ = function of composition (of nickel),

and

$x(E)$ = function of composition (of element E).

"Best values" represent arithmetic means without weighting factors. "Uncertainties" represent computed standard deviations, and they include variations of samples, experimental methods, etc. Systematic error is believed negligible compared to imprecision. All data were included in the averages with the following exceptions. Data corresponding to severely deformed specimens were omitted as being non-representative. When the "same" materials were tested by different experimental methods, only a single average data point was included. "Different" materials measured by the same experimental method and by the same investigator were included as multiple data points.

24. Tables and Figures

TABLE 1. Connecting identities $X=X(Y,Z)$ for elastic constants of quasi-isotropic solids

X	Y,Z									
	E, G	E, B	E, ν	G, B	G, ν	B, ν	λ, μ	c^0_{11}, c^0_{12}	s^0_{11}, s^0_{12}	v_l, v_t
E				$\frac{9GB}{G+3B}$	$2G(1+\nu)$	$3B(1-2\nu)$	$\frac{\mu(3\lambda+2\mu)}{\lambda+\mu}$	$\frac{(c^0_{11}-c^0_{12})(c^0_{11}+2c^0_{12})}{c^0_{11}+c^0_{12}}$	$\frac{1}{s^0_{11}}$	$3\rho v_t^2(v_l^2-\frac{4}{3}v_t^2)/(v_l^2-v_t^2)$
$G(=\mu=\rho v_t^2)$		$\frac{3BE}{9B-E}$	$\frac{E}{2(1+\nu)}$			$\frac{3B}{2}\cdot\frac{1-2\nu}{1+\nu}$		$\frac{1}{2}(c^0_{11}-c^0_{12})=c^0_{44}$	$\frac{1}{2(s^0_{11}-s^0_{12})}=\frac{1}{s^0_{44}}$	
B	$\frac{GE}{3(3G-E)}$		$\frac{E}{3(1-2\nu)}$		$\frac{2G}{3}\cdot\frac{1+\nu}{1-2\nu}$		$\lambda+\frac{2}{3}\mu$	$\frac{c^0_{11}+2c^0_{12}}{3}$	$\frac{1}{s_{11}+2s_{12}}$	$\rho\left(v_l^2-\frac{4}{3}v_t^2\right)$
ν	$\frac{E}{2G}-1$	$\frac{1}{2}-\frac{E}{6B}$		$\frac{1}{2}\cdot\frac{3B-2G}{3B+G}$			$\frac{\lambda}{2(\lambda+\mu)}$	$\frac{c^0_{12}}{c^0_{11}+c^0_{12}}$	$-\frac{s^0_{12}}{s^0_{11}}$	$\frac{1}{2}(v_l^2-2v_t^2)/(v_l^2-v_t^2)$
λ	$G\frac{E-2G}{3G-E}$	$3B\frac{3B-E}{9B-E}$	$\frac{\nu E}{(1+\nu)(1-2\nu)}$	$B-\frac{2}{3}G$	$\frac{2\nu G}{1-2\nu}$	$\frac{3\nu B}{1+\nu}$		c^0_{12}	$\frac{-s^0_{12}}{(s^0_{11}-s^0_{12})(s^0_{11}+2s^0_{12})}$	$\rho(v_l^2-2v_t^2)$
ρv_l^2	$G\frac{4G-E}{3G-E}$	$\frac{3B(3B+E)}{9B-E}$	$\frac{E(1-\nu)}{(1+\nu)(1-2\nu)}$	$B+\frac{4}{3}G$	$G\frac{2(1-\nu)}{1-2\nu}$	$3B\frac{1-\nu}{1+\nu}$	$\lambda+2\mu$	c^0_{11}	$\frac{s^0_{11}+s^0_{12}}{(s^0_{11}-s^0_{12})(s^0_{11}+2s^0_{12})}$	

Besides the symbols already defined in the text, ρ = mass density, v_l = velocity of longitudinal elastic wave, and v_t = velocity of transverse elastic wave. The c^0_{ij} satisfy the isotropy condition $c_{11}-c_{12}=2c_{44}$. Similarly, the s^0_{ij} satisfy the isotropy condition $2(s_{11}-s_{12})=s_{44}$.

TABLE 2. Expressions for engineering elastic constants of cubic single crystals

Young's modulus

$$E_l^{-1}=s'_{11}=s_{11}-S\Gamma$$

Shear modulus

$$G_l^{-1}=s'_{44}=s_{44}+2S\Gamma$$

Bulk modulus

$$B=\tfrac{1}{3}\,(s_{11}+2s_{12})^{-1}=\tfrac{1}{3}\,(c_{11}+2c_{12})\ \text{(independent of } l\text{)}$$

Poisson ratio

$$\nu_{l,m}=-s'_{12}/s'_{11}=-(s_{12}+S\Lambda)/(s_{11}-S\Gamma)$$

where

$$S=(2s_{11}-2s_{12}-s_{44}),$$

$\Gamma=l_1^2l_2^2+l_2^2l_3^2+l_3^2l_1^2$ where l_1, l_2, l_3 = direction cosines of an arbitrary crystallographic direction;

$\Lambda=l_1^2m_1^2+l_2^2m_2^2+l_3^2m_3^2$ where m_1, m_2, m_3 = direction cosines of an arbitrary vector perpendicular to l.

TABLE 3. Conversions between elastic stiffnesses c_{ij} and elastic compliances s_{ij} for cubic crystals

$$c_{11}=\frac{s_{11}+s_{12}}{(s_{11}-s_{12})(s_{11}+2s_{12})} \qquad s_{11}=\frac{c_{11}+c_{12}}{(c_{11}-c_{12})(c_{11}+2c_{12})}$$

$$c_{12}=\frac{-s_{12}}{(s_{11}-s_{12})(s_{11}+2s_{12})} \qquad s_{12}=\frac{-c_{12}}{(c_{11}-c_{12})(c_{11}+2c_{12})}$$

$$c_{44}=\frac{1}{s_{44}} \qquad s_{44}=\frac{1}{c_{44}}$$

And, by derivation:

$$c_{11}-c_{12}=\frac{1}{s_{11}-s_{12}} \qquad s_{11}-s_{12}=\frac{1}{c_{11}-c_{12}}$$

$$c_{11}+2c_{12}=\frac{1}{s_{11}+2s_{12}} \qquad s_{11}+2s_{12}=\frac{1}{c_{11}+2c_{12}}$$

TABLE 4. Selected properties of iron and nickel

	Fe	Ni
Atomic number	26	28
Atomic weight, mkg/mol	55.85	58.71
Electronic structure	$[\mathrm{Ar}]3d^64s^2$	$[\mathrm{Ar}]3d^84s^2$
Ionic (Goldschmidt, 12-fold coordination) radius, nm	0.127	0.124
Distance of closest approach, nm	0.24823	0.24919
Lattice parameter, nm, 293 K	0.28664	0.35238
Density, kkg/m³, 293 K	7.87	8.91
Melting point, K	1810	1726
Boiling point, K	3106	3059
Heat of fusion, kJ/mol	15.3	17.7
Heat of vaporization, MJ/mol	0.416	0.430

TABLE 5. Second-order elastic stiffnesses c_{ij} of iron

Investigator(s) (Year)	Composition	Technique	Specimen, Test Conditions	c_{11}	c_{12}	c_{44}
				(10^{12} dyn/cm²)		
Goens, Schmid (1931)	99.85 Fe (0.025 Mn, 0.03C, 0.01 P, 0.08 S, 0.06 Cu, trace Si)	Transv. res. freq.	Strain-ann. crystals. No field.	2.37	1.41	1.16
Kimura, Ohno (1934)		Bending, torsion opt. microscope.	Recrystallized. No field.	2.41	1.46	1.12
Kimura (1939)		a) Long. res. freq.	No field.	2.09	1.14	1.11
		b) Long. res. freq.	Saturated field.	2.10	1.13	1.12
		c) Bending, torsion.	No field.	2.28	1.33	1.11
Yamamoto (1941, 1943)	Fe (0.03 C, 0.01 Si, 0.04 Mn, 0.01 P, 0.04 S, 0.06 Cu)	Magnetostrictive oscillation. Bridgman (1940) compressibility data.	No field.	2.34	1.35	1.176
Moller, Brasse (1955)	Fe (0.02–0.2 Mn, 0.01–0.06 Si, 0.015 C, 0.01 P, 0.02 S, 0.15 O)	Tension, induction.	H_2 ann., 1223 K; 3–10% strain; vac. ann. 1153 K, 72 h.	2.28	1.40	1.12
Markham (1957)		5–20 MHz pulse-echo.	One crystal. No field.	2.330	1.392	1.162

TABLE 5. Second-order elastic stiffnesses c_{ij} of iron—Continued

Investigator(s) (Year)	Composition	Technique	Specimen, Test Conditions	c_{11}	c_{12}	c_{44}
				(10^{12} dyn/cm^2)		
Rayne, Chandrasekhar (1961)	99.99 Fe	10 MHz pulse-echo.	Strain-ann. crystal. No field, $f(T)$ in figure 15.	2.331	1.354	1.178
Lord, Beshers (1965)	99.8 Fe	7, 10 MHz pulse-echo.	11 kOe field (saturated). [100], [110] crystals ann., wet H_2, 993 K, 216 h, slow cool. [111] crystal vac. ann. 1123 K, 176 h, slow cool. Strain-ann. crystals, $f(T)$ in figure 15.	2.28	1.32	1.165
Truell (1965)		Pulse-echo.		2.23	1.27	1.15
Rotter, Smith (1966)	99.99 Fe (Cr, Mn traces)	10 MHz pulse-echo.	Specimens from crystal of Rayne, Chandrasekhar (1961); no field, $f(P)$.	2.314	1.346	1.164
Leamy, Gibson, Kayser (1967)	Fe, 1-25 Al alloys	10 MHz pulse-echo. Extrapolated from alloy data.	Bridgman technique crystals, ann. 1173 K, 72 h, extremely slowly cooled (60 days), argon atmos; $f(T)$ in figure 15.	2.338	1.378	1.186
Leese, Lord (1968)	99.8 Fe	30-60 MHz pulse-echo.	Specimens and treatment from Lord, Beshers (1965); no field; $f(T)$ in figure 15.	2.26	1.40	1.16
Guinan, Beshers (1968)	99.8 Fe	10 MHz pulse-echo.	Specimens from Lord, Beshers (1965), no field, $f(P)$.	2.301	1.346	1.167
Dever (1972)	Ferrovac	40, 70 MHz phase comparison	Two crystals, no field, $f(T)$ in figure 15.	2.322	1.356	1.170
			Best values	2.29	1.34	1.15
			Uncertainties	0.09	0.09	0.03

TABLE 6. Second-order elastic stiffnesses c_{ij} of nickel

Investigator(s) (Year)	Composition	Technique	Specimen, Test Conditions	c_{11}	c_{12}	c_{44}
				(10^{12} dyn/cm^2)		
Honda, Shirakawa (1937, 1949)		Bending, opt. microscope.	Bridgman method crystals.	2.52	1.51	1.04
Bozorth, Mason, McSkimin, Walker (1949)	99.95 Ni	10 MHz pulse-echo.	Bridgman method, dry H_2, crystals.	2.50	1.60	1.185
Bozorth, Mason, McSkimin (1951)	99.95 Ni	10 MHz pulse-echo.	Bridgman method, dry H_2, crystals; f(freq.); a) no field, b) saturated field.	2.517 2.523	1.574 1.566	1.226 1.23
Neighbours, Bratten, Smith (1952)	99.9 Ni	10 MHz pulse-echo.	Bridgman method crystals, annealed 2 h in H_2, 5 kOe transv. field.	2.53	1.52	1.24
Yamamoto (1942, 1950, 1951)	Ni(0.02–0.19 Fe, 0.01 P, S, Al, 0.03 C, Si, Mn, 0.01–0.20 Co, Cu)	Magnetostrictive oscillation.	Bridgman method crystals; vac. ann. 1273 K, 1 h.	2.44	1.58	1.02
Levy, Truell (1953)	99.9 Ni	27, 30 MHz pulse-echo.	Bridgman method crystals; $f(H,$ freq.); saturated field.	2.47	1.52	1.21

TABLE 6. Second-order elastic stiffnesses c_{ij} of nickel—Continued

Investigator(s) (Year)	Composition	Technique	Specimen, Test Conditions	c_{11}	c_{12}	c_{44}
				(10^{12} dyn/cm		
DeKlerk, Musgrave (1955)		2–10 MHz pulse-echo.	a) No field, b) saturated field.	2.43 2.46	1.49 1.47	1.19 1.24
Shirakawa, Numakura (1957)	Ni(0.06 C, 0.02 Si, 0.05 Fe, 0.02 Co)	Tension, opt. microscope.	X(Cu)	2.55	1.69	0.902
DeKlerk (1959)		2–10 MHz pulse-echo.	F(freq.). a) No field, b) saturated field ‖ to [001].	2.459 2.461	1.500 1.475	1.213 1.220
Alers, Neighbours, Sato (1960)	"Electrolytic"	10 MHz pulse-echo.	Bridgman method crystals, 10 kOe field, $f(T)$ in figure 16.	2.508	1.500	1.235
Sakurai (1964)	99.95 Ni	1–5 MHz pulse-echo.	Bridgman method crystals, 10 kOe field.	2.51	1.53	1.24
Sakurai, Fujii, Nakamura, Takaki (1964)		1–5 MHz pulse-echo.	Bridgman method crystals, X(Cu, Fe).	$c_{11}-c_{12}$	$=0.93$	1.24
Epstein, Carlson, (1965)	99.95 Ni	10 MHz pulse-echo.	Bridgman method crystals; ann. 1373 K, 200 h; X(Cu); a) no field, b) saturated field.	2.481 2.504	1.54 1.57	1.242 1.256
Vintaikin (1966)		X-ray, thermal diffuse scattering.	Bridgman method crystals; ann. 1173 K, 3 h.	2.47	1.44	1.24
Salama, Alers (1969)	"Pure"	Change of sound velocity under uniaxial stress.	Saturated, 10 kOe, field.	2.516	1.544	1.220
Shirakawa, et al. (1969)	Ni (0.012 Fe, 0.007 Si, 0.008 Cu, 0.003 Mn)	Single-crystal resonant frequency.	Saturated field.	2.88	1.81	1.24
			Best values (no field) (sat. field)	2.49 2.54	1.55 1.55	1.14 1.23
			Uncertainties (no field) (sat. field)	0.04 0.12	0.07 0.10	0.12 0.01

TABLE 7. Second-order elastic stiffnesses c_{ij} of iron-nickel alloys

Investigator(s) (Year)	Composition	Technique	Specimen, Test Conditions	c_{11}	c_{12}	c_{44}
				(10^{12} dyn/cm^2)		
Alers, Neighbours, Sato (1960)	Fe-30.0 Ni	10 MHz pulse-echo.	Bridgman method crystals, $f(T)$ in figure 17, a) $H=0$, b) $H=10$kOe.	1.473 1.463	0.888 0.881	1.135 1.132
Einspruch, Clairborne (1964)	Fe-73.8 Ni	Pulse-echo.	Bridgman method crystals, no field and saturated field.	2.304	1.444	1.192
Sakurai, Fujii Nakamura, Takaki (1964)	a) Fe-59 Ni b) Fe-75 Ni c) Fe-90 Ni d) 100 Ni	1–5 MHz pulse-echo.	Bridgman method crystals, 2–4 kOe field, ΔE effect$=1-2\%$.	$c_{11}-c_{12}$ $c_{11}-c_{12}$ $c_{11}-c_{12}$ $c_{11}-c_{12}$	$=0.72$ $=0.89$ $=0.95$ $=0.94$	1.22 1.27 1.25 1.24
Salama, Alers (1968)	Fe-30.0 Ni	10 MHz pulse-echo.	Specimens from Alers, Neighbours, Sato (1960); 10 kOe field; $f(T)$ in figure 17.	1.474	0.894	1.134

TABLE 7. Second-order elastic stiffnesses c_{ij} of iron-nickel alloys—Continued

Investigator(s) (Year)	Composition	Technique	Specimen, Test Conditions	c_{11}	c_{12}	c_{44}
				(10^{12} dyn/cm^2)		
Bower, Claridge, Tsong (1968)	a) Fe-36.1 Ni	10 MHz pulse-echo.	Bridgman method crystals (quenched), measured at T=4K.	1.573	1.235	1.006
	b) Fe-38.2 Ni			1.545	1.211	0.992
	c) Fe-60.8 Ni			2.283	1.501	1.176
	d) Fe-61.8 Ni			2.286	1.500	1.184
	e) Fe-78.4 Ni			2.476	1.512	1.277
	f) Fe-89.8 Ni			2.627	1.528	1.300
	g) Ni			2.614	1.548	1.309
Shirakawa, et al. (1969)	a) Fe-35 Ni	Single-crystal, resonant frequency.	Saturated field.	1.40	0.92	1.11
	b) Fe-40 Ni			1.57	1.09	0.96
	c) Fe-45 Ni			1.96	1.42	0.83
	d) Fe-50 Ni			2.12	1.55	0.90
	e) Fe-60 Ni			2.24	1.51	1.12
	f) Fe-70 Ni			2.33	1.46	1.27
	g) Fe-80 Ni			2.41	1.43	1.38
	h) Fe-90 Ni			2.52	1.43	1.39
	i) Ni			2.88	1.81	1.24
Diesburg (1971)	a) Fe-28.2 Ni	10 MHz pulse-echo-overlap.	Bridgman method crystals, homog. 1473 K 120h, $f(T)$ in figure 17, no field.	1.6080	0.9578	1.1598
	b) Fe-30.0 Ni			1.5258	0.9157	1.1313
	c) Fe-34.4 Ni			1.3328	0.8570	1.0591
Hausch, Warlimont (1973)	a) Fe-31.5 Ni	10 MHz pulse-echo.	Bridgman method crystals, 6kOe field, $f(T)$ in figure 17.	1.404	0.840	1.121
				1.362	0.852	1.086
				1.379	0.899	1.058
				1.356	0.910	1.042
				1.507	1.077	1.020
				1.592	1.162	1.024
				1.713	1.261	1.029
				1.860	1.372	1.035
				2.053	1.459	1.059

TABLE 8. Young's modulus E of iron

Investigator(s) (Year)	Composition	Technique	Specimen, Test Conditions	E (10^{12} dyn/cm^2)
Guillaume (1897)		Spring tension.	X(Fe).	1.96
Schaefer (1901)		Res. freq.		1.80
Benton (1903)	"Steel"	Tension.	$F(T$, 76–300 K), relative to 300 K.	
Morrow (1903)	"Wrought iron"	Compression, opt. lever.	Range of values: 2.01–2.12.	2.06
Carpenter, Hadfield, Longmuir (1905)	Fe(0.95 Mn, 0.17 Si, 0.47 C, 0.04 S, 0.02 P)	Tension, extensometer.	Ann. 1023 K, x(Ni).	2.21
Grüneisen (1907)	99.5 Fe(0.1 C, 0.2 Si, 0.1 Mn)	a) Tension, opt. lever.		2.10
		b) Transv. res. freq.		2.10
Honda, Terada (1907)	"Swedish steel"	Tension opt. lever.	Ann., $f(S)$, x(Ni).	2.0
Grüneisen (1908)	a) "Steel"	Res. freq.		2.09
	b) "Iron"	Res. freq.		2.13
Grüneisen (1910)		Bending.	Range of values=2.05–2.11.	2.08
Honda (1919)		Bending, opt. lever.	Ann. 1173 K, x(Ni).	2.05
Honda (1919)	Fe(0.29 Cu, 0.31 Mn, 0.11 Si, 0.09 C, 0.3 P, S)	Bending, opt. lever.	X(Cu).	2.1

TABLE 8. Young's modulus E of iron—Continued

Investigator(s) (Year)	Composition	Technique	Specimen, Test Conditions	E (10^{12} dyn/cm^2)
Bach, Baumann (1921)			$F(T$, 293–773 K).	2.03
Honda, Hasimoto (1921)	Fe(0.18 C, 0.20 Mn+Si)	Bending, opt. lever.	a) Ann. 1173 K, slow cool. b) Ann. 1173 K, quench. X(C).	2.055 1.955
Koch, Dieterle (1922)		Res. freq.	$F(T$, 285–873 K).	1.4
Lea (1922)	"Armco iron"	Tension, opt. lever.	$F(T$, 293–573 K).	2.0
Carrington (1924)	a) "Wrought iron"	Tension.	Ann. 1183 K, slow cool, $f(T$, 293–590 K).	2.00
	b) Fe(0.19 C)	Tension.	Ann. 1183 K, slow cool, $f(T$, 293–590 K).	1.98
Kimball, Lovell (1925)	Fe(0.15 C)	Res. freq.	$F(T$, 290–790 K).	
Honda, Tanaka (1926)	a) Fe(0.31 Mn, 0.29 Cu, 0.09 C, 0.11 Si, 0.03 P, S) b) Fe(0.38 Mn, 0.1 C, 0.02 P, S)	Bending, opt. lever.	Ann. 1173 K, 2 h, slow cool. Ann. 1173 K, 1/2 h, slow cool. Ann. 1173 K, 1/2 h, oil quench. X(Ni, Co, C), $f(H)$.	2.087 2.045 1.942
Nishiyama (1929)	a) Fe(0.1 C)	Bending, opt. lever.	Ann. 1173 K in vac., 1 h, furnace cooled; x(Si, V, Al, W, Mn, Cr, Co, Ni).	2.12
	b) "Armco iron"			2.11
	c) "Electrolytic iron"			2.13
Kawai (1930)	"Armco iron"	Tension.	Ann. 1273 K, $f(D)$ in figure 9.	2.13
Jacquerod, Mugeli (1931)		Bending.	Ann., $f(T$, 273–390 K), relative to 273 K.	2.09
Everett (1931)	Fe(0.35 C, 0.80 Mn, 0.10 Si, 0.02 P, 0.03 S)	Tension, opt. lever.	a) Ann. 1173 K, ½ h, slow cool. b) Unannealed.	2.01 2.11
Keulegan, Houseman (1933)	Fe(0.66 C, 0.8 Mn, 0.01 P)	Loaded helical springs.	Detm. temp. coeff., 223–323 K.	–
Bez-Bardili (1935)		Long. and transv. res., 1–20 MHz.		2.18
Verse (1935)	a) Fe(0.43 C, 0.86 Mn, 0.04 S, 0.02 P, 0.14 Si)	Tension, cathetometer.	Ann., $f(T$, 298–733 K).	2.06
	b) Fe(0.34 C, 0.80 Mn, 0.10 Si, 0.02 P, 0.03 S)	Long. torsional res. freq.	Ann. 1173 K, $f(T)$ in figure 18.	2.08
Nakamura (1935)	99.94 Fe	Long. res. freq.	Ann. 1273 K, 1 h, slow cool; x(Ni); $f(H)$.	2.107
Cooke (1936)	"Armco iron"	Long. (56 MHz), torsional.	a) Ann, 1200 K, 2 h, H_2 atmos., slow cool (8 h), $H=0$. b) Cold rolled, $H=0$. $F(H)$.	1.99 1.86
Förster, Köster (1937)		Transv. res. freq.	Ann. 1200 K, ½ h. air cool.	2.13
Engler (1938)		Long. res. freq.	$F(H)$ 0–0.575kOe, $f(T)$ in figure 18.	2.12
Yamamoto (1938)	"Armco iron"	Magnetostrictive oscillation.	Ann. 1203 K, 1 h; $X(C)$; $f(H)$.	2.11
Kimura (1939)	"Armco iron"	Long. res. freq.	Ann., H_2 atmos.; $f(H)$, $f(T)$ in figure 18.	2.17
Köster (1940)	"Armco iron"	Transv. res. freq.	X(Co, Cr, C, Ni), $f(D)$ in figure 9. $f(T$, 293-1173 K), $f(GS, A, R)$.	2.12

TABLE 8. Young's modulus E of iron—Continued

Investigator(s) (Year)	Composition	Technique	Specimen, Test Conditions	E (10^{12} dyn/cm^2)
Yamamoto (1941, 1943)	a) "Electrolytic" b) Fe(0.03 C, 0.01 Si, 0.39 Mn, 0.01 P, 0.04 S, 0.06 Cu)	Magnetostrictive oscillation.	Vac. ann. 1203 K, 1.5 h, furnace cool. Vac. ann. 1203 K, 1 h, furnace cool. $F(H)$.	2.140 2.058
Köster (1943)		Transv. res. freq.	Ann. 1273 K, 1 h, $H=0$. a) Bcc crystal structure. b) Fcc crystal structure (extrapolated). F(Ni), $f(T)$ in figure 18, $f(H), f(O)$.	 2.12 2.20
Smith, Wood (1941)	99.95 Fe	Tension, x-ray spectometer.	Vac. ann. 0.050 in. sheet.	1.79
Seager, Thompson (1943)	a) Fe(0.8 Mn, 0.06 Si, 0.18 C, 0.08 S, 0.02 P) b) "Armco iron"	Bending, interferometer. Bending, interferometer.	Hot rolled, $f(T$, 295–500 $K($, $f($Impurities). Cold rolled, ann., $f(T)$ in figure 18.	1.94 1.81
Everett, Miklowitz (1944)	Fe(0.15 0.25 C, 0.3–0.6 Mn, 0.04 P, 0.05 S) [SAE1020]	Bending, opt. lever.	$F(T$, 293–810 K).	2.03
Scheil, Reinacher (1944)		Res. freq.	X (Ni), $f(T)$ in figure 18.	2.11
Roberts, Nortcliffe (1947)	Fe(0.09 Ni, 0.22 Mn, 0.21 Si, 0.06 Cr, 0.09 C)	a) Transv. res. freq. b) "Static".	Ann. 1200 K, $f(T)$ in figure 18. Ann. 1200 K, $f(T)$, 293–673 K.	2.09 2.06
Köster (1948)		Transv. res. freq.	Worked, ann. 1273 K; $f(T)$ in figure 18.	2.11
Bennett, Davies (1949)	99.75 Fe 98.83 Fe(0.25 C, 0.65 Mn)	Res. freq.	Ann. 973 K, 6 h; $f(T)$; relative values, 273–850 K.	....
Andrews (1950)	99.97 Fe(0.01 C, 0.02 Mn)	Transv. res. freq.	0.03 in. sheet; $f(T)$ in figure 18.	2.12
Frederick (1947)	"Armco iron"	0.5–15 MHz pulse-echo.	$F(T)$.	2.089
Garofalo, Malenock, Smith (1952)	Fe(0.45 Mn, 0.19 Si, 0.13 C, 0.01 P, 0.02 S)[SAE1015]	Tension, opt. lever.	Ann. 1173 K, ½ h, air cool; $f(T)$ in figure 18.	2.03
Hughes, Kelly (1953)	"Armco iron"	Pulse-echo.	$F(P)$.	2.11
Yamamoto, Taniguchi (1954)	Fe(0.02 Al)	Magnetostrictive.	Ann., x(Al, $f(H)$.	2.152
Burnett (1956)	99.8 Fe	Res. freq., bending.	$F(T)$ in figure 18.	1.98
Yamamoto (1959)	Fe(0.06 Mn, 0.03 Si, C, S, 0.02 P)	Magnetostrictive oscillation.	Ann. 1273 K, 2 h, H_2 atmos.; x(Ni); $f(H)$, a) $H=0$, b) H sat.	2.091 2.096
Hill, Shimmin, Wilcox (1961)	Fe(0.30 Mn, 0.24 C, 0.01 Si; P, 0.04 S)[SAE1020]	a) Long. res. freq. b) Tension, opt. strain gauges.	"Warm rolled", $f(T)$ in figure 18.	2.10 2.08
Voronov, Vereshchagin (1961)	99.8 Fe(0.02 Mn, Si, 0.01 C, 0.03 P, S)	10 MHz pulse-echo.	Annealed.	2.09
Durham, et al. (1963)	Fe(0.08 C, 0.3 Mn, 0.15 Si) [SAE1075]	Tension, strain gage extensometer.	Ann. 1060 K, 1 h, oil quench, 655 K, 1 h, air cool, $f(T)$ in figure 18.	2.07
Kamber (1963)	Fe(0.002 C, P, S, Mn, 0.001 Cr, V, 0.003 Mo, Al, 0.004 Si, 0.011 Ni, 0.014 Cu, 0.040 xy)	1 MHz, transv. res. freq.	a) 1 mm GS, $H=0$, b) 1 mm GS, $H=1.5$ kOe. Strained 3%, ann. 1173 K, 25 h c) 30 mm GS, $H=0$, d) 30 mm GS, $H=1.5$ kOe. $F(T)$ in figure 18.	2.04 2.06 1.94 1.94
Masumoto, Saito, Kobayashi (1963)	"Electrolytic"	Long. res. freq.	Vac. ann. 1273 K, 1 h, slow cool; x(Pd).	1.97

TABLE 8. Young's modulus E of iron—Continued

Investigator(s) (Year)	Composition	Technique	Specimen, Test Conditions	E (10^{12} dyn/cm^2)
Shved (1964)	"Armco iron"	X-ray scattering, uniaxial tension.		2.21
Smith, Stern, Stephens (1966)	a) Fe(0.4 C, 0.35i, 0.8 Mn) b) Fe(0.6 C, 0.25 i, 0.8 Mn)	Long. transv. pulse-echo.	$F(P)$.	2.11 2.11
Masumoto, Sawaya, Kikuchi (1971)	"Electrolytic" Fe(0.004 Cu, trace Al, 0.005 Mn, 0.005 Si, 0.005 C, 0.005 S, 0.004 P)	Resonance frequency, 700–900 Hz.	Vac. ann. 1 h at 1273 K, cooled at ~573 K/h; $f(T)$ in figure 18.	1.97
Speich, Schwoeble, Leslie (1972)	Fe(0.057 C)	80 kHz pulse-echo.	Austenitized 1 h at 1273 K and water quenched.	2.082
			Best value	2.05
			Uncertainty	0.12

TABLE 9. Young's modulus E of nickel

Investigator(s) (Year)	Composition	Technique	Specimen, Test Conditions	E (10^{12} dyn/cm^2)
Guillaume (1897)		Spring tension.	X(Ni).	1.92
Schaefer (1901)		Res. freq.		2.31
Honda, Terada (1907)	a) "Pure" b) "Commercial"	Tension, opt. lever.	Ann., $f(S)$, x(Fe).	1.9 2.2
Grüneisen (1907)	97.0 Ni(1.4 Co, 0.4 Fe, 1.0 Mn, 0.1 Cu, Si)	a) Transv. res. freq. b) Tension, opt. lever.	Hard drawn.	1.95 2.01
Kurnakow, Rapke (1914)	99.9 Ni	Tension, opt.	Ann. 820–870 K, x(Cu).	1.97
Harrison (1915)		Tension, opt. mic.	Ann. 773 K, $f(T$, 293–740 K).	2.16
Koch, Dieterle (1922)		Res. freq.	$F(T$, 285–1273 K).	1.7
Honda, Tanaka (1926)	Ni(0.145 C, 0.05 Si, 0.01 Cu, 0.15 Fe, 0.04 S)	Bending, opt. lever.	Ann. 1173 K, $\frac{1}{2}$ h; x(Fe, Co, C); $f(H)$.	1.93
Mudge, Luff (1928)	99.18 Ni(0.01 C, 0.16 Cu, 0.06 Si, Mn, 0.4 Fe, 0.01 S)	Tension.	a) Hot rolled. b) Ann. 1030 K, 4 h.	2.13 2.15
Nishiyama (1929)	Ni(0.10 Fe, 0.03 Co, 0.05 Si, 0.02 P, 0.01 S)	Bending, opt. lever.	Vac. ann. 1173 K, 2 h, furnace cool.	1.99
Kawai (1930)		Tension, opt. lever.	Ann. 1173 K; $f(D$(tension)), $f(T$(anneal)).	2.10

Giebe, Blechschmidt (1931)		Res. freq.	a) Cold worked, $H=0$;
			b) Cold worked, $H=6.2$ kOe;
			c) Ann. 973 K, 12 h, slow cool;
			d) Ann. 973 K, 12 h, slow cool. $H=6.2$ kOe;
			e) Ann. 973 K, 2 h quenched, $H=0$,
			f) Ann. 973 K, 2 h, quenched, $H=6.2$ kOe.
				2.259
				2.285
				1.908
				2.256
				2.063
				2.207

Jacquerod, Mugeli (1931)	"Pure"	Bending.	a) As received. b) Ann. 858 K, H_2 atmos., 16 h; $f(T)$ in figure 19.	2.17 2.00

TABLE 9. Young's modulus E of nickel—Continued

Investigator(s) (Year)	Composition	Technique	Specimen, Test Conditions	E (10^{12} dyn/cm^2)
Zacharias (1933)	Ni(0.41 Fe, 0.13 Cu, 0.02 Mn, 0.09 Si, 0.11 C, 0.3–0.4 Co, 0.01 S) 99.9 Ni(< 0.003 Cu, 0.11 Mo)	Long. res. freq.	a) Ann. 973 K, slow cool.	2.141
			b) Ann. 1173 K, 2 h, slow cool.	1.986
			c) Ann. 1373 K, 2 h, slow cool.	2.077
			d) Ann. 1373 K, 2 h, reheated 1373 K, H_2O quench.	2.301
			a) Single crystal from melt, ann. 1373 K, H_2O quench.	2.138
			b) Single crystal from melt, slow cool from 1723 K. $F(T)$ in figure 19.	2.076
Nakamura (1935)	99.84 Ni	Long. res. freq.	Vac. ann., 1273 K, 1 h, slow cool; x(Fe).	
			a) $H=0$,	1.940
			b) $H=0.325$ kOe.	2.275
Nakamura (1936)		Long. res. freq.	F(Cu), $f(T$, 288–743 K).	1.950
Siegel, Quimby (1936)	99.715 Ni(0.01 Si, S 0.02 Cu, 0.11 Fe, Mg 0.05 C)	Long. res. freq.	Ann. 1373 K, 4 h, H_2 atmos., slow figure 33. cool; $GS=0.4$ mm.; $f(H, T)$ in	
			a) $H=0$,	2.085
			b) H sat.	2.218
Davies, Thomas (1937)	99.2 Ni	Res. freq.	a) Ann. 1123 K, 45 h.	1.937
			b) Unannealed. x(Fe).	1.918
Förster, Köster (1937a, 1938)		Transv. res. freq.	Ann. 973 K, ½ h, x(Fe), $f(T$, 293–745 K).	2.15
Förster, Köster (1937b)		Transv. res. freq.	Ann. 973 K, 1 h, slow cool; x(Fe); f(vibr. ampl.).	2.1193
Engler (1938)	99 Ni	Long. res. freq.	Ann. 973 K; $f(T, H)$ in figure 33.	
			a) $H=0$,	2.06
			b) $H=0.575$ kOe.	2.21
Kimura (1939)	"Electrolytic"	Long. res. freq.	Ann. 1223 K, 3 h, slow cool; $f(T, H)$ in figure 33;	
			a) $H=0$,	1.921
			b) H sat.	2.174
Köster (1940)		Transv. res. freq.	Ann. 973 K, 1 h, slow cool; x(Fe).	2.11
Aoyama, Fukuroi (1941)	98.9 Ni(0.3 Mn, 0.05 Fe)	"Dynamic".	Vac. ann. 1173 K, 6 h, f(Cu);	
			a) $T=289$ K.	1.70
			b) $T=78$ K.	1.95
Yamamoto (1941, 1943)	"Electrolytic"	Magnetoscillation.	Vac. ann. 1273 K, 2 h, slow cool; $f(H)$.	2.012
Yamamoto (1942, 1954)	99.6 Ni(0.08 Fe, 0.32 Co, 0.01 Si, 0.02 C)	Magnetoscillation.	Vac. ann. 1173 K, 2 h, x(Cu); $f(H)$;	
			a) $H=0$,	1.86
			b) $H=0.6$ kOe.	2.17
Köster (1943a)	Ni(0.5 Mn)	Transv. res. freq.	a) Ann. 1273 K: cold rolled 80%	2.15
			b) Vac. ann. 973 K	2.00
			c) Vac. ann. 1173 K	1.92
			d) Vac. ann. 1573 K, $H=0$	1.82
			e) Vac. ann. 1573 K, H sat.	2.19
			$F(T, GS, T$ anneal) in figure 14.	
Köster (1943b)	Ni(0.5 Mn)	Transv. res. freq.	Vac. ann. 913 K, 1 h, slow cool; x(Fe); $f(H)$; $f(T$, 293–973 K);	

TABLE 9. Young's modulus E of nickel—Continued

Investigator(s) (Year)	Composition	Technique	Specimen, Test Conditions	E (10^{12} dyn/cm^2)
			a) $H=0$, b) $H=0.5$ kOe. (Extrapolated paramagnetic fcc phase to 293 K.)	1.87 2.19 (2.16)
Masumoto, Saito (1944)	99.6 Ni(0.02 Fe, 0.02 C, 0.01 Si)	"Static", helical coils.	Vac. ann. 1273 K, 1 h, x(Cu).	1.68
Köster (1948)		Transv. res. freq.	Ann. 1173 K; $f(T)$ in figure 19; a) $H=0$, b) H sat.	 1.93 2.18
Köster, Rauscher (1948)		Transv. res. freq.	X(Cu); a) $H=0$, b) H sat.	 2.01 2.16
Bennett, Davies (1949)	99.9 Ni, 99.2 Ni	Transv. res. freq.	923 K ann. 8–29 h, $f(T$, 273–850 K) relative values, x(Fe).	
Fukuroi, Shibuya (1950)	98.9 Ni(0.3 Mn, 0.05 Fe)	Bending, interferometer.	Vac. ann. 1173 K, 1 h x(Cu).	1.65
Beck, Kouvelites, McKeehan (1951)	"Commercially pure"	Long res. freq.	a) Ann. at 923 K, 3 h, in H_2. b) Unannealed. $F(H)$ in figure 37. $\Delta E/E$ data in Kouvelites, McKeehan (1952)	1.873 2.010
Frederick (1947)		0.5–15 MHz pulse-echo.	$F(T)$ in figure 19.	2.075
Yamamoto, Taniguchi (1951, 1955)		Magnetostrictive oscillation.	Vac. ann. 1273 K, 2 h; f(Co conc.), Ni values obtained by extrapolation of Ni-Co data; $f(H)$; a) $H=0$, b) H sat.	 1.99 2.24
Umekawa (1954)		Transv. res. freq.	Vac. ann. 1123 K, ½ h; x(Cu, Co).	1.72
Burnett (1956)	99.8 Ni(0.04 Fe, 0.03 Mn, 0.11 Si, 0.01 Cu, C)	Res. freq. in bending.	$F(T)$ in figure 19.	1.89
Pavlov, Kirutchkov, Fedotov (1957)	99.99 Ni	0.7 MHz transv. res. freq.	Vac. ann. 1073 K, 3 h; x(Cu); $f(T)$ in figure 19.	2.00
Shirakawa, Numakura (1958)	Ni(0.09 Mn, 0.01 C)	Bending.	a) Vac. ann. 973 K, 1 h, $GS=0.060$ mm. b) Vac. ann. 1073 K, 1 h, $GS=0.069$ mm. c) Vac. ann. 1173 K, 1 h, $GS=0.082$ mm. d) Vac. ann. 1273 K, 1 h, $GS=0.111$ mm. e) Vac. ann. 1373 K, 1 h, $GS=0.110$ mm.	1.70 1.69 1.68 1.66 1.65
Yamamoto (1959)	Ni(0.1 Fe, 0.01 Si, Cu, 0.04 C, 0.02 S)	Magnetostrictive oscillation.	Ann. 1273 K, H_2 atmos., 1 h; reannealed 1273 K, vac., 1½ h; x(Fe); $f(H)$, a) $H=0$, b) H sat.	 1.749 1.915
Hill, Shimmin, Wilcox (1961)	Ni(0.01 C, Si, P)	Long. res. freq.	$F(T$, 293–920 K).	2.02
Durham, et al. (1963)	Ni(0.3 Mn, 0.1 Fe, 0.06 C, 0.1 S)	Tension, strain-gauge extensometer.	Ann. 1213 K, ½ h; $f(T)$ in figure 19.	1.96

TABLE 9. Young's modulus E of nickel—Continued

Investigator(s) (Year)	Composition	Technique	Specimen, Test Conditions	E (10^{12} dyn/cm^2)
Kamber (1963)	"A" Nickel; Ni(0.1 Cu, C, 0.15 Fe, 0.20 Mn, 0.05 Si, 0.005 S)	1.2 MHz transv. res. freq.	a) ann. 1623 K, H_2 atmos., ½ h, $GS=1$ mm; *no field*. b) ann. 1623 K, H_2 atmos., ½ h, $GS=1$ mm; saturated field. c) ann. 1173 K, H_2 atmos., 1 h, $GS=$ 0.13 mm. $F(T)$ in figure 19.	1.90 2.16 2.10
Tino, Maeda (1963)	Electrolytic Ni	Res. freq., 20–30 kHz.	a) $H=0$, b) $H=320$ Oe. $F(T, H)$ in figure 33.	2.06 2.17
Armstrong, Brown (1964)	Ni(0.55 metallic, 0.05 C, 0.005 S+O)	Long. res. freq.	Ann. 1173, $f(T)$ in figure 19.	2.06
Orlov, Fedotov (1966)	99.98 Ni	Trans., long. res. freq.	Vac. electron arc melting, x(Cu), $f(T)$ in figure 19.	2.08
Masumoto, Saito, Murakami, Kikuchi (1968)	Ni(0.19 Co, 0.01 Fe, Al, 0.02 C)	Res. freq.	$F(T)$ in figure 19.	1.95
Faninger (1969)	99.99 Ni	Tension, x-ray.	X(Cu), $f(H)$.	2.15
Masumoto, Saito, Sawaya (1970)	Electrolytic 99.98 Ni (0.016 Co, 0.001 Cu, 0.001 Fe, 0.002 S, 0.000 Si, Mn, Pb, C)	600–800 Hz oscillator.	Vac. ann. 30 min. at 1173 K, cooled 300 °C/h.	1.96
			Best values (no field) *(sat. field)*	1.97 2.18
			Uncertainties (no field) (sat. field)	0.15 0.09

TABLE 10. Young's modulus E of iron-nickel alloys

Investigator(s) (Year)	Composition	Technique	Specimen, Test Conditions	E (10^{12} dyn/cm^2)
Guillaume (1897, 1898, 1927)	15 alloys	Spring tension.	X(Cr, C), $f(T$, 243–313 K).	Figure 5
Angenheister (1903)	Fe-24.1 Ni (0.36 C, 0.41 Mn)	Tension.	a) Ann. "non-magnetic", b) Cooled to 76 K, "magnetic".	1.74 1.53
Carpenter, Hadfield, Longmuir (1905)	6 alloys, impurities (0.40–0.52 C, 0.8–0.18 Si, 0.01–0.04 S, P	Tension extensometer.	Ann. 1030 K, slow cool.	Figure 5
Honda, Terada (1907)	6 alloys	Tension, opt. lever.	$F(S)$.	Figure 5
Honda (1919)	14 alloys	Bending, opt. lever.	Ann. 1173 K.	Figure 5
Müller (1922)	12 alloys, impurities (0.12–0.73 C, 0.34–1.24 Mn, 0.13–0.27 Si, ≤ 0.02 P, ≤ 0.04 S)	Tension, opt. microscope).	Ann. 813–1073 K.	Figure 5
Carrington (1924)	Fe-3.41 Ni (0.19 C, 0.55 Mn, 0.03 P, S, 0.10 Si)	Bending.	Ann. 1180 K, ½ h, slow cool; $f(T)$ in figure 21.	2.07
Kimball, Lovell (1925)	Fe-3.5 Ni (0.35 C, 0.21 Si, 0.02 S, P, 0.58 Mn)	Transv. res. freq.	Ann. 1123 K, *oil quench, drawn* 923 K, $f(T)$ in figure 22.	
Honda, Tanaka (1926)	12 alloys	Bending, opt. lever.	Ann. 1173 K, 2 h, slow cool; $f(H)$.	Figure 5

TABLE 10. Young's modulus E of iron-nickel alloys—Continued

Investigator(s) (Year)	Composition	Technique	Specimen, Test Conditions	E (10^{12} dyn/cm^2)
Chevenard (1927, 1943) also Chevenard, Crussard (1943)	33 alloys	Bending, torsion.	Ann. 1173 K.	Figure 5
Nishiyama (1929)	9 alloys from electrolytic Fe, Mond Ni	Bending, opt. lever.	Ann. 1173 K, 2 h, furnace cooled.	Figure 5
Kawai (1930)	Fe-3 Ni (0.3 C)	Tension.	a) Ann. 1133 K, b) tensile elongation = 2.1%, c) tensile elongation = 5.3%, d) tensile elongation = 8.0%, e) tensile elongation = 12.9%.	2.07 2.01 1.99 1.97 2.02
Honegger (1932)	a) Fe-5 Ni b) Fe-3 Ni	Transv. res. freq.		1.99 1.94
Keulegan, Houseman (1933)		Tension, torsion.	$F(T$, 295–906 K) in Fe-3.5–5.0 Ni, ann. ½ h, furnace cooled or water quenched; Fe-35 Ni as received; $f(T)$, temp. coeff. at 273 K.	
Nakamura (1935)	10 alloys from 99.94 Fe, Ni	Long. res. freq.	Vac. ann. 1273 K, 1 h, slow cool, $f(H)$.	Figure 5
Moller, Barbers (1936)	Fe-0.02 C, Si, S, 0.37 Mn, 0.05 P)	a) X-ray. b) Tension.	Vac. ann. 873 K, 1 h, slow cool.	1.79 1.98
Förster, Köster (1937)	Fe-22.4 Ni	Transv. res. freq.	$F(T)$, in figure 38.	1.49
Förster, Köster (1937)	6 alloys	Transv. res. freq.	F(vibr. ampl.).	Figure 5
Davies, Thomas (1937)	Fe-48 Ni	Res. freq.	a) Ann. 1173 K, 7 h. b) As received.	1.365 1.529
Döring (1938)	Fe-42 Ni	Res. freq.	a) $H = 0$. b) $H = 0.575$ kOe. $F(T)$ in figure 20.	1.575 1.62
Engler (1938)	4 alloys (0.4 Mn, 0.1 Si)	Long. res. freq.	Ann 973 K, 3 h, slow cool; $f(T, X)$ in figure 20; $f(H, X)$ in figure 33. $f(D, X)$ in figure 13.	Figure 5
Scheil, Thiele (1938)	Fe-22.4 Ni (0.2 Mn, 0.28 Si, 0.03 C, 0.01 P, S	Res. freq.	Ann. 1083K, H_2, $f(T)$ in figure 21.	1.50
Williams, Bozorth, Christensen (1941)	Fe-68 Ni (0.3 Mn)	Long. res. freq.	a) Rolled (83% red. thick.), i) $H = 0$, ii) H Sat. b) Ann. 1273 K, 1 h, H_2, slow cool, i) $H = 0$, ii) H Sat. c) Treatment (b), then 873 K, rapid cool, i) $H = 0$, ii) H Sat. d) Treatment (b), then 873 K, H_2 cool in 0.01 kOe long. field, i) $H = 0$, ii) H Sat. e) Treatment (b); then 873 K, H_2, cool in 0.01 kOe transv. field, i) $H = 0$, ii) H Sat.	1.8145 1.8161 1.783 1.870 1.654 1.826 1.843 1.930 2.105 2.181
Chevenard, Crussard (1943)	a) Fe-49 Ni b) 12 alloys	Bending, torsion.	Cold worked 44%; $f(T)$ in figure 20. Annealed.	1.93 Figure 5
Seager, Thompson (1943)	Fe-3.1 Ni (0.51 Mn, 0.16 Si, 0.2 C, 0.01 S, P)	Bending, interferometric.	Ann., $f(T)$ in figure 21.	1.92
Köster (1943b)	11 alloys	Transv. res. freq.	Ann. 1273 K, 1 h; f(Ni). $F(H)$, $f(T)$ in figure 20.	Figure 5

TABLE 10. Young's modulus E of iron-nickel alloys—Continued

Investigator(s) (Year)	Composition	Technique	Specimen, Test Conditions	E (10^{12} dyn/cm^2)
Scheil, Reinacher (1944)	7 alloys (0.1-0.9 Mn, 0.1-0.3 Si)	Transv. res. freq.	Ann. 1173 K, H_2 atmos., $\frac{1}{2}$ h., slow cool; $f(T)$ in figure 20.	Figure 5
Fontana (1948)	Fe-8.6 Ni (0.77 Mn, 0.23 Si, 0.05 Al, 0.05 Ti, 0.01 C, P 0.02 S)	Tension, strain gauges.	Ann. 1173 K, 1 h, air cool then 1063 K, 1 h, air cool; then 838 K, 2 h, air cool; $f(T)$ in figure 21.	1.91
Bennett, Davies (1949)	Fe-48 Ni	Res. Freq.	Ann. 923 K, 10 h; $f(T)$ in figure 22.	
Fine, Ellis (1950)	15 alloys (0-0.4 Co, 0.0.7 Mn)	Long. res. freq.	Cold swaged 74%; ann. 1223 K. 1 h; $f(T)$ in figure 20. Cold swaged 41, 55%; ann. 673 K, not plotted.	Figure 5
Beck, Kouvelites, McKeehan (1951)	5 alloys (46.2, 69.1, 84.9, 88.5, 100 Ni)	Long. res. freq.	Ann. at 923 K, 3 h, in H_2. $F(H)$ in figure 37. $\Delta E/E$ data in Kouvelites, McKeehan (1952).	Figure 5
Ochsenfeld (1955)	Fe-60 Ni	Res. freq.	a) No field, b) Saturated field.	1.76 1.86
Markham (1957)	Fe-3 Ni	a) Tension. b) 10 MHz pulse-echo.		2.01 2.05
Yamamoto (1959)	12 alloys from Armco iron, Mond nickel	Magnetostrictive vibration.	Ann. 1273 K, 1 h, H_2; then vac. ann. 1273 K, $1\frac{1}{2}$ h; $f(H, x)$.	Figure 5
Hill, Shimmin, Wilcox (1961)	Fe-35.6 Ni	Long. res. freq.	"Recrystallized"; $f(T)$ in figure 20.	1.48
Durham, et al. (1963)	Fe-36 Ni (0.8 Mn, 0.4 Si, 0.2 Se, 0.08 C, 0.01 P, S)	Torsion, opt. lever.	Cold drawn 12–15%, $f(T)$ in figure 20.	1.45
Tino, Maeda (1963)	6 alloys, 26.2-100 Ni	Res. freq., 20-30 kHz.	$F(T, H)$ in figure 34, $f(D)$ in figure 13.	Figure 5
Goldman, Robertson (1964)	Fe-29.9 Ni (0.004 C) Fe-25.1 Ni (0.26 C)	Long. res. freq.	Vac. ann. 1173 K, $\frac{1}{2}$ h; 0.035 mm GS; $f(T)$ in figure 38.	Figure 5
Doroshek (1964)	6 alloys (0.4-0.5 Mn, 0.14-0.48 Si, 0.17-0.38 Cr, 0.01 Al, 0.02-0.03 C, 0.02-0.04 P, S)	Res. freq.		Figure 5
Smith, Stern, Stephens (1966)	Fe-2.5 Ni (0.4 C, 0.6 Cr, 0.5 Mo)	Long, transv. pulse-echo.	$F(P)$, third-order stiffnesses.	2.10
Eganyan, Selissikiy (1967)	Fe-75 Ni	Res. freq.	$F(H)$, a) $H = 0$, b) $H = 1$ kOe. $F(T)$ in figure 20.	2.06 2.16
Kototayev, Koneva (1968)	Fe-75 Ni	Res. freq.	$F(T)$ in figure 22, relative values.	....
Khomenko, Tseytlin (1969)	9 alloys, 30.2-46.4 Ni	Res. freq.	Vac. ann. at 1173 K, 2 h, cooled at 100°/h. a) 30.2 Ni, $H = 0$; b) 30.2 Ni, $H =$ sat.; c) 46.4 Ni, $H = 0$; d) 46.4 Ni, $H =$ sat.	1.67 1.67 1.33 1.49
Shirakawa, et al. (1969)	9 alloys, 26.2-100 Ni	Res. freq.	H sat. Polycrystal and ⟨100⟩, ⟨110⟩, ⟨111⟩ single crystals.	Figure 5
Maeda (1971)	Fe-35 Ni	Res. freq.	Vac. ann. at 1273 K, 10 h,	

TABLE 10. Young's modulus E of iron-nickel alloys—Continued

Investigator(s) (Year)	Composition	Technique	Specimen, Test Conditions	E (10^{12} dyn/cm^2)
			a) $H=0$, b) $H=190$ Oe, c) $H=1900$ Oe. $F(T, H)$ in figure 34.	1.26 1.36 1.38
Diesburg (1971)	3 alloys	10 MHz pulse-echo-overlap.	Calculated from c_{ij} by V-R-H method.	Figure 5
Hausch, Warlimont (1972)	9 alloys	10 MHz pulse-echo.	Calculated from c_{ij} by V-R-H method.	Figure 5

TABLE 11. Shear modulus G of iron

Investigator(s) (Year)	Composition	Technique	Specimen, Test Conditions	G (10^{12} dyn/cm^2)
Earlier reports (1853-1900)			Range = 0.68 – 0.83.	average = 0.76
Schaefer (1901)		Torsional res. freq.		0.719
Benton (1903)	"Steel"	Torsion	$F(T$, 76–300 K), relative to 300 K.	
Horton (1905)		Res. freq.	$F(T), f(A)$.	0.826
Grüneisen (1908)	a) "Steel" b) "Iron"	Long. res. freq.		0.812 0.831
Guye, Freedericksz (1909)		Torsion pendulum.	$F(T)$ in figure 23.	0.805
Koch, Dannecker (1915)		Torsion	$F(T)$ in figure 23.	0.79
Honda (1919)	Fe (0.29 Cu, 0.31 Mn, 0.11 Si, 0.09 C, 0.03 P, S)	Torsion, opt. lever.	X(Co).	0.84
Honda (1919)		Torsion, opt. lever.	Ann. 1173 K, $f(X)$.	0.834
Honda, Hasimoto (1921)	Fe (0.18 C, 0.2 Si + Mn)	Torsion, opt. lever.	Ann. 1173 K, a) slow cool, b) oil quench. X(C), $f(CR)$.	0.832 0.806
Iokibe, Sakai (1921)	99.98 Fe (0.0085 C)	Torsional oscillations.	Ann. 1973 K, $f(T)$ in figure 23.	0.78
Kikuta (1921)	Fe (0.35 C)	Res. freq.	Ann. 1173 K, $f(T)$ in figure 23.	0.807
Honda, Tanaka (1926)	Fe (0.38 Mn, 0.1 C, 0.02 P, S) Fe (0.31 Mn, 0.11 Si, 0.09 C, 0.29 Cu, 0.03 P, S)	Torsion, opt. lever.	X(Ni, Co, C), $f(H)$. a) Ann. 1173 K, ½ h slow cool. b) Ann. 1173 K, ½ h oil quench. c) Ann. 1173 K, 2 h., slow cool.	 0.813 0.792 0.834
Chevenard (1927)		Torsion.	X (Ni, Cr, C).	0.85
Goens (1930)		a) Res. freq. b) Torsion.		0.800 0.808
Gutenberg, Schlechtweg (1930)		Res. freq., torsion.		0.78
Everett (1931)	Fe (0.35 C, 0.80 Mn, 0.10 Si, 0.02 P, 0.03 S)	Torsion, dial gauge, mech. lever.	Ann. 1173 K, ½ h, slow cool $F(T$, 295–773K).	0.794
Kawai (1931)	"Armco iron"	Torsion, opt. lever.	Ann. 1273 K, $f(D)$ in figure 10.	0.812
M'Farlene (1931)	"Soft iron"	Torsion pendulum.	$F(D)$ in figure 10.	0.78

TABLE 11. Shear modulus G of iron—Continued

Investigator(s) (Year)	Composition	Technique	Specimen, Test Conditions	G (10^{12} dyn/cm^2)
Keulegan, Houseman (1933)	Fe (0.66 C, 0.8 Mn, 0.01 P, 0.04 S)	Helical loaded springs.	Temp. coeff., 223–323 K.	
Verse (1935)	a) Fe (0.4 C, 0.86 Mn, 0.04 S, 0.02 P, 0.14 Si)	Torsion.	Ann., $f(T$, 298–773 K).	0.796
	b) Fe (0.34 C, 0.80 Mn, 0.10 Si 0.02 P, 0.03 S)	Long. torsional res. freq.	Ann. 1173 K, $f(T)$ in figure 23.	0.798
Bez-Bardili (1935)		Long., transv. sound-wave velocities, 1–20 MHz.		0.845
Brown (1936)	"Armco iron"	Long. (56 MHz), torsional (39 MHz) res. freq.	Ann., $f(H)$.	0.846
Glocker, Schaaber (1938)	Fe (0.06 C)	Torsion, x-ray		0.798
Everett, Miklowitz (1944)	Fe (0.15–0.25 C, 0.3–0.6 Mn, 0.04 P, 0.05 S); SAE 1020	Torsion, opt. lever.	$F(T)$ in figure 23.	0.78
Garofalo, Malenock, Smith (1952)	Fe (0.45 Mn, 0.19 Si, 0.13 C, 0.01 P, 0.02 S); (SAE 1015)	Torsion, opt. lever.	Ann. 1170 K, ½ h air cooled; $f(T)$ in figure 23.	0.80
Hughes, Kelly (1953)	"Armco iron"	Pulse-echo.	$F(P)$.	0.820
Burnett (1956)	99.8 Fe	"Free-free sonic vibration", res. freq. in torsion.	$F(T)$ in figure 23.	0.78
Hughes, Maurette (1956)	"Armco iron"	Pulse-echo.	$F(P)$, $f(T)$ in figure 23.	0.814
Voronov, Vereshchagin (1961)	99.8 Fe (0.02 Mn, 0.02 Si, 0.012 C, 0.03 P, S)	10 MHz pulse-echo.	Ann.; $f(P)$.	0.812
Durham, McClintock, Reed, Warren, Guntner (1963)	Fe (0.8 C, 0.3 Mn, 0.15 Si)	Torsion, opt. lever.	Ann. 1056 K, 1 h, oil quench, temper 655 K, 1 h, air cool; $f(T)$ in figure 23.	0.795
Smith, Stern, Stephens (1966)	a) Fe (0.8 Mn, 0.3 Si, 0.4 C)	Long. and transv. pulse-echo.	X(Ni), $f(P)$, third-order polycrystalline moduli.	0.821
	b) Fe (0.8 Mn, 0.2 Si, 0.6 C)			0.820
Frederick (1947)	"Armco iron"	0.5–15 MHz pulse-echo.	$F(T)$.	0.808
Speich, Schwoeble, Leslie (1972)	Fe (0.057 C)	80 kHz pulse-echo.	Austenitized 1 h at 1000 °C and water quenched.	0.806
			Best value	0.81
			Uncertainty	0.03

TABLE 12. Shear modulus G of nickel

Investigator(s) (Year)	Composition	Technique	Specimen, Test Conditions	G (10^{12} dyn/cm^2)
Earlier reports (1853–1900)			Range: 0.68–0.83	average 0.76
Schaefer (1901)		Torsion, res. freq.		0.933
Grüneisen (1908)		Long. res. freq.	Hard drawn.	0.770
Guye, Schapper (1910)		Torsional oscillations.	$F(T)$ in figure 24.	0.762
Koch, Dannecker (1915)		Res. freq.	$F(T)$ in figure 24.	0.716

TABLE 12. Shear modulus G of nickel—Continued

Investigator(s) (Year)	Composition	Technique	Specimen, Test Conditions	G (10^{12} dyn/cm^2)
Iokibe, Sakai (1921)		Torsional oscillations under tensile load.	Vac. ann. 1073 K, $f(T)$ in figure 24.	0.723
Kikuta (1921)		Torsional oscillations under tensile load.	Ann., $f(T)$ in figure 24.	0.782
Honda, Tanaka (1926)	99.6 Ni (0.15 Fe, 0.14 C, 0.01 Cu, 0.05 Si, 0.04 S)	Torsion, opt. lever.	Ann. 1173 K, 0.5 h; $f(H)+x$(Fe).	0.750
Chevenard (1927)		Torsion.	X(Fe, Cr).	0.86
Mudge, Luff (1928)	99.18 Ni (0.1 C, 0.16 Cu, 0.06 Si, 0.01 S, 0.4 Fe, 0.05 Mn)	Torsion.	a) Hot rolled. b) Ann. 1030 K, 4 h.	0.78 0.758
Gutenberg, Schechtweg (1930)		Res. freq. in torsion.		0.80
Kawai (1931)	99.5 Ni	Torsion, opt. lever.	Ann. 1073 K, $f(D$, tension) in figure 11, $f(R)$.	0.785
Mobius (1932, 1934)		Res. freq.	$F(H)$; $f(T$, 293–673 K).	
Kikuchi (1936)		Torsion.	X(Cu).	0.710
Landon, Davies (1938)	99.2 Ni	Res. freq. in torsion.	a) Ann. 1133 K, $\frac{1}{4}$ h, cold rolled, Brinnell hardness = 210. b) Ann. 1133 K, $\frac{1}{4}$ h, cold rolled, ann. 1133 K, $\frac{1}{4}$ h.	0.800 0.827
Burnett (1956)	99.8 Ni (0.04 Fe, 0.03 Mn, 0.11 Si, 0.01 Cu, C)	Res. freq. in torsion.	$F(T)$ in figure 24.	0.738
Susse (1956)	99.7 Ni	Torsional res. freq.	$F(T)$ in figure 24.	0.79
Orlov, Fedotov (1966)	99.98 Ni	Long., transv., torsional res. freq.	Ann., x(Cu), $f(T)$ in figure 24.	0.805
Faninger (1969)	99.99 Ni	X-ray, tension.	X(Cu), $f(H)$.	0.83
Shirakawa, et al. (1969)	Electrolytic Ni (0.012 Fe, 0.007 Si, 0.008 Cu, 0.003 Mn)	Res. freq.	H sat., 1 mm GS.	0.83
Frederick (1947)		0–15 MHz pulse-echo.	$F(T)$.	0.808
			Best value	0.78_5
			Uncertainty	0.05

TABLE 13. Shear modulus G of iron-nickel alloys

Investigator(s) (Year)	Composition	Technique	Specimen, Test Conditions	G (10^{12} dyn/cm^2)
Angerheister (1903)	Fe-24.1 Ni (0.36 C, 0.41 Mn)	Tension, torsion, res. freq.	a) Ann. "non-magnetic", fcc. b) Cooled to 76K, "magnetic", bcc.	0.67 0.56
Guye, Woelfle (1907)	Fe-36.118 Ni (0.02 Cu)	Res. freq.	$F(T)$ in figure 25.	0.563
Honda (1919)	13 alloys	Torsion, opt. lever.	Ann. 1173K.	Figure 6
Chevenard (1920)	Fe-36 Ni	Res. freq. in torsion.	Ann. 973K, cold worked, tempered, ann. $F(T)$ in figure 25.	
Honda, Tanaka (1926)	12 alloys	Torsion, opt. lever.	Ann. 1173 K, $\frac{1}{2}$ h; $f(H)$.	Figure 6

TABLE 13. Shear modulus G of iron-nickel alloys — Continued

Investigator(s) (Year)	Composition	Technique	Specimen, Test Conditions	G (10^{12} dyn/cm^2)
Chevenard (1927)	35 alloys	Res. freq. in torsion.	Ann. 1023K, x(Cr); $f(T)$, relative in figure 26.	Figure 6
Landon, Davies (1938)	Fe-48 Ni	Res. freq. in torsion.	a) Unannealed 1173K, 20 min., rolled 40%. b) Ann. 1173K, 20 min., rolled 40%, ann. 1173K, 20 min.	0.601 0.596
Burnett (1956)	66.97 Fe, 31.95 Ni (0.81 Mn, 0.14 Si, 0.05 Cr, 0.08 C)	Res. freq. in torsion.	$F(T)$ in figure 25.	0.58
Markham (1957)	Fe-3 Ni	a) 10 MHz pulse-echo. b) Torsion.		0.797 0.790
Bungardt, Preisendanz, Brandis (1962)	a) 90.68 Fe, 9.21 Ni (0.05 Mn, 0.02 C, 0.01 P, S, N) b) 82.74 Fe, 17.14 Ni (0.05 Mn, 0.02 C, 0.01 P, S, N)	Res. freq. in torsion.	Ann. 1173 K, 1 h; $F(T$, 100–1100 K), relative, in figure 26.	
Durham, McClintock, Guntner, Warren (1963)	Fe-36 Ni (0.8 Mn, 0.2 Se, 0.08 C, 0.01 P, S)	Torsion, opt. lever.	Cold drawn 12-15%., $f(T)$ in figure 25.	0.565
Goldman, Robertson (1964)	a) Fe-29.9 Ni (0.004 C) b) Fe-25.1 Ni (0.26 C)	Long., torsional res. freq.	Vac. ann. 1173 K, ½ h, 0.035 mm GS; $f(T)$ in figure 25. i) fcc ii) bcc i) fcc ii) bcc	 0.68 0.54 0.72 0.625
Smith, Stern, Stephens (1966)	Fe-2.5 Ni (0.4 C, 0.6 Cr, 0.5 Mo)	Long., transv. pulse-echo.	$F(P)$, third-order stiffnesses.	0.818
Roberts, Owen (1967)	6 alloys (50 ppm C)	Res. freq. in torsion.	Ann. 1198K, ½ h, 2% H_2 atmos., quenched.	Figure 6
Meincke, Litva (1969)	Fe-35 Ni	Sound velocity measurements.	Ann. 1273K, air cool. $F(T)$ in figure 25.	0.56
Maeda (1971)	Fe-35 Ni	Res. freq.	Vac. ann. 1273 K, 10 h, a) $H = 0$, b) $H = 190$ Oe, c) $H = 1900$ Oe. $F(T, H)$ in figure 3.	 0.407 0.458 0.473
Shirakawa, et al. (1969)	9 alloys, 26.2-100 Ni	Res. freq.	H sat. Polycrystal and ⟨100⟩, ⟨110⟩, ⟨111⟩ single crystals.	Figure 6
Diesburg (1971)	3 alloys	10 MHz pulse-echo-overlap.	Calculated from c_{ij} by V-R-H method.	Figure 6
Hausch, Warlimont (1972)	9 alloys	10 MHz pulse-echo	Calculated from c_{ij} by V-R-H method.	Figure 6

TABLE 14. Bulk modulus B and compressibility B^{-1} of iron

Investigator(s) (Year)	Composition	Technique	Specimen, Test Conditions	B_s	dB_S/dP	$B^{-1}=a^*$	B_T	b^*
				(10^{12} dyn/cm^2		(10^{-7} cm^2/dyn)	(10^{12} dyn/cm^2)	(10^{-24} cm^4/dyn^2)
Richards (1907)						0.40		
Grüneisen (1908)		Res. freq., $\Delta l/l$ measurements.				0.62	1.61	
Grüneisen (1908)		$\Delta l/l$ measurements.	Range: 0.570–0.641. $f(T)$ in figure 27.			0.61 0.61	1.64 1.64	
Richards, Bartlett (1915)		$\Delta V/V$ measurements, Hg bath.	$100 < P < 500$ bar.					
Bridgman (1923)	99.97 Fe	$\Delta l/l$ of rod under hydrostatic pressure.	$P \leq 10$ k bar. a) 303 K b) 348 K			0.599 0.605 0.603	1.669 1.653 1.658	2.18 2.18 1.37
Ebert (1935)		$\Delta l/l$ of rod, comparative.	Single crystal, $P \leq 5$ kbar.			0.612	1.634	
Ebert, Kussmann (1937)	99.99 Fe	Pressure dep. in magnetic field.	X(Ni), $f(H)$, saturated field.					
Bridgman (1940a, 1940b)		$\Delta l/l$, lever piezometer.	$P \leq 30$ kbar, Slater (1940) correction, a) 297 K, b) 348 K.			0.595 0.601 0.5941	1.680 1.664 1.683	0.82 0.82 0.83
Birch (1947)		Correction to Bridgman data.	$T=297$ K.			0.590	1.695	0.843
Bridgman (1949)	Fe(0.008 Ni, C, 0.002 i, 0.001, < 0.001 Co, Cr, Mo, Mn, 0, < 0.005 Cr)	$\Delta l/l$, lever improved piezometer; Compared to Fe, Bridgman (1940).	$P \leq 30$ kbar, $T=296–299$ K.	1.641	2.7±1.6	6.093	1.641	
Hughes, Kelly (1953)	"Armco Iron"	Pulsed ultrasound velocities.	Simple compression and hydrostatic pressure to 9 kbar.		4.30	0.6033	1.656	0.947

Hughes, Maurette (1956)	"Armco iron"	Pulse-echo.	Polycrystals;
			$f(T)$ in figure 27;
			isothermal data calculated;
			a) $P=1$ bar, $T=303$ K;
			b) $P=1$ bar, $T=373$ K;
			c) $P=9$ kbar, $T=303$ K;
			d) $P=9$ kbar, $T=373$ K.
				1.686
				1.683
				1.735
				1.712
				1.667
					5.13	0.606	1.650	1.10

TABLE 14. Bulk modulus B and compressibility B^{-1} of iron—Continued

Investigator(s) (Year)	Composition	Technique	Specimen, Test Conditions	B_s	dB_S/dP	$B_T^{-1}=a$*	B_T	b*
				(10^{12} dyn/cm^2)		(10^{-12} cm^2/dyn)	(10^{12} dyn/cm^2)	(10^{-24} cm^4/dyn^2)
Voronov, Vereshchagin (1961)	99.8 Fe(0.02 Mn, Si, 0.01 C, 0.03 P, S)	10 MHz pulse-echo.	Ann. polycrystals, up to 10 kbar, isothermal data calculated.					
Rotter, Smith (1966)	99.99 Fe(Cr, Mn traces)	10 MHz pulse-echo.	Specimens from crystal of Rayne, Chandrasekhar (1961), $f(P)$.	1.569	5.97	0.6098	1.637	1.29
Aliev, Lazarev, Sudovtsov (1967)		Bimetallic helix.	T=4.2 K.			0.58	1.72	
Guinan, Beshers (1968)	"Armco iron"	10 MHz pulse-echo.	Specimens from Lord, Beshers (1965), single crystals; $f(P)$; isothermal data calculated.	1.564	5.29	0.6117	1.635	1.15
Takahashi, Bassett, Mao (1968)		High pressure x-ray diffraction, NaCl standard.	a) From Murnaghan molar volume eqn. b) From 1st-order Birch molar volume eqn.			0.618 0.625	1.62 1.60	
			Best values	1.564	4.68	0.606	1.649	1.17
			Uncertainties	0.015	1.26	0.009	0.025	0.43

*a and b are coefficients in the equation $\Delta V/V_0 = aP + bP^2$.

TABLE 15. Bulk modulus B and compressibility B^{-1} of nickel

Investigator(s) (Year)	Composition	Technique	Specimen, Test Conditions	$B_T^{-1}=a^*$ (10^{-12} cm^2/dyn)	B_T (10^{12} dyn/cm^2)	b^* (10^{-24} cm^4/dyn^2)
Grüneisen (1908)		Res. freq., $\Delta l/l$ measurements.		0.57	1.75	
Bridgman † (1923)	a) 99 Ni.	$\Delta l/l$ Fe standard, piezometer, hydrostatic P.	Ann. 2 h. $F(P, \leq 1$ kbar).			
			i) $T=303$ K,	0.535	1.869	2.14
			ii) $T=348$ K.	0.539	1.855	2.14
	b) "Pure"	$\Delta l/l$ tensile.	Drawn, ann. to "bright red"			
			i) $T=303$ K,	0.540	1.853	2.14
			ii) $T=348$ K.	0.546	1.832	2.14
Ebert, Kussmann (1937)	Ni (0.12 Fe, 0.04 Mn, Si, 0.1 Co., 0.05 Cu)	$\Delta A/A$ in magnetic field.	Saturated field. $F(H), X(\mathrm{Ni}), P \leq 10$ kbar.	0.542	1.845	
Bridgman (1949)	about 99.98 Ni	Piezometer, Fe standard, hydrostatic P, $\Delta l/l$.	Ann., H_2, ~ 1650 K. $F(P, \leq 30$ kbar). $T=296-299$ K.	0.488	2.048	
Aliev, Lazarev Sudovtsov (1967)		Bimetallic helix, differential, compared to Pb	$T=4.2$ K.	0.49	2.02	
Tanji, et al. (1970), reported also in Shirakawa, et al. (1969)		Calc. from E, G data.	Ann. 1273 K, 3 h.			
			a) $H=0$,	0.46	2.17	
			b) H sat.	0.54	1.85	
			Best values	0.526	1.903	2.14
			Uncertainties	0.036	0.127	—

*a and b are coefficients in the equation $\Delta V/V_0=aP+bP^2$.

†Original values corrected according to Bridgman (1946, 1949).

TABLE 16. Bulk modulus B and compressibility B^{-1} of iron-nickel alloys

Investigator(s) (Year)	Composition	Technique	Specimen, Test Conditions	B^{-1} (10^{-12} cm^2/dyn)	B (10^{12} dyn/cm^2)
Ebert, Kussmann (1937)	13 alloys from 99.99 Fe, Ni(0.12 Fe, 0.04 Mn, 0.1 Co, 0.05 Cu, 0.04 Si)	Pressure dependence in magnetic field.	X(Co, Cr, Pt).	Figure 7	
Takahashi, Bassett, Mao (1968)	Fe-5.15 Ni	P to 300 kbars, H to 15 kOe, x-ray diffraction, NaCl standard, molar volume detn.	a) Using Murnaghan eqn.	0.645	1.55
			b) Using 1st order Birch eqn.	0.641	1.56
	Fe-10.26 Ni		a) Using Murnaghan eqn.	0.645	1.55
			b) Using 1st order Birch eqn.	0.654	1.53
Meincke, Litva (1969)	Fe-35 Ni	Sound velocity measurements.	Ann. 1273 K, air cool; $f(T)$ in figure 29.	0.90	1.11
Maeda (1971)	Fe-35 Ni	Flexural and torsional resonance of a bar specimen. Calc. from E and G data.	Vac. ann. at 1273 for 10 h.		
			a) $H=190$ Oe,	0.813	1.23
			b) $H=1900$ Oe. $F(T), f(H)$ in figure 36.	0.847	1.18
Diesburg (1971)	3 alloys	10 MHz pulse-echo-overlap	Calculated from c_{ij} by V–R–H method.	Figure 7	
Hausch, Warlimont (1972)	9 alloys	10 MHz pulse-echo.	Calculated from c_{ij} by V–R–H method.	Figure 7	

TABLE 17. Poisson ratio ν of iron

Investigator(s) (Year)	Composition	Technique	Specimen, Test Conditions	ν
Earlier publications (1879–1903)	a) "Steel" b) "Iron"		Range = 0.27 – 0.30. Range = 0.26 – 0.32.	average 0.29 average 0.28
Benton (1901)	"Iron"	Interference microscope.		0.29
Schaefer (1901)		Torsion, res. freq.		0.247
Morrow (1903)	"Wrought iron"	Meas. of lateral and long. strains under compression.	Range = 0.270 – 0.289.	0.275
Grüneisen (1908)	a) "Steel" b) "Iron"	Res. freq.		0.287 0.280
Grüneisen (1910)		Bending, torsion.	Range = 0.28 – 0.293.	average 0.284
Carrington (1924)	a) "Wrought iron" b) Fe(0.19 C)	Flexure.	Ann. 1183 K, slow cool, $f(T)$ in figure 30. Ann. 1183 K, slow cool, $f(T)$ in figure 30.	0.23 0.27
Honda, Tanaka (1926)	Fe(0.09 C, 0.11 Si, 0.31 Mn, 0.03 P, S, 0.29 Cu)	Bending torsion.	Ann. 1173 K, ½ h, $f(H)$, x(Ni).	0.27
Keulegan, Houseman (1933)	Fe(0.66 C, 0.8 M, 0.01 P, 0.04 S)	Loaded helical springs.	Detm. temp. coeff., 223–323 K.	
Verse (1935)	a) Fe(0.43 C, 0.86 Mn, 0.04 S, 0.02 P, 0.14 Si) b) Fe(0.34 C, 0.80 Mn, 0.10 Si, 0.02 P, 0.03 S)	Tension cathetometer torsion. Long., torsional res. freq.	Ann. $f(T$, 298–733 K). Ann. 1173 K, $f(T)$ in figure 30.	0.295 0.307
Bez-Bardili (1935)		Long., transv. sound-wave velocities, 1–20 MHz.	Calc. from meas. E, G.	0.290
Smith, Wood (1941)	99.95 Fe	Tension, x-ray spectrometer.	Vac. ann. 0.050 in. sheet.	0.27
Everett, Miklowitz (1944)	Fe(0.15–0.25 C, 0.3–0.6 Mn, 0.04 P, 0.05 S) [SAE 1020]	Bending, torsion.	a) Hot rolled, b) Cold rolled. $F(T)$ in figure 30.	0.313 0.286
Garofalo, Malenock, Smith (1952)	Fe(0.45 Mn, 0.19 Si, 0.13 C, 0.01 P, 0.02 S) [SAE 1015]	Bending, torsion.	Ann. 1170 K, ½ h, air cooled. $F(T)$ in figure 30.	0.265
Burnett (1956)	99.8 Fe	"Free-free sonic vibration," res. freq. in torsion.	$F(T)$ in figure 30.	0.275
Voronov, Vereshchagin (1961)	99.8 Fe(0.01 C, 0.02 Si, Mn, 0.03 P, S)	10 MHz pulse-echo.	Ann., a) Hydrostatic $P = 0$, b) Hydrostatic $P = 9.8$ bar.	0.290 2.292
Shved (1964)	"Armco iron"	X-ray scattering, uniaxial tension.		0.283
			Best value	0.282
			Uncertainty	0.019

Table 18. Poisson ratio ν of nickel

Investigator(s) (Year)	Composition	Technique	Specimen, Test Conditions	ν
Schaefer (1901)		Torsion, res. freq.		0.240
Benton (1901)		Interference microscope.	0.96 Diam. wire. 1.49 diam. wire.	0.375 0.271
Grüneisen (1908)		Static.		0.309
Honda, Tanaka (1926)	Ni(0.05 Si, 0.01 Ca, 0.15 Fe, 0.04 S, 0.14 C)	Bending, torsion.	Ann. 1173 K, ½ h; $f(H)$; X(Fe).	0.29
Burnett (1956)	99.8 Ni(0.04 Fe, 0.03 Mn, 0.11 Si, 0.01 Cu)	Res. freq. in bending, torsion.		0.280
Köster (1961)		Calculated from Köster E, G data.		0.31
			Best value	0.296
			Uncertainty	0.029

Table 19. Poisson ratio ν of iron-nickel alloys

Investigator(s) (Year)	Composition	Technique	Specimen, Test Conditions	ν
Angenheister (1903)	Fe-24.1 Ni(0.36 C, 0.41 Mn)	Tension, torsion, res. freq.	Ann., non-magnetic, fcc. Cooled to 76 K, magnetic, bcc.	0.298 0.358
Carrington (1924)	Fe-3.4 Ni(0.19 C, 0.55 Mn, 0.03 P, S, 0.01 Si)	Bending.	Ann. 1180 K, ½ h, slow cool; $f(T)$ in figure 32.	0.27
Honda, Tanaka (1926)	12 alloys	Torsion, bending.	Ann. 1173 K, ½ h; $f(H)$.	Figure 8
Chevenard, Crussard (1942)	a) Fe-6 Ni	Torsion-flexure.	i) Cold worked. ii) Ann. 1073 K.	0.27 0.29
	b) Fe-36 Ni		Ann. 1073 K; $f(T)$ in figure 32.	0.28
Chevenard, Crussard (1943)	a) Fe-49 Ni b) 12 alloys	Torsion-flexure.	Cold worked 44%; $f(T)$ in figure 32. Ann. 1173 K, cold worked 44%.	0.56 Figure 8
Goldman, Robertson (1964)	a) Fe-29.9 Ni(0.004 C) b) Fe-25.1 Ni(0.26 C)	Long., torsional res. freq.	Vac. ann. 1173 K, ½ h, 0.035 mm GS; $f(T)$ in figure 32. fcc, 293 K; bcc, 293 K; fcc, 217 K; bcc, 217 K.	0.28 0.26 0.23 0.22 0.20
Diesburg (1971)	3 alloys	10 MHz pulse-echo-overlap.	Calculated from c_{ij} by V–R–H method.	Figure 8
Hausch, Warlimont (1972)	9 alloys	10 MHz pulse-echo	Calculated from c_{ij} by V–R–H method.	Figure 8

TABLE 20. Third-order elastic stiffnesses c_{ijk} of iron

Investigator(s) (Year)	Technique	c_{111}	c_{112}	c_{123}	c_{144}	c_{166}	c_{456}
		(10^{12} dyn/cm^2)					
Hughes, Kelly (1953)*	Ultrasound velocities under tension and hydrostatic pressure.			−3.48	−10.31		9.81
Seeger, Buck (1960)*	Poynting effect.			−1.67	−7.55		−14.9
Powell, Skove (1968)	Measured deviations from Hooke's law of single crystals. Calculated using Rotter, Smith (1966) pressure derivatives of second-order stiffnesses.	−28.29	−8.00	−6.07			
Tietz (1969)*	Ultrasound velocities under tension and hydrostatic pressure.				5.99		−9.44
Mathur, Sharma (1970)	Calculated using Morse central-force potential and Girifalco, Weizer (1959) parameters.	−16.44	−2.60	−3.00	−3.00	−2.60	−3.00

*Determined isotropic constants c°_{123}, c°_{144}, and c°_{456}: see text for relationship of these to other c_{ijk}.

TABLE 21. Third-order and fourth-order elastic stiffnesses c_{ijk} and c_{ijkl} of nickel

Investigator(s) (Year)	Technique	c_{111}	c_{112}	c_{123}	c_{144}	c_{166}	c_{456}	c_{1111}	c_{1112}	c_{1122}	c_{1123}
		(10^{12} dyn/cm^2)									
Rose (1966)	Calc. from data in Huntington (1958) using finite strain theory and central-force potential.	−14.37	−10.53	1.19	1.19	−10.53	1.19	102.70	58.63	65.48	−3.47
Salama, Alers (1969	Change of sound velocity under uniaxial stress, specimens neutron irradiated to pin dislocations, saturated, 10 kOe field.	−20.32	−10.43	−2.20	−1.38	−9.10	−0.70				
Sarma, Mathur (1969)	Calc. from 9 nn Morse potential.	−17.896	−11.420	0.814	0.814	−11.420	0.814	−15.366	−0.741	−0.141	−0.083
Sarma, Reddy (1973)	Change of sound velocity under uniaxial stress, specimens neutron irradiated to pin dislocations, saturated, 8 kOe field.	−21.04	−13.45	0.59	−1.80	−7.57	−0.42				

TABLE 22. Pressure derivatives dc_{ij}/dP of elastic stiffnesses of iron and nickel

	c_{11}	c_{12}	c_{44}	$(c_{11}+2c_{12})/3$	$(c_{11}-c_{12})/2$
Fe: Rotter, Smith (1966)	7.51	5.19	2.66	5.97	1.16
Fe: Guinan, Beshers (1968)	6.72	4.58	2.59	5.29	1.07
Ni: Salama, Alers (1967)	6.03	4.87	2.38	5.26	0.58
Ni: Sarma, Mathur (1969)	5.70	4.58	2.65	4.95	0.70

TABLE 23. Relative elastic constants based on a hard-sphere model, $B=1$ arbitrarily

	c^r_{11}	c^r_{12}	c^r_{44}	$\dot{C}'$	B^r	G^r	E^r	ν	A
b. c. c.	1.000	1.000	0.667	0.000	1.000	0.200	0.563	0.406	∞
Fe (obs.)	1.375	0.838	0.726	0.481	1.000	0.489	1.246	0.282	2.43
f. c. c.	1.333	0.833	0.500	0.250	1.000	0.379	1.000	0.333	2.00
Ni (obs.)	1.350	0.825	0.666	0.486	1.000	0.413	1.145	0.296	2.54

TABLE 24. Debye characteristic temperatures θ of iron, nickel, and iron-nickel alloys calculated from single-crystal elastic data

Low-temperature			Room-temperature		
Wt. %Ni	θ, K	Ref.	Wt. %Ni	θ, K	Ref.
0	472	Lord, Beshers (1965)	29.82	435	Tanji (1971)
35.3	351	Hausch, Warlimont (1972)	35.7	405	Tanji (1971)
36.1	348	Bower, et al. (1968)	39.62	398	Tanji (1971)
37.7	358	Hausch, Warlimont (1972)	44.43	410	Tanji (1971)
38.2	346	Bower, et al. (1968)	49.96	425	Tanji (1971)
40.0	369	Hausch, Warlimont (1972)	60.7	458	Tanji (1971)
42.5	383	Hausch, Warlimont (1972)	70.02	465	Tanji (1971)
45.2	396	Hausch, Warlimont (1972)	78.5	478	Tanji (1971)
51.4	419	Hausch, Warlimont (1972)	89.6	475	Tanji (1971)
60.8	436	Hausch, Warlimont (1972)	99.98	474	Tanji (1971)
61.9	437	Hausch, Warlimont (1972)	See tables 5–7 for details.		
78.5	463	Hausch, Warlimont (1972)			
89.7	468	Hausch, Warlimont (1972)			
100.0	472	Hausch, Warlimont (1972)			
100.0	476	Alers, et al. (1960)			

TABLE 25. Conversions among commonly used stress units

	N/m²	dyn/cm²	bar	kbar	kg/cm²	kg/mm²	atm	psi
1 Newton/sq. meter (N/m²)	1	10^1	10^{-5}	10^{-8}	1.01972×10^{-5}	1.01972×10^{-7}	0.98692×10^{-5}	1.45038×10^{-4}
1 dyne/sq. cm. (dyn/cm²)	10^{-1}	1	10^{-6}	10^{-9}	1.01972×10^{-6}	1.01972×10^{-8}	0.98692×10^{-6}	1.45038×10^{-5}
1 bar	10^5	10^6	1	10^{-3}	1.01972	1.01972×10^{-2}	0.98692	1.45038×10^1
1 kilobar (kbar)	10^8	10^9	10^3	1	1.01972×10^3	1.01972×10^1	0.98692×10^3	1.45038×10^4
1 kilogram/sq. cm. (kg/cm²)	0.98066×10^5	0.98066×10^6	0.98066	0.98066×10^{-3}	1	10^{-2}	0.96784	1.42233×10^1
1 kilogram/sq. mm. (kg/mm²)	0.98066×10^7	0.98066×10^8	0.98066×10^2	0.98066×10^{-1}	10^2	1	0.96784×10^2	1.42233×10^3
1 atmosphere (atm)	1.01325×10^5	1.01325×10^6	1.01325	1.01325×10^{-3}	1.03323	1.03323×10^{-2}	1	1.46959×10^1
1 pound/sq. in. (psi)	0.68948×10^4	0.68948×10^5	0.68948×10^{-1}	0.68948×10^{-4}	0.70307×10^{-1}	0.70307×10^{-3}	0.68046×10^{-1}	1

The S.I. unit for pressure and stress is the pascal (Pa), 1 Newton/sq. meter (N/m²).

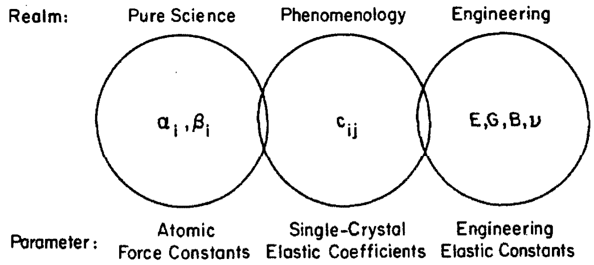

FIGURE 1. Schematic interconnectivity of elastic parameters of solids

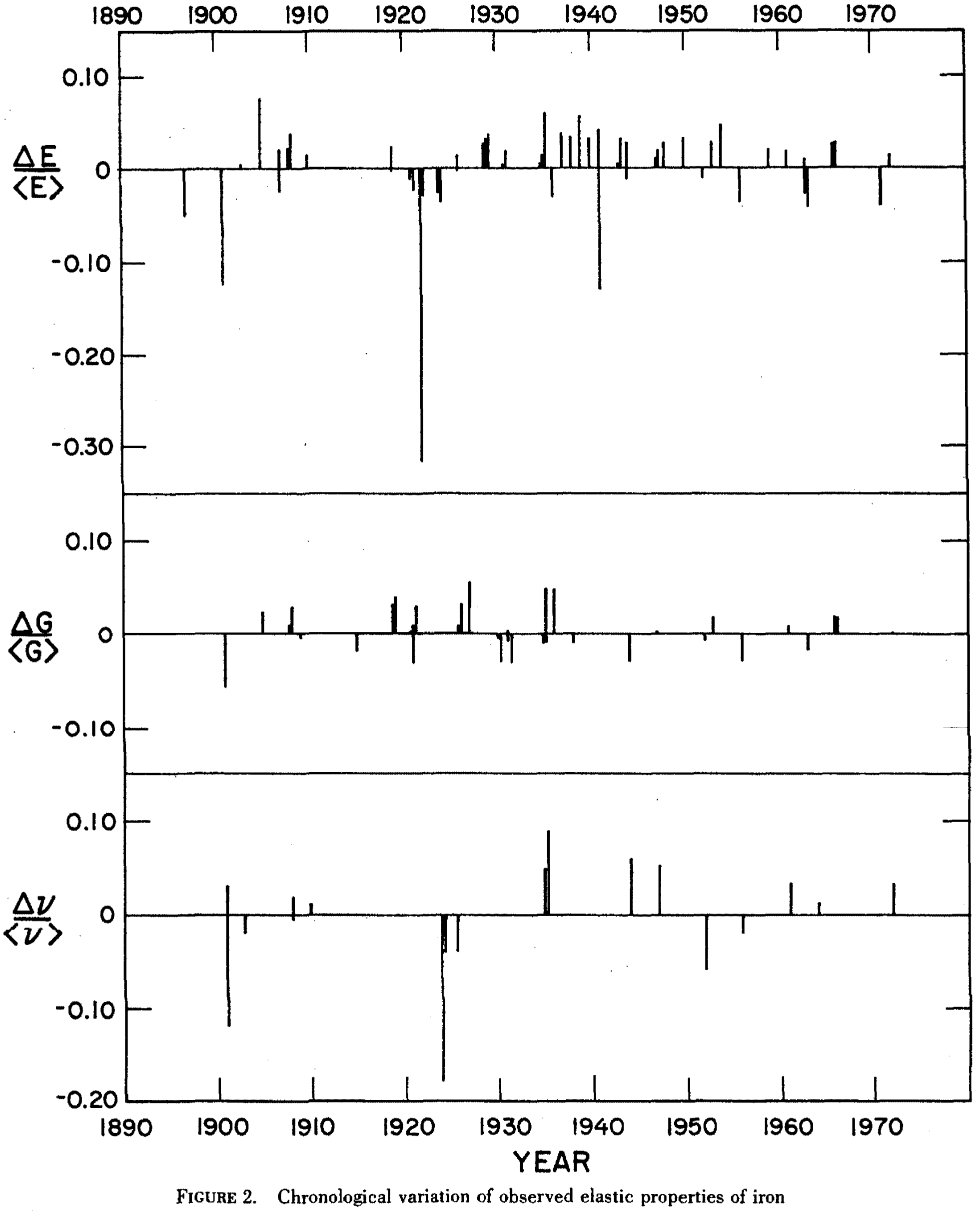

FIGURE 2. Chronological variation of observed elastic properties of iron

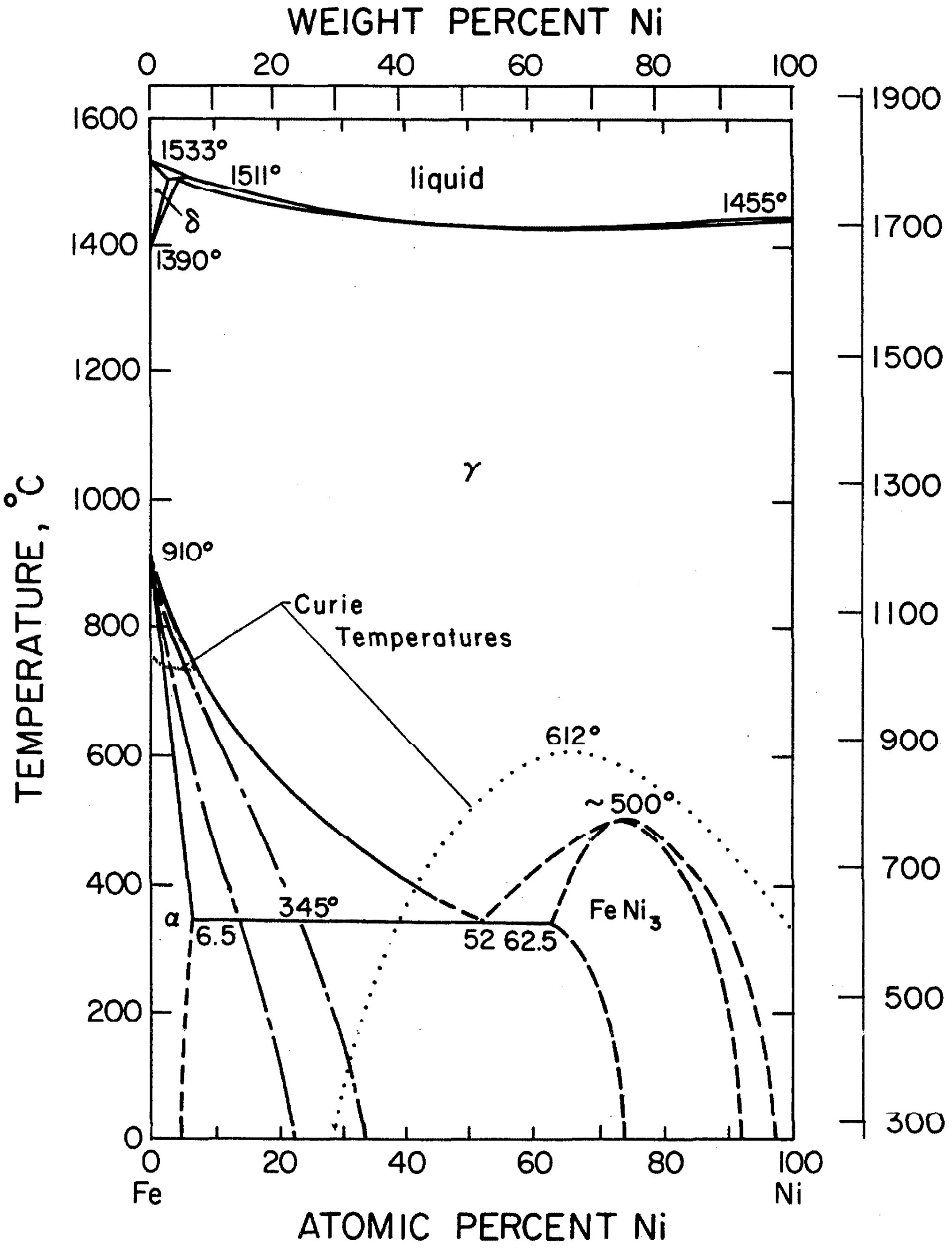

FIGURE 3. Iron-nickel phase diagram.

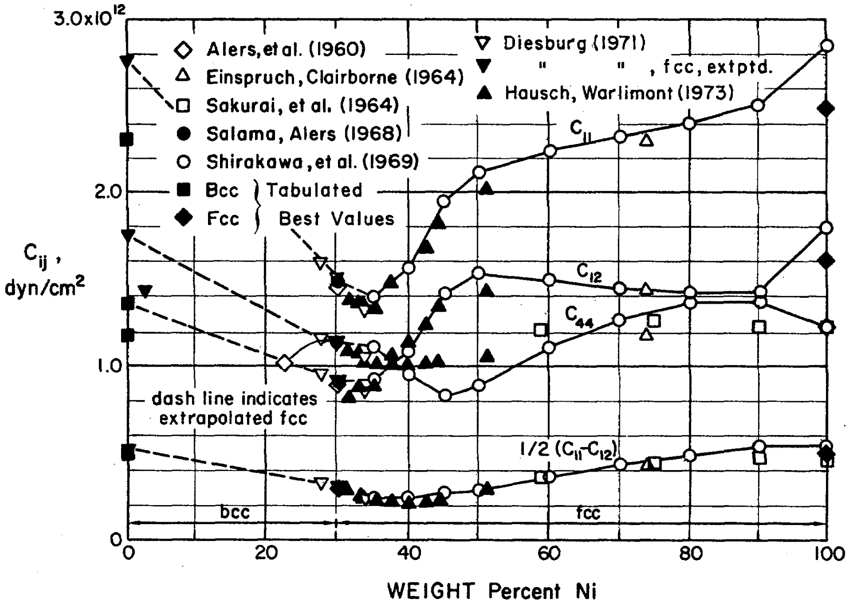

FIGURE 4. Compositional variation of elastic stiffnesses c_{ij} of iron-nickel alloys

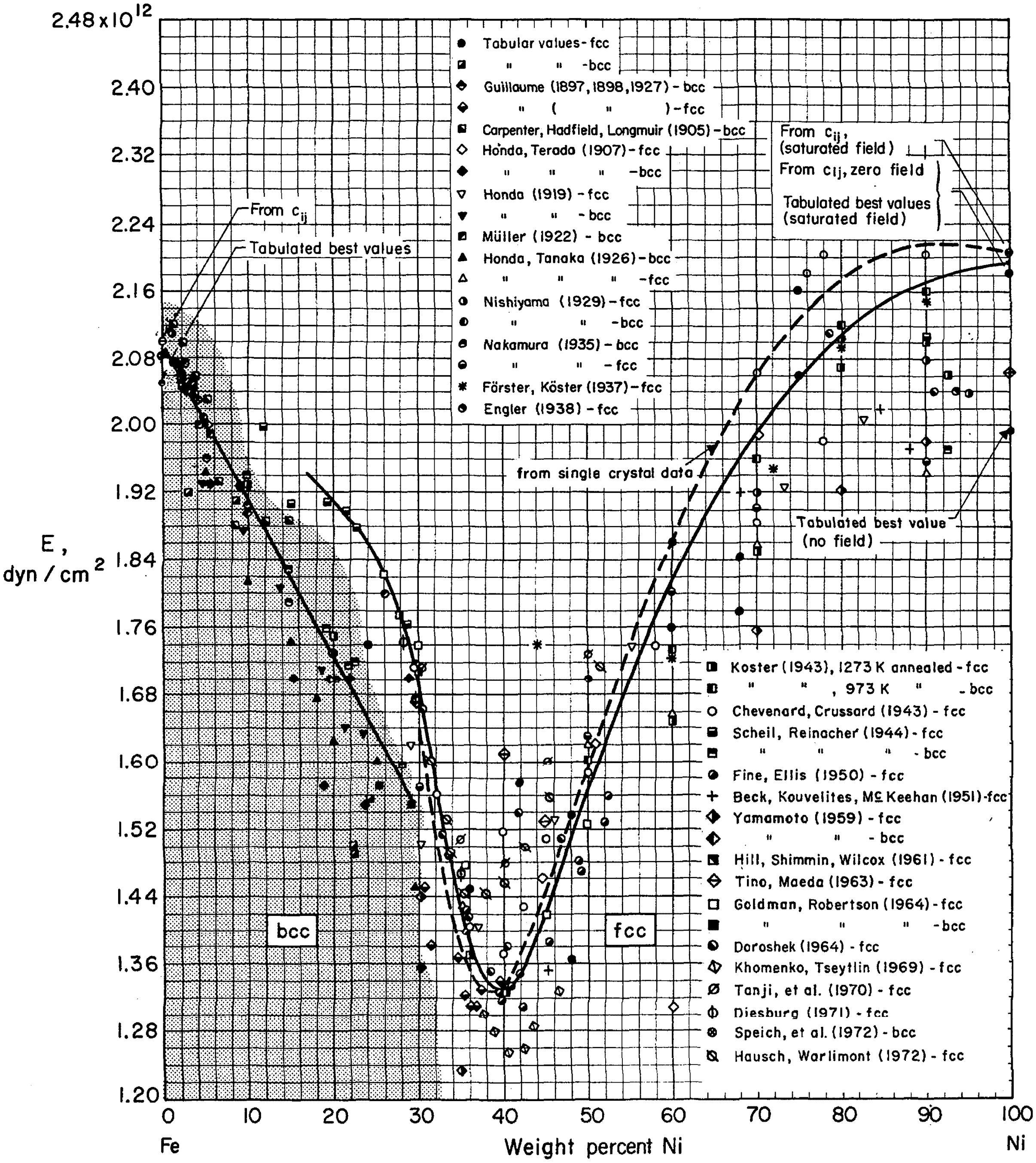

FIGURE 5. Compositional variation of Young's modulus E of iron-nickel alloys

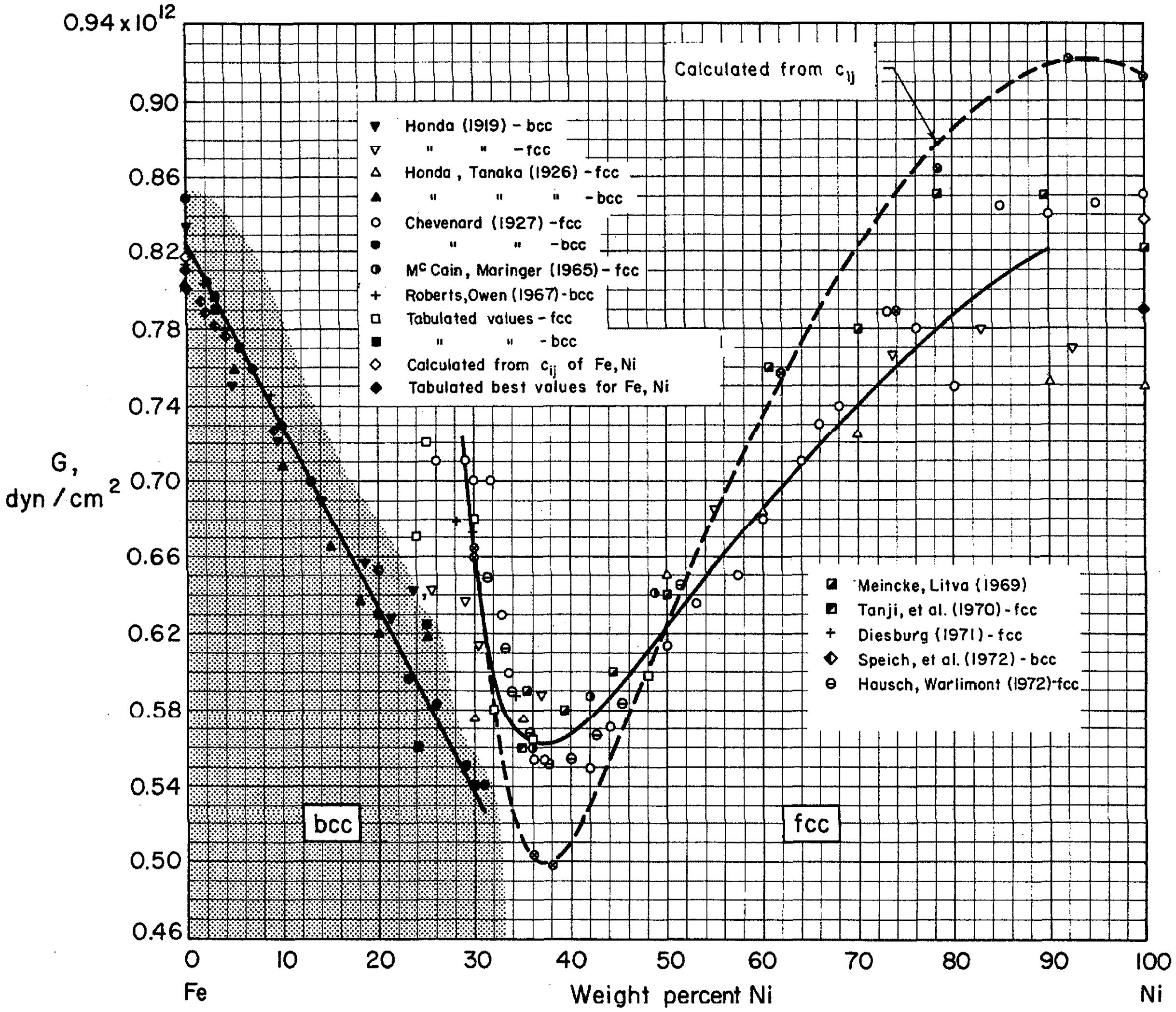

FIGURE 6. Compositional variation of shear modulus G of iron-nickel alloys

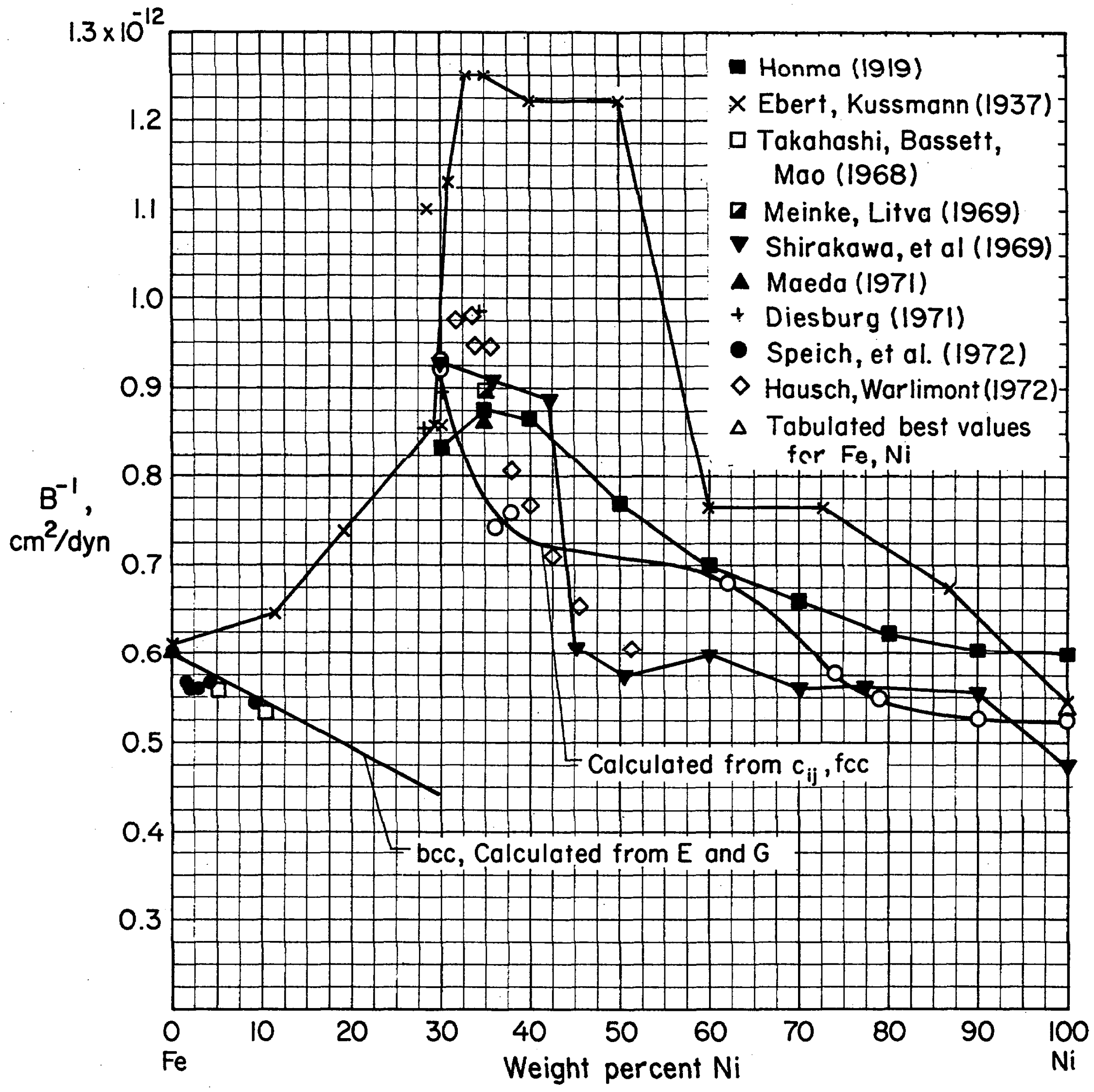

FIGURE 7. Compositional variation of compressibility B^{-1} of iron-nickel alloys

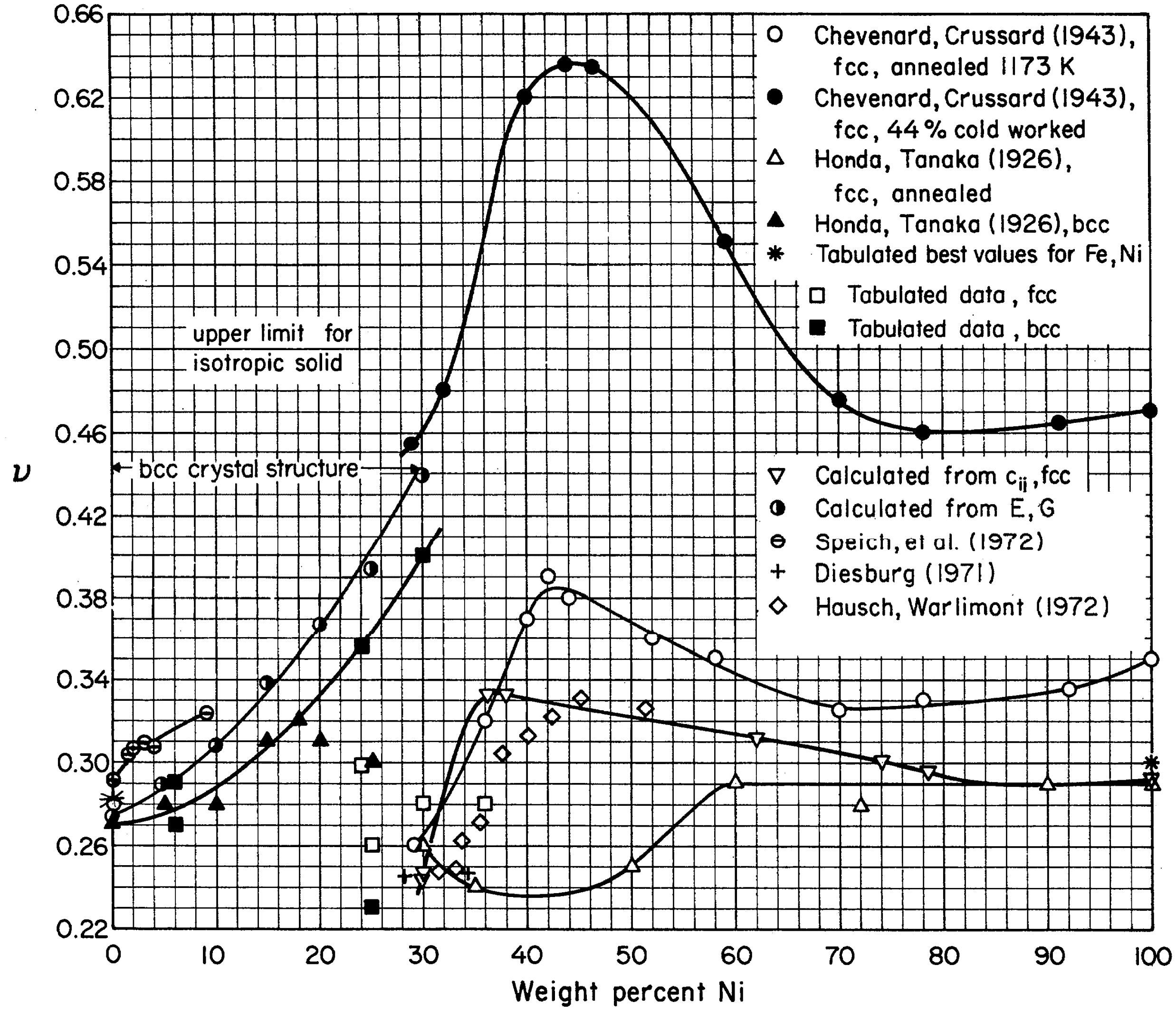

FIGURE 8. Compositional variation of Poisson ratio ν of iron-nickel alloys

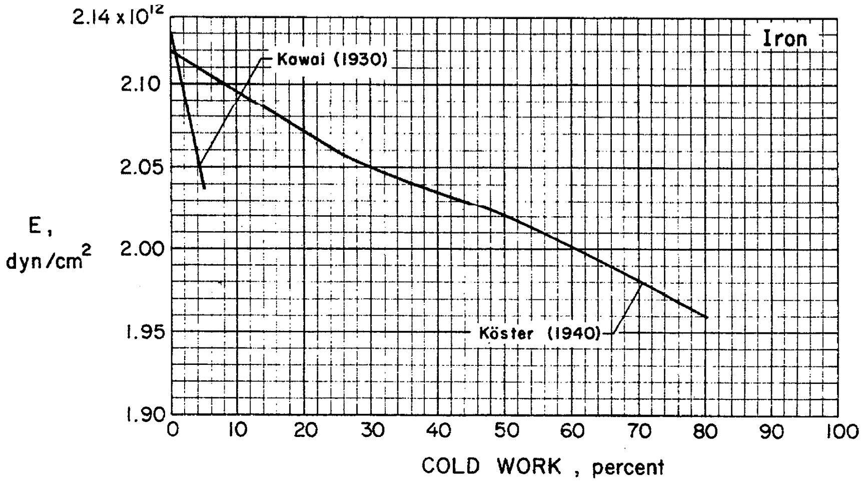

FIGURE 9. Cold-work dependence of Young's modulus E of iron

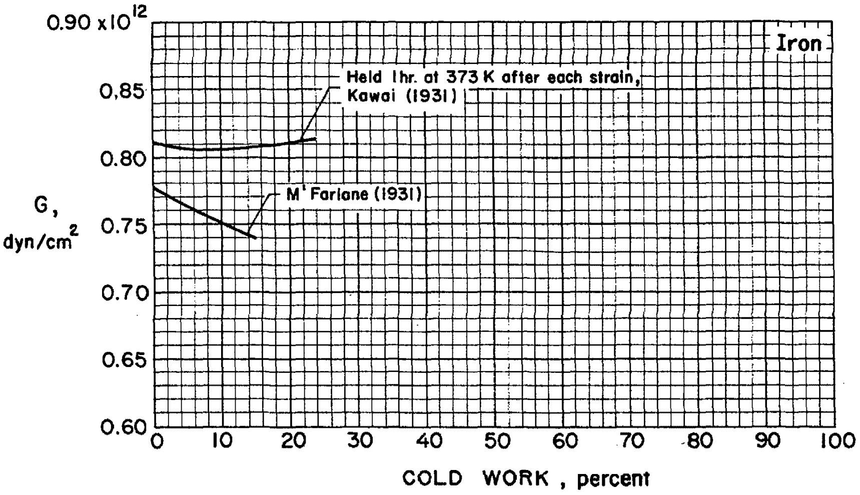

FIGURE 10. Cold work dependence of shear modulus G of iron

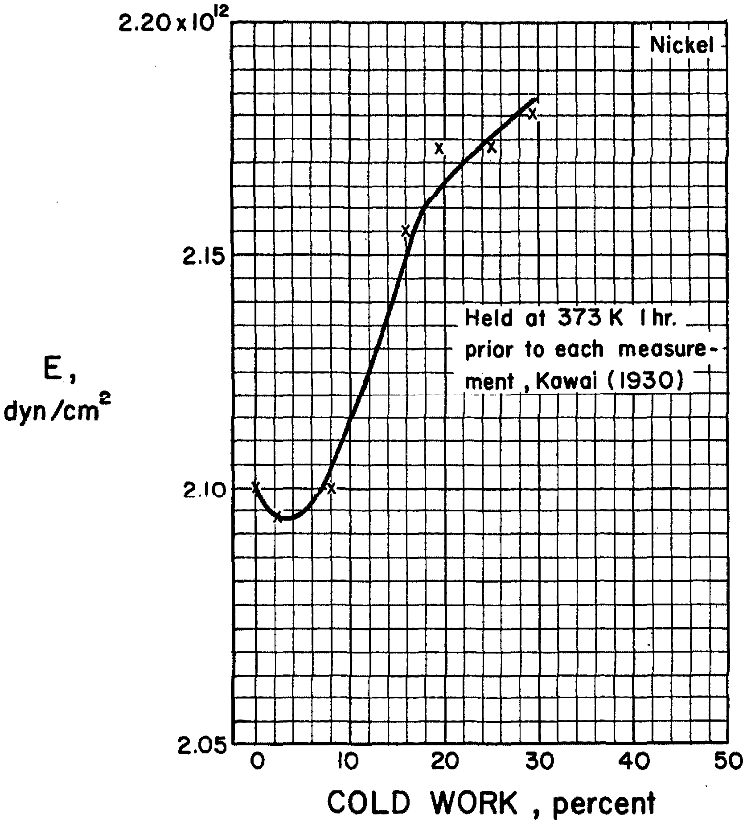

FIGURE 11. Cold work effect on Young's modulus E of nickel

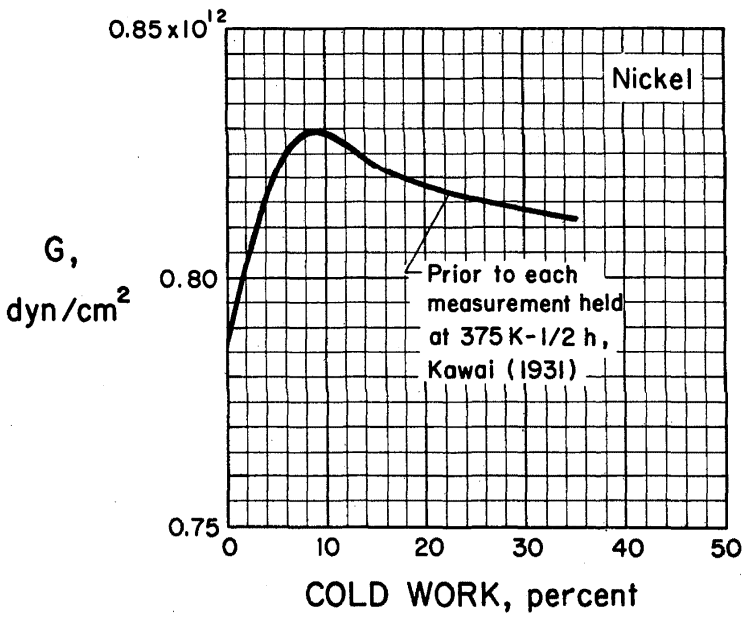

FIGURE 12. Cold work effect on shear modulus G of nickel

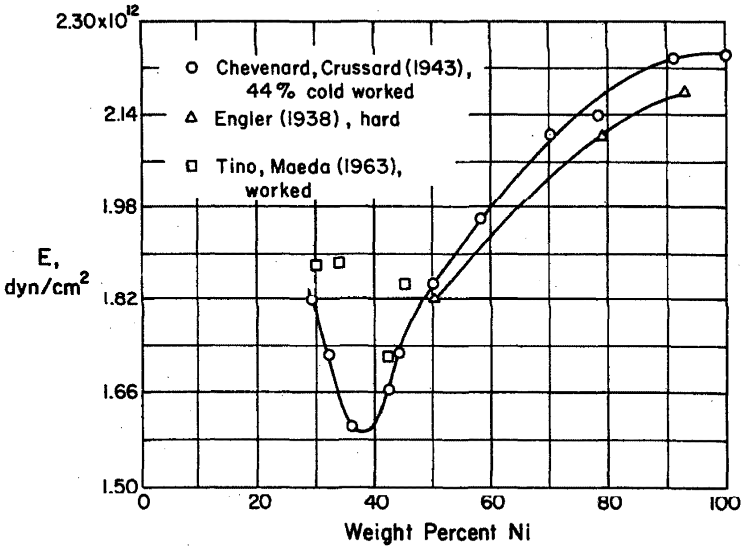

FIGURE 13. Cold work effect on Young's modulus E of face-centered cubic iron-nickel alloys

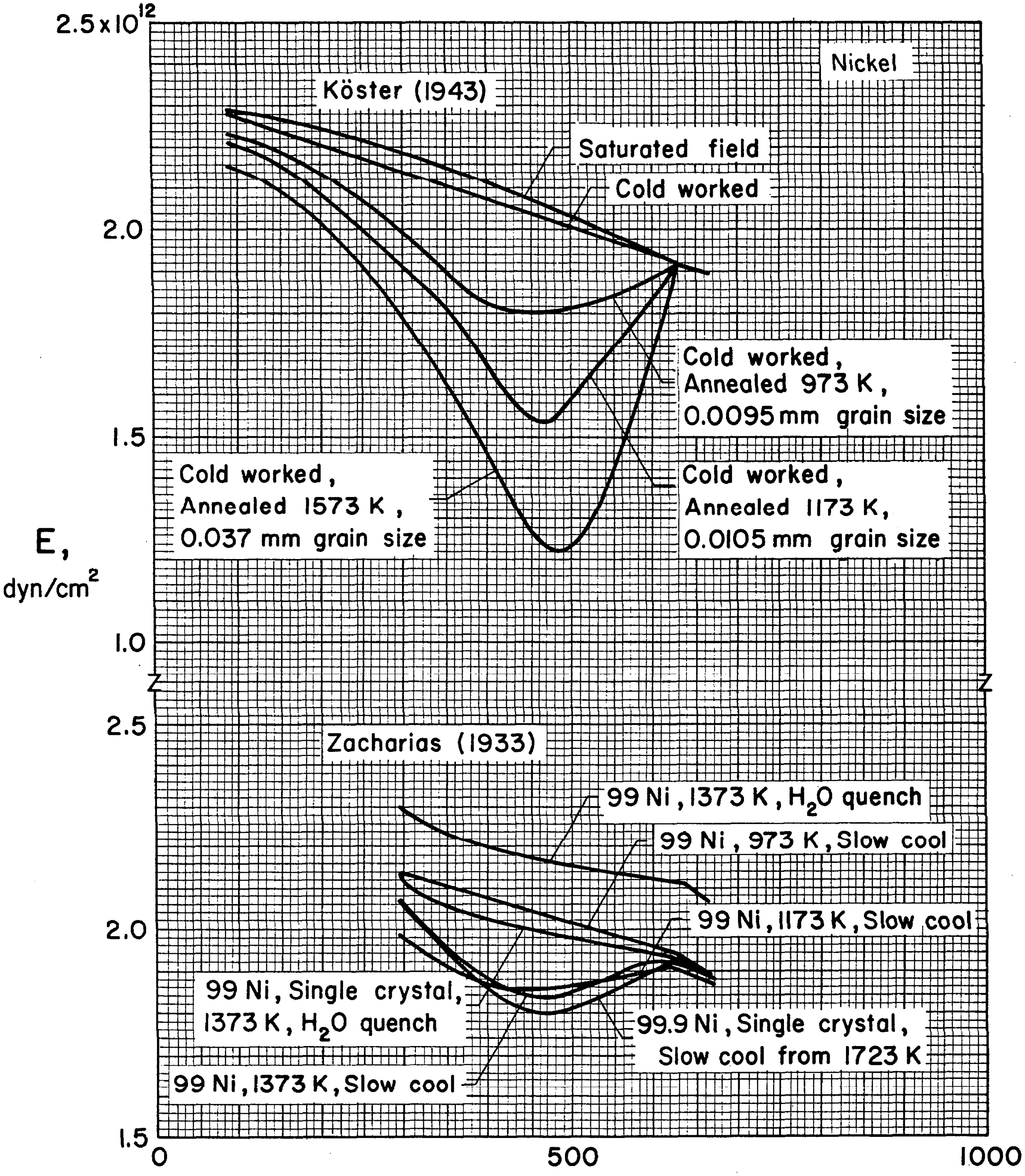

FIGURE 14. Annealing effect on Young's modulus E of nickel

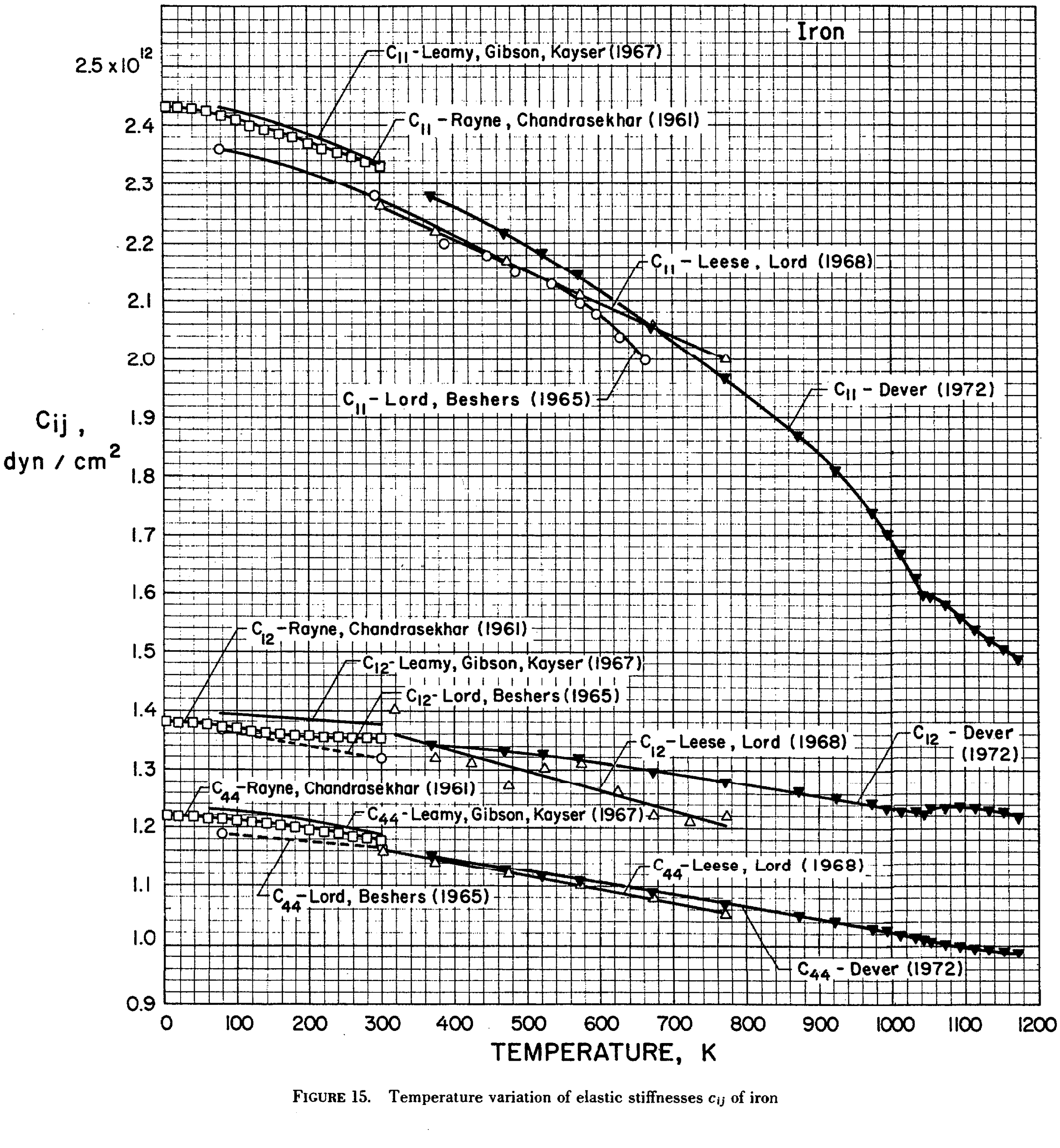

FIGURE 15. Temperature variation of elastic stiffnesses c_{ij} of iron

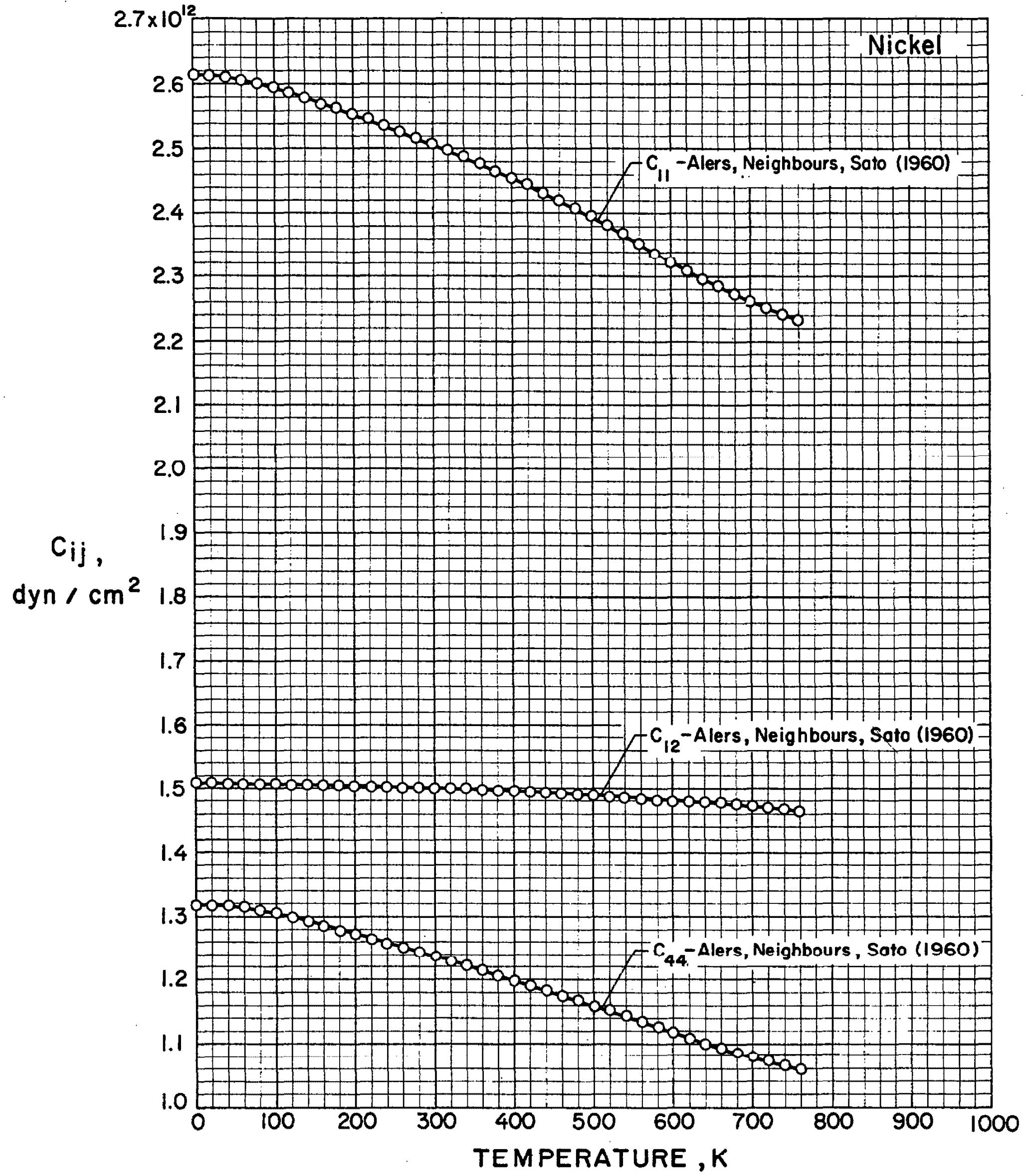

FIGURE 16. Temperature variation of elastic stiffnesses c_{ij} of nickel

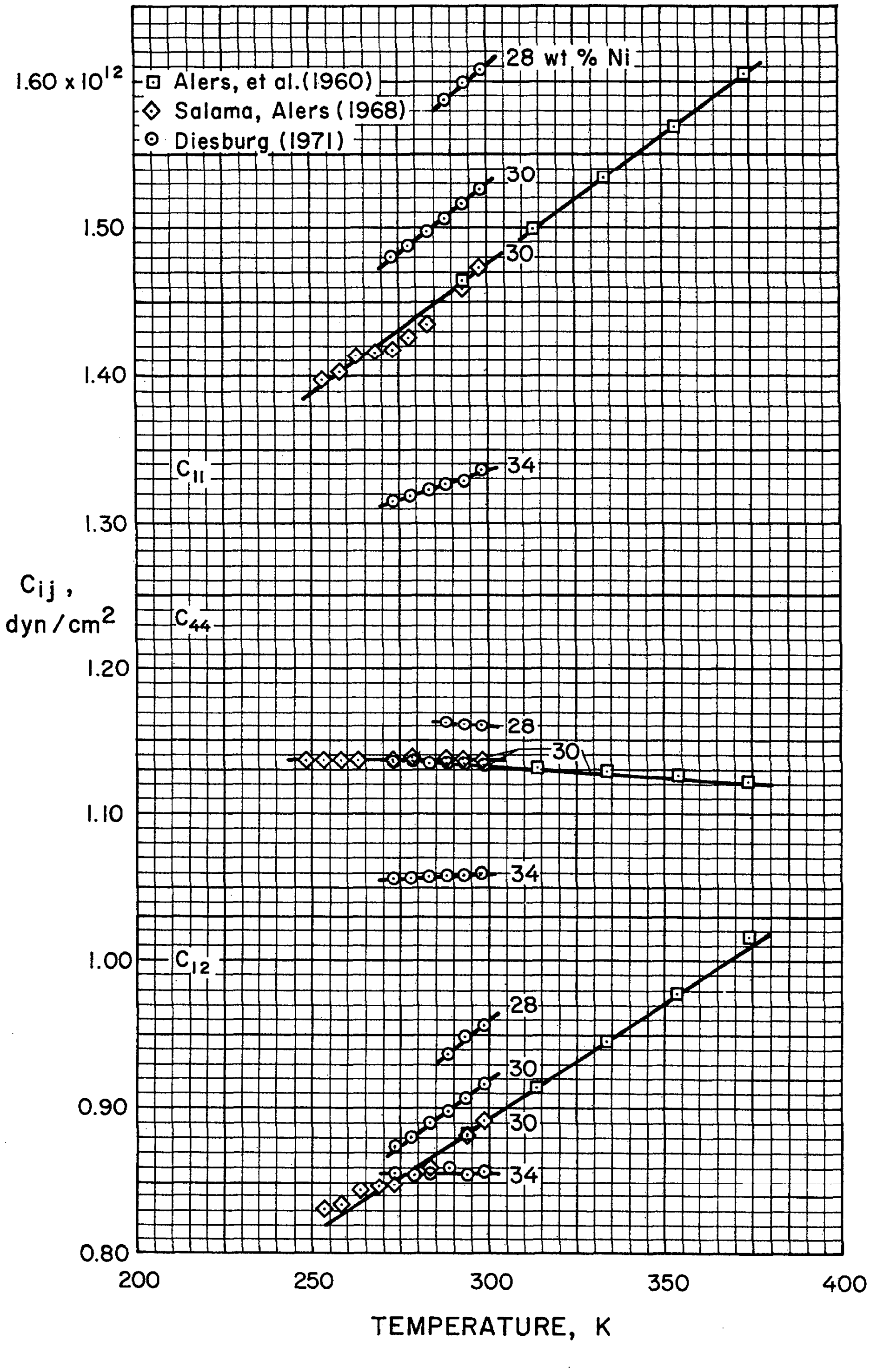

FIGURE 17a. Temperature variation of elastic stiffnesses c_{ij} of iron-nickel alloys

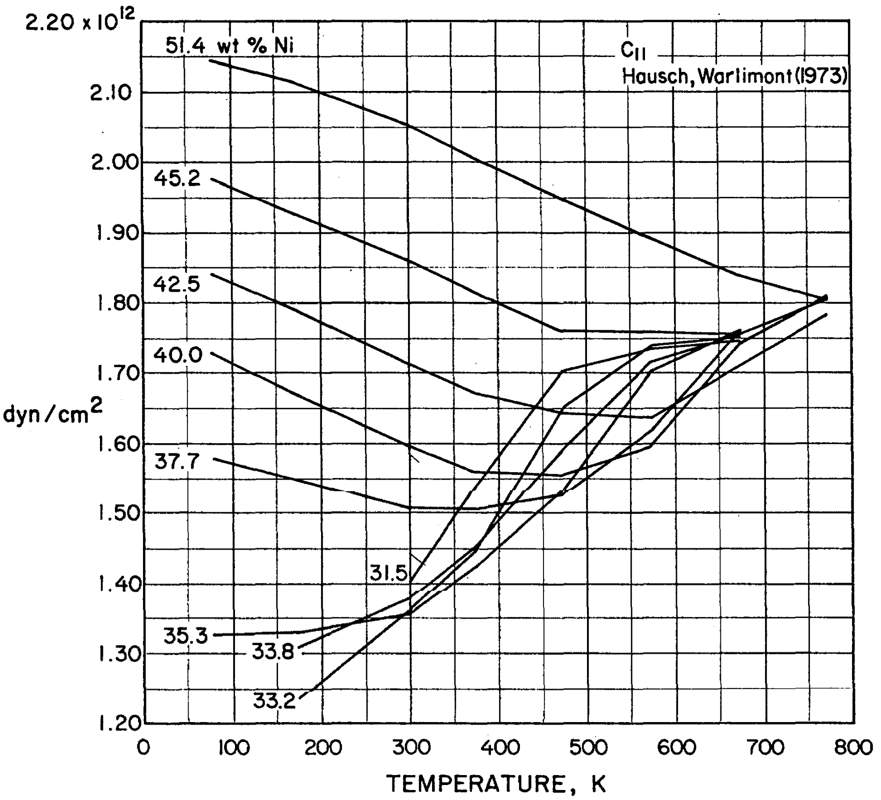

FIGURE 17b. Temperature variation of elastic stiffness c_{11} of iron-nickel alloys

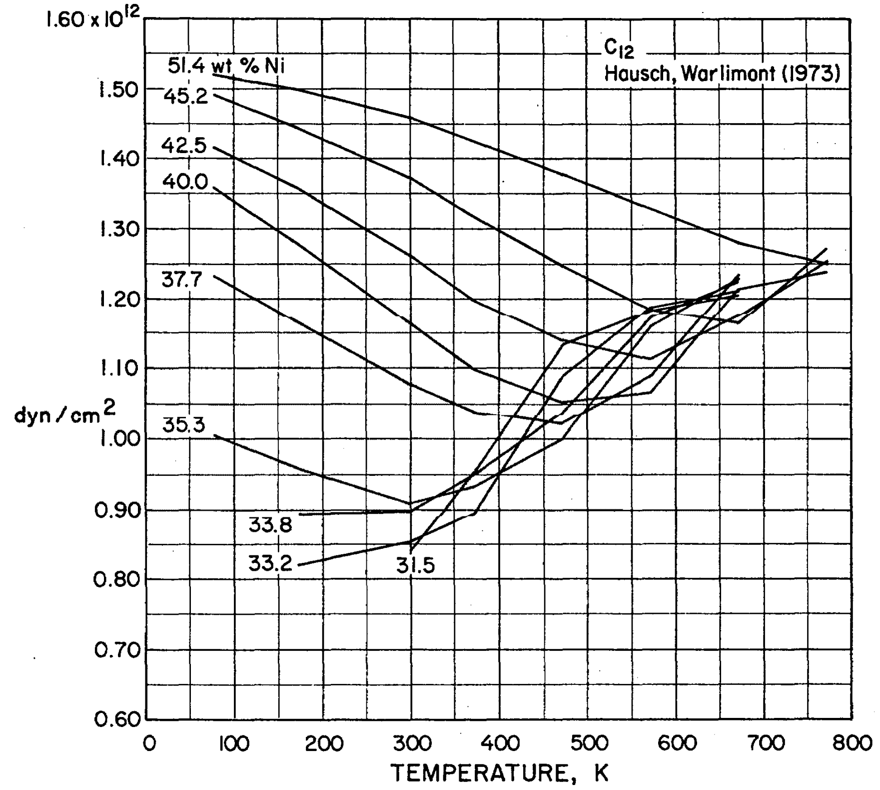

FIGURE 17c. Temperature variation of elastic stiffness c_{12} of iron-nickel alloys

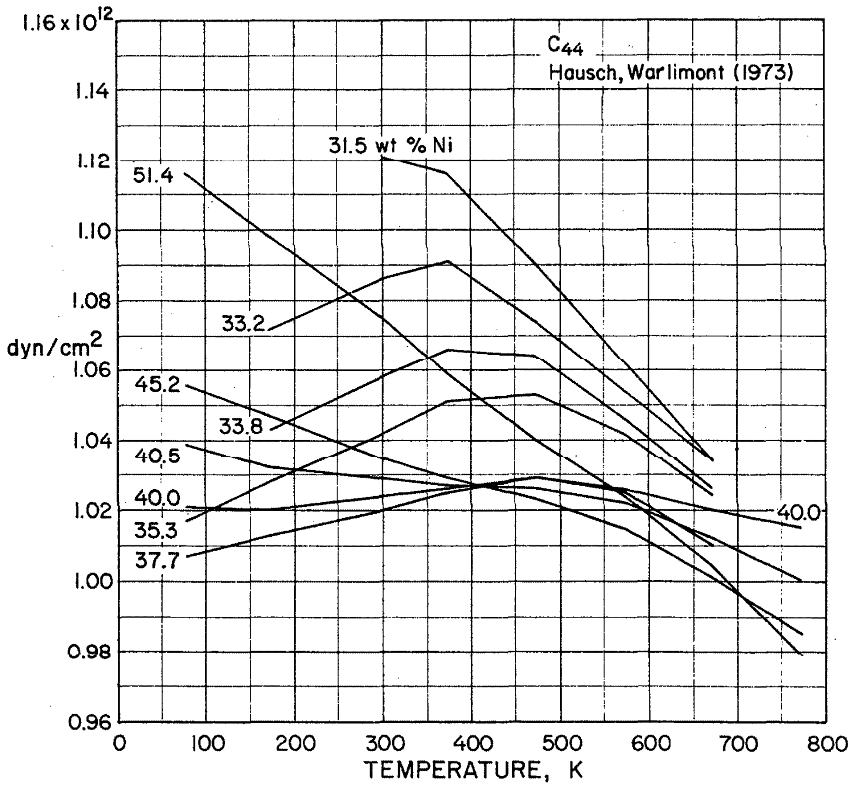

FIGURE 17d. Temperature variation of elastic stiffness c_{44} of iron-nickel alloys

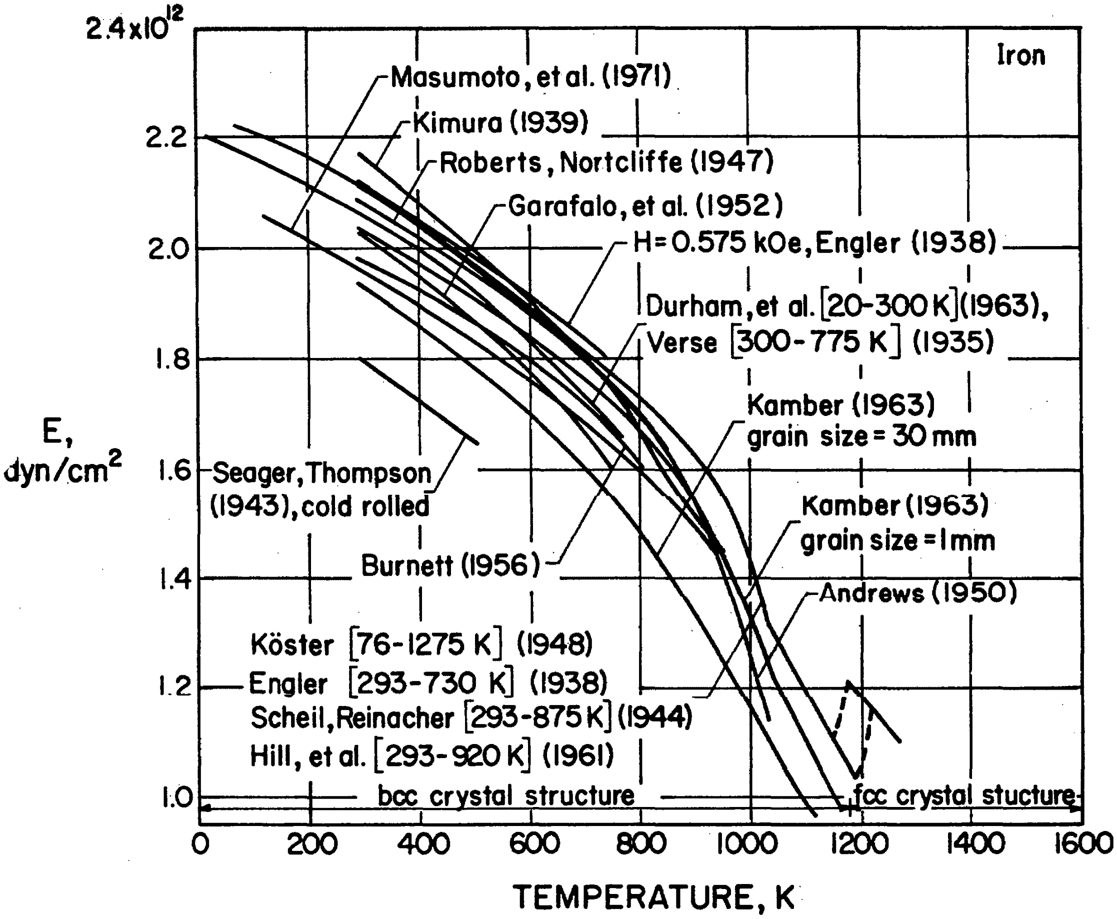

FIGURE 18. Temperature variation of Young's modulus E of iron

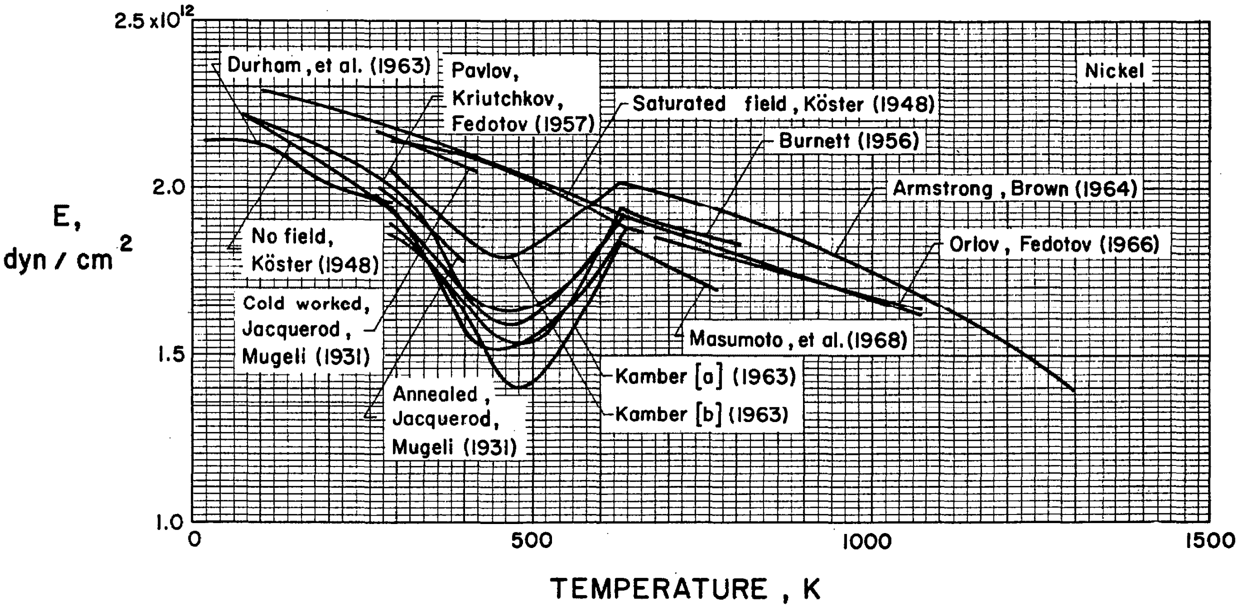

FIGURE 19. Temperature variation of Young's modulus E of nickel

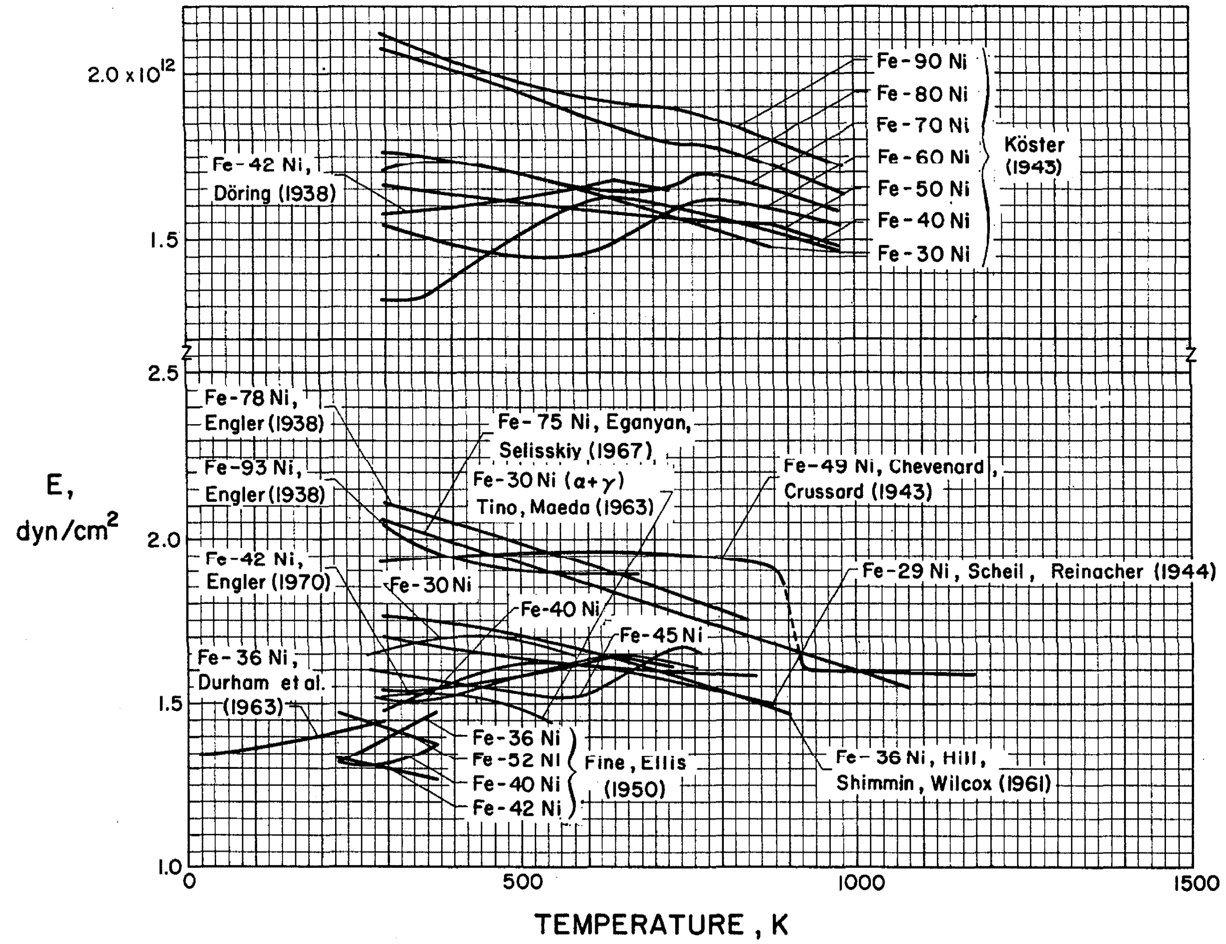

FIGURE 20. Temperature variation of Young's modulus E of iron-nickel alloys—face-centered cubic

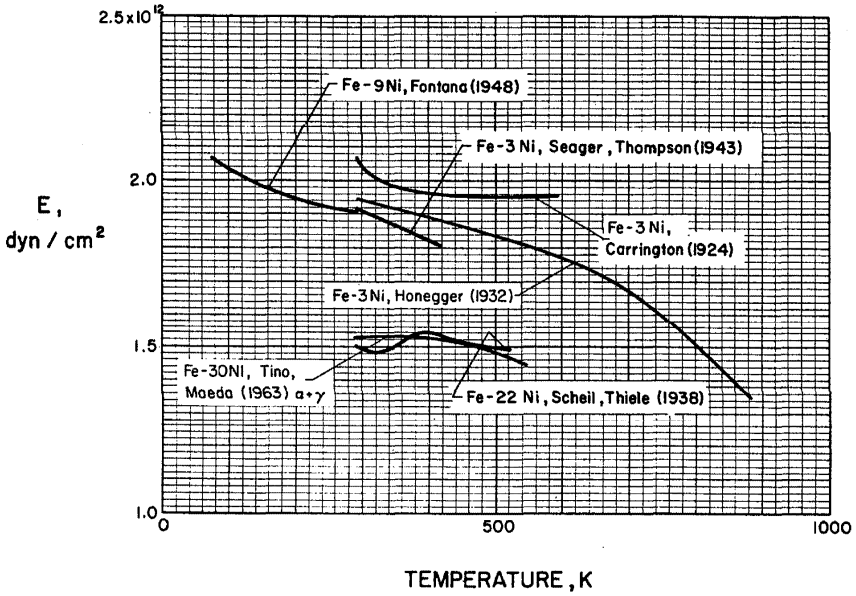

FIGURE 21. Temperature variation of Young's modulus E of iron-nickel alloys—body-centered cubic

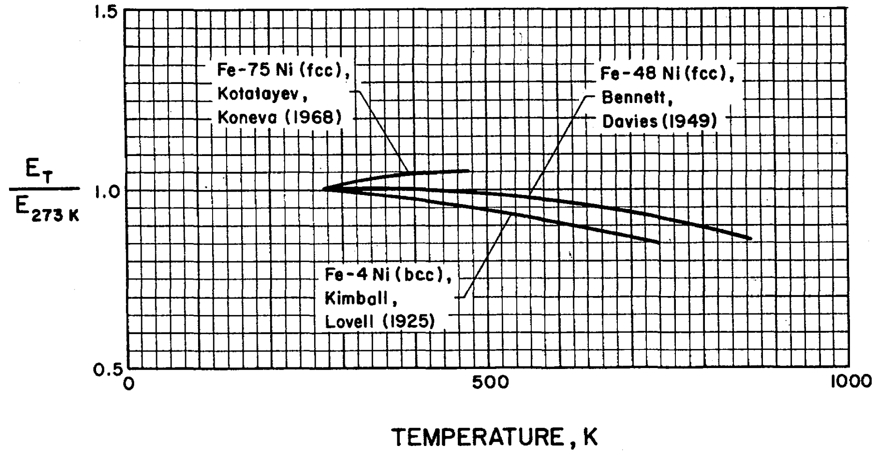

FIGURE 22. Relative temperature variation of Young's modulus E of some iron-nickel alloys

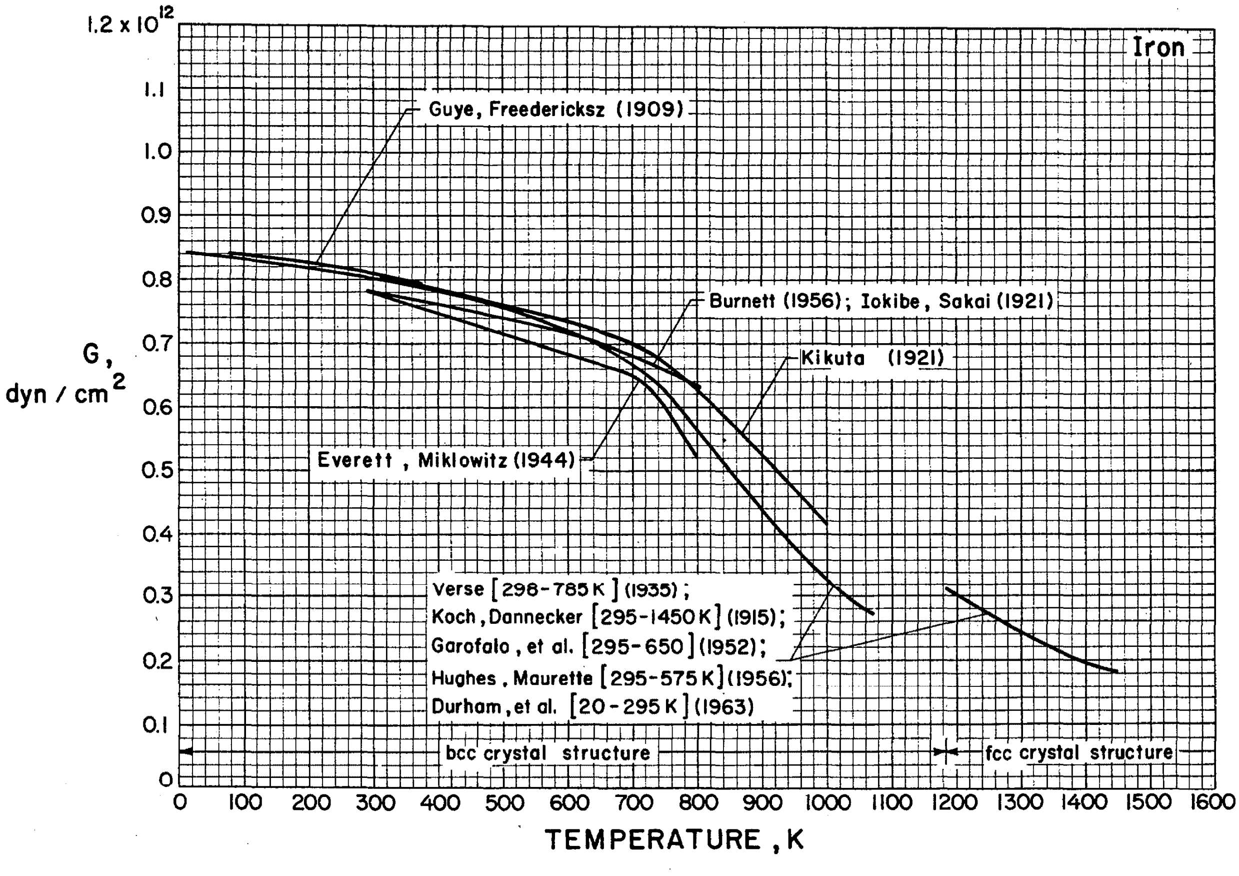

FIGURE 23. Temperature variation of shear modulus G of iron

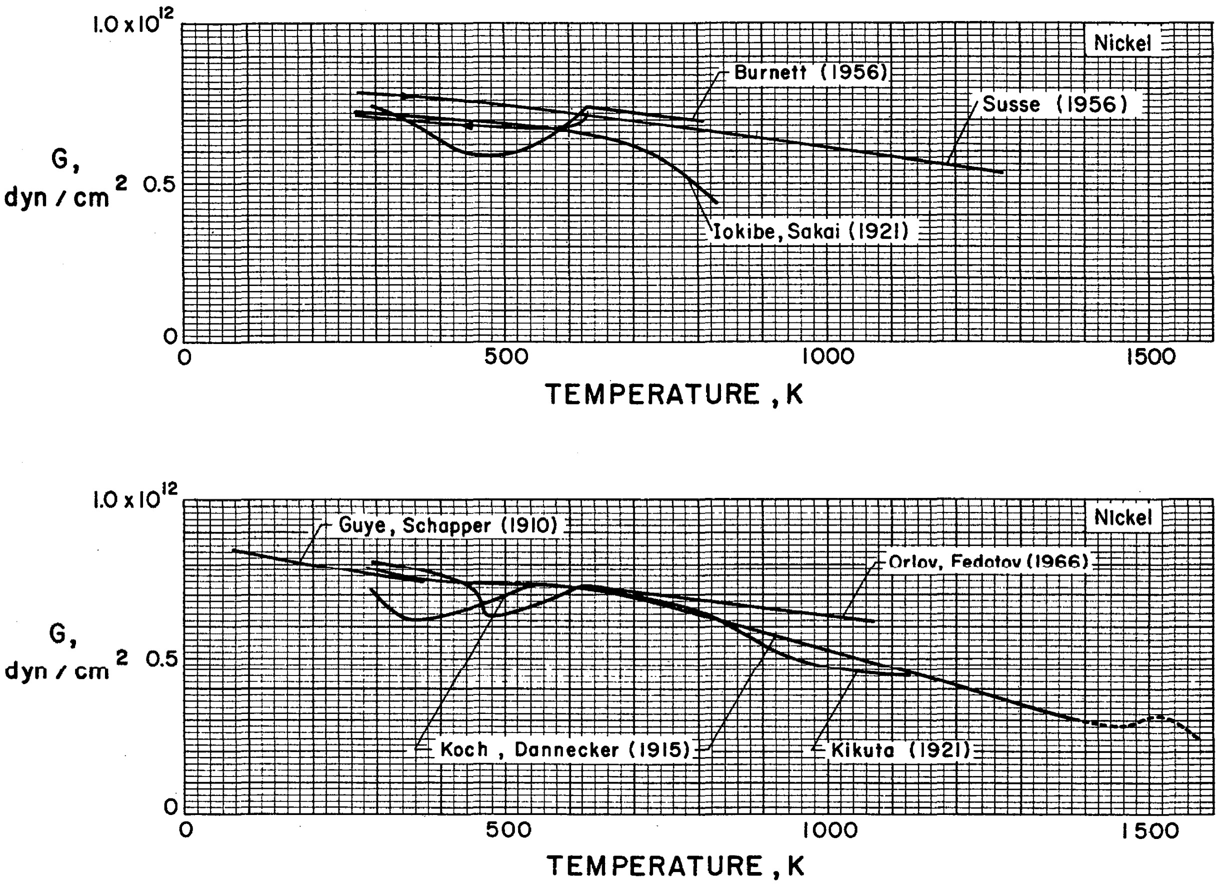

FIGURE 24. Temperature variation of shear modulus G of nickel

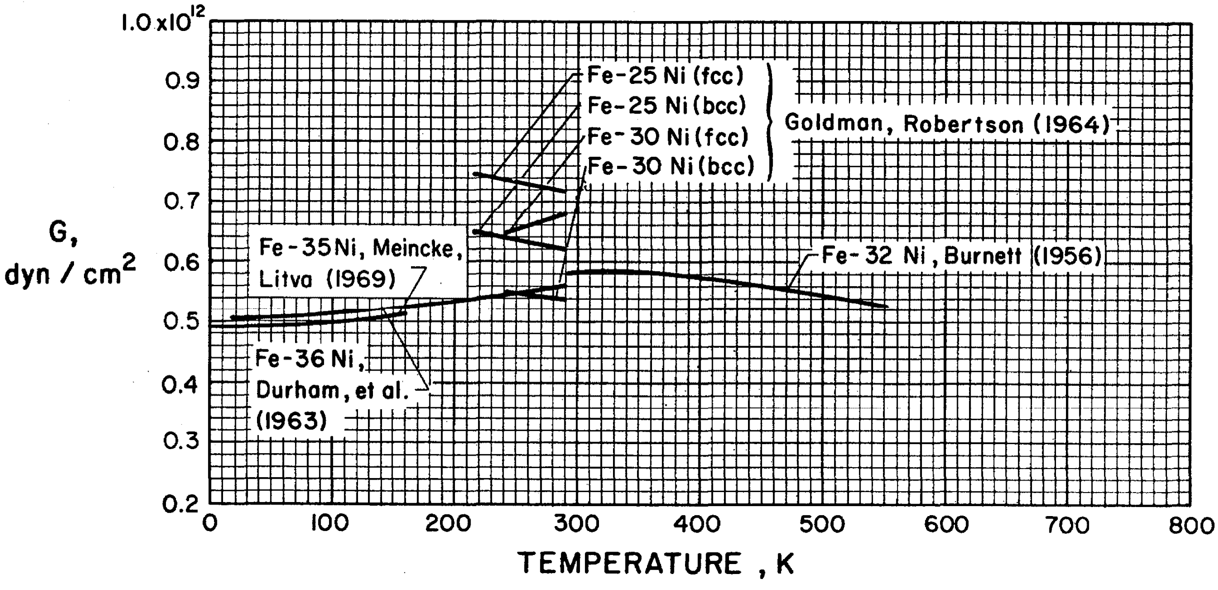

FIGURE 25. Temperature variation of shear modulus G of iron-nickel alloys

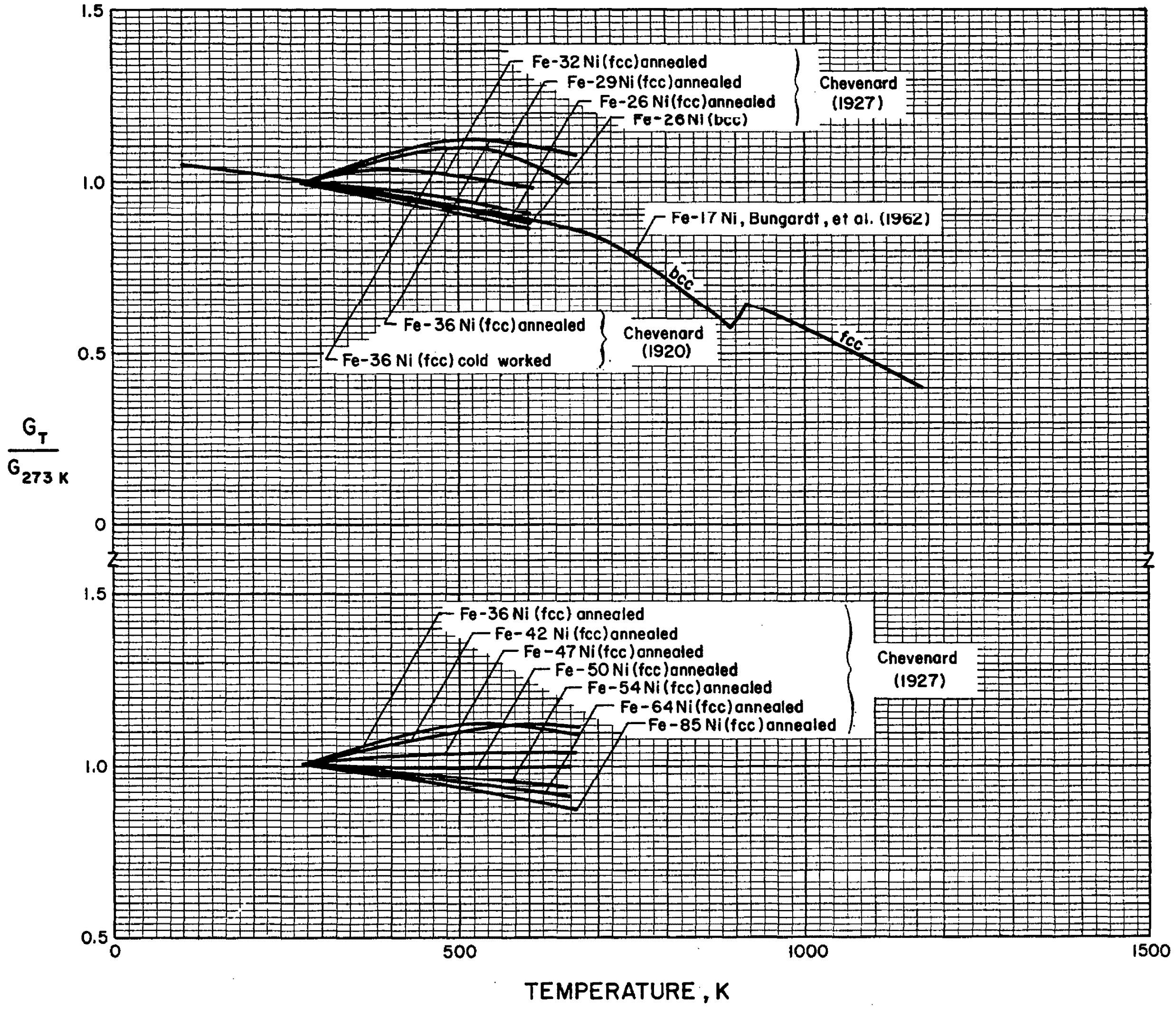

FIGURE 26. Relative temperature variation of shear modulus G of some iron-nickel alloys

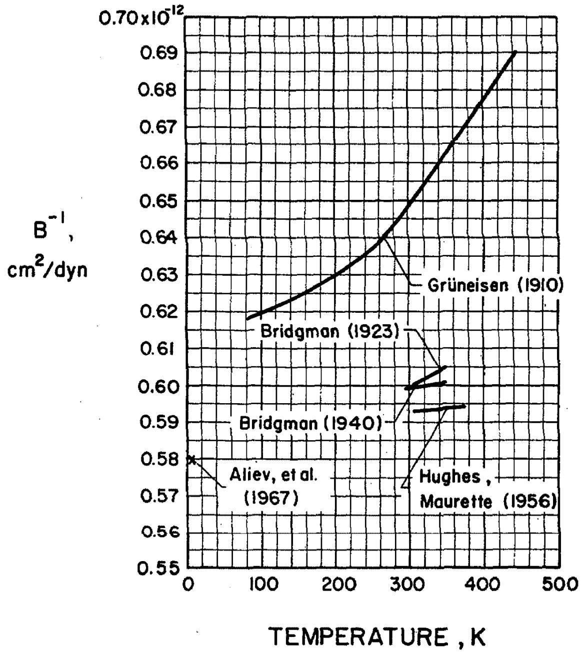

FIGURE 27. Temperature variation of compressibility B^{-1} of iron

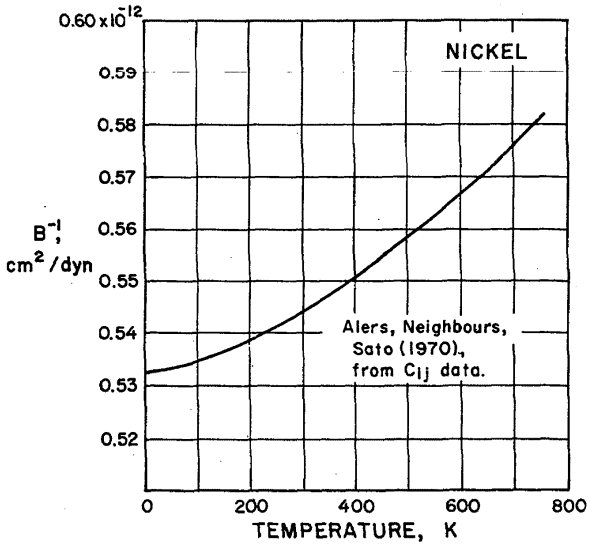

FIGURE 28. Temperature variation of compressibility B^{-1} of nickel

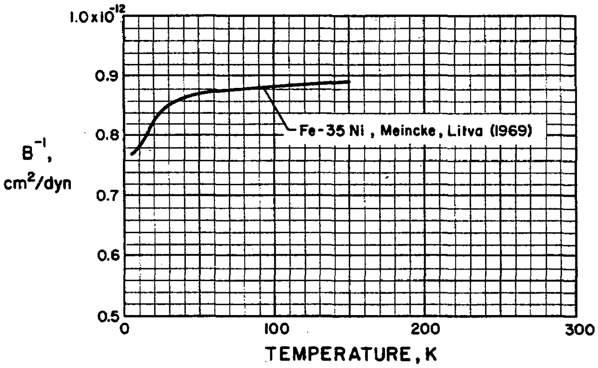

FIGURE 29. Temperature variation of compressibility B^{-1} of iron-nickel alloys

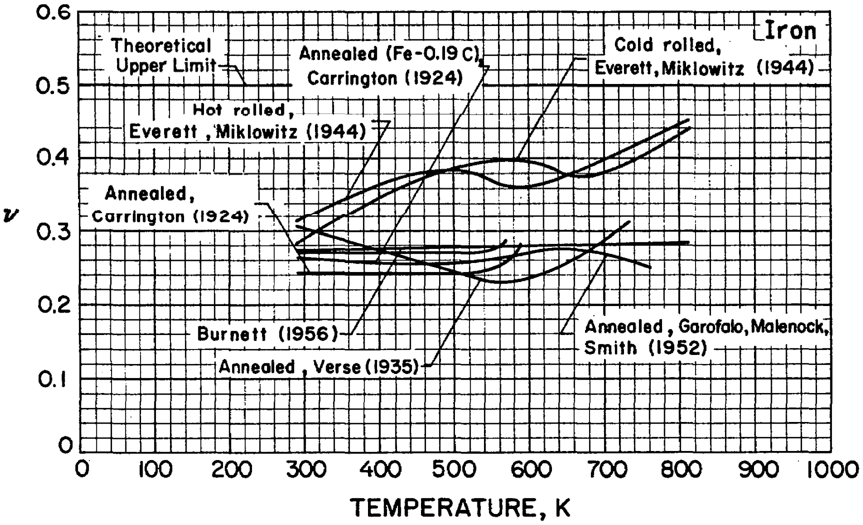

FIGURE 30. Temperature variation of Poisson ratio ν of iron

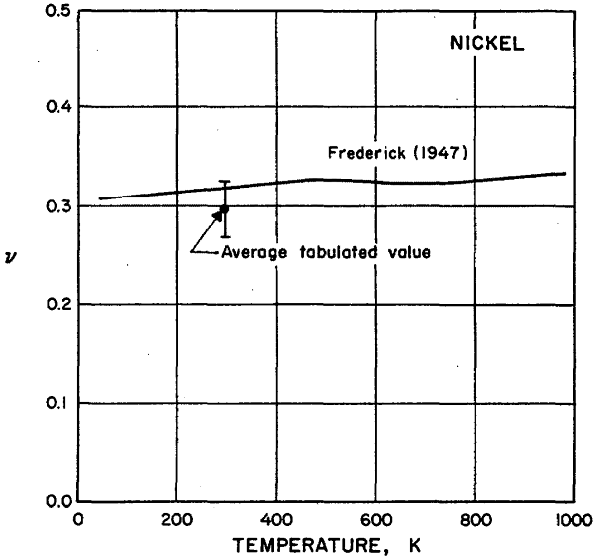

FIGURE 31. Temperature variation of Poisson ratio ν of nickel

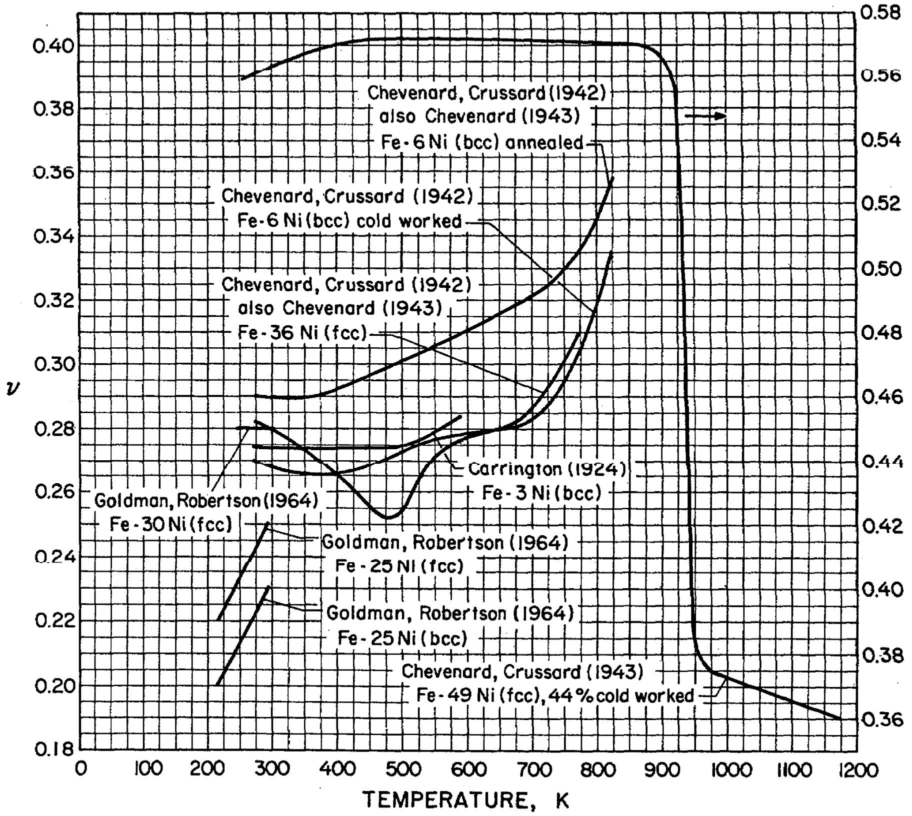

FIGURE 32. Temperature variation of Poisson ratio ν of iron-nickel alloys

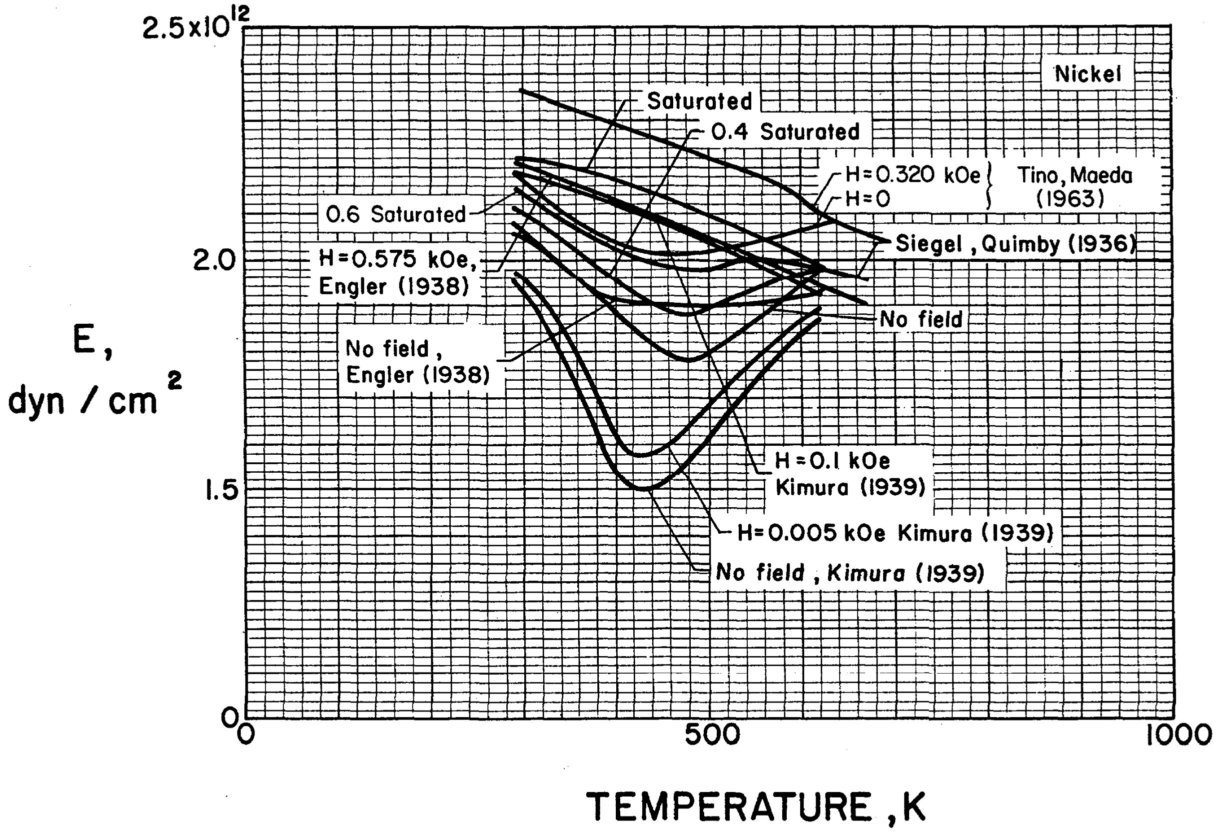

FIGURE 33. Magnetic field and temperature effects on Young's modulus E of nickel

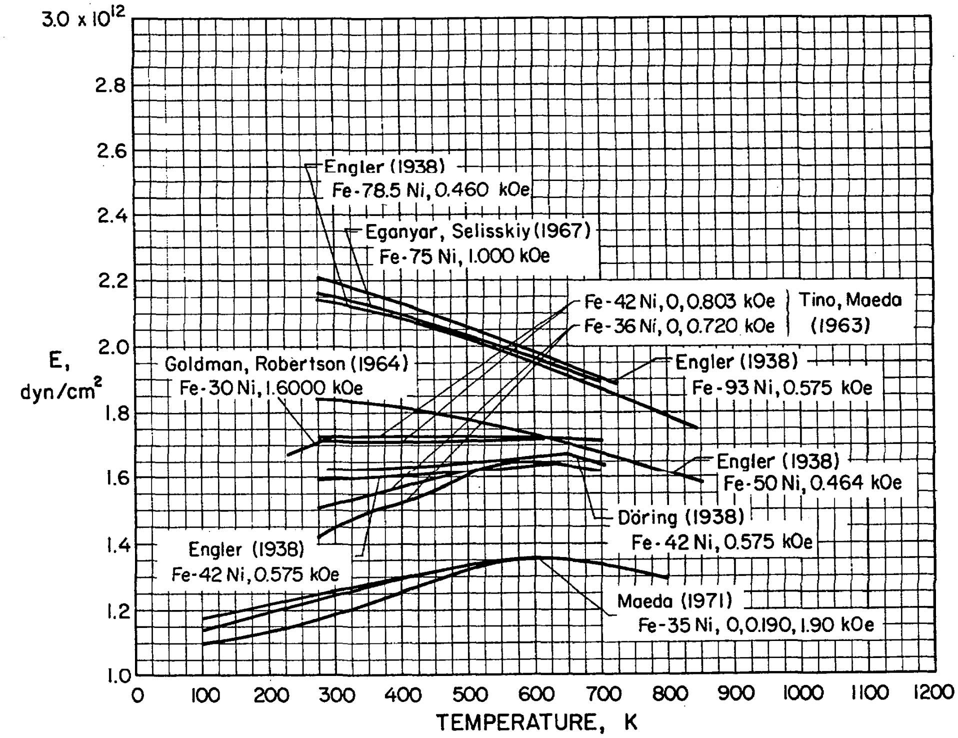

FIGURE 34. Magnetic field and temperature effects on Young's modulus E of iron-nickel alloys

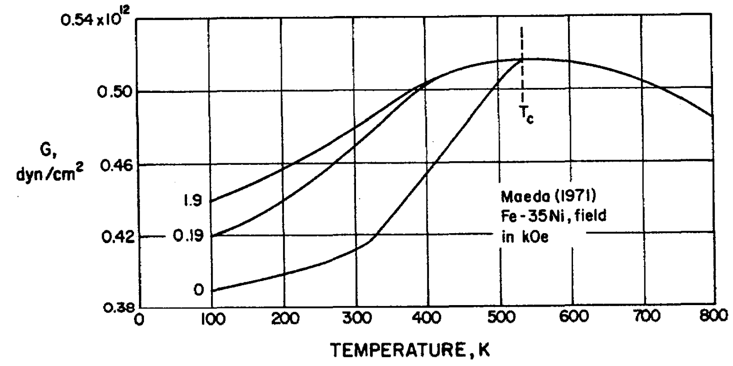

FIGURE 35. Magnetic field and temperature effects on shear modulus G of an iron-nickel alloy

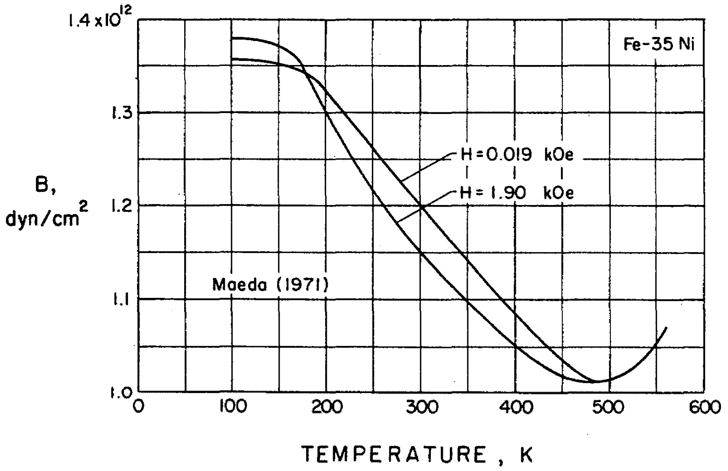

FIGURE 36. Magnetic field and temperature effects on bulk modulus B of an iron-nickel alloy

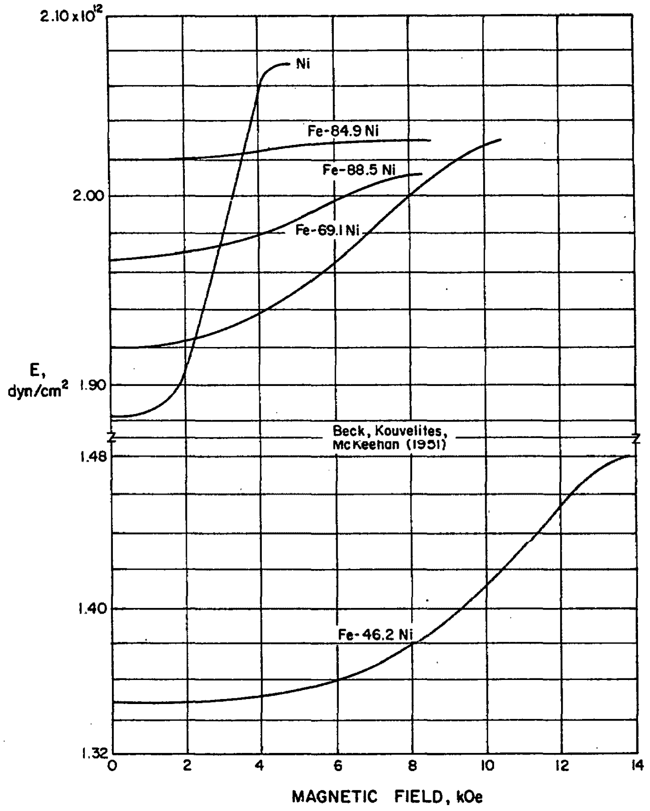

FIGURE 37. Magnetic field effect on Young's modulus E of nickel and iron-nickel alloys

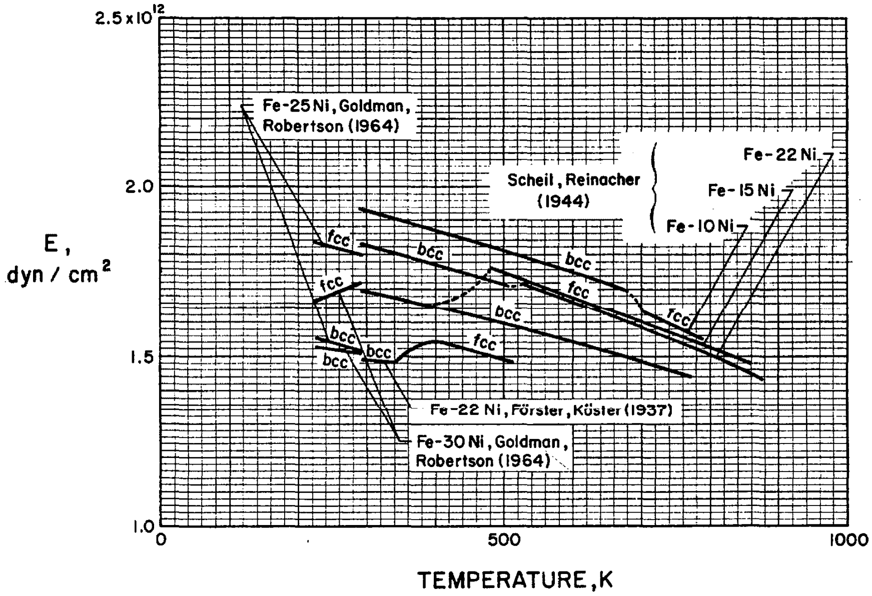

FIGURE 38. Phase transformation (bcc to fcc on heating) effect on Young's modulus E of iron-nickel alloys

25. References for Tables and Figures

[1] Alers, G. A., Neighbours, J. R., and Sato, H., Temperature dependent magnetic contributions to the high field elastic constants of nickel and an Fe-Ni alloy, J. Phys. Chem. Solids **13**, 40 (1960).

[2] Aliev, F. Y., Lazarev, B. G., and Sudovtsov, A. I., Compressibility of iron and nickel at 4.2 °K, Ukr. Phys. J. **12**, 1189 (1967). Reported also in Phys. Abstr. **71**, 400 (1968).

[3] Andrews, C. W., Effect of temperature on the modulus of elasticity, Metal Progr. **58**, 85 (1950).

[4] Angenheister, G., Beitrage zur Kenntnis von der Elastizität der Metalle, Ann. Phys. (Leipzig) **11**, 188 (1903).

[5] Aoyama, S., and Fukuroi, T., On Young's modulus of metals and alloys at low temperatures, Bull. Sci. Res. Inst. (Tokyo) **20**, 809 (1941), in Japanese.

[6] Armstrong, P. E., and Brown, H. L., Dynamic Young's modulus measurements above 1000 °C on some pure polycrystalline metals and commercial graphites, Trans. Met. Soc. AIME **230**, 962 (1964).

[7] Bach, C., and Baumann, R., Festigkeitseigenschaften und Getugebilder der Konstruktionsmaterialien, (Springer, Berlin, 1921).

[8] Beck, F. J., Kouvelites, J. S., and McKeehan, L. W., Magnetostrictive vibration of prolate spheroids. Analysis and experimental results, Phys. Rev. **84**, 957 (1951).

[9] Bennett, G. E., and Davies, R. M., An experimental investigation by a dynamical method of the variation of Young's modulus with temperature, J. Inst. Metals **16**, 759 (1949).

[10] Benton, J. R., Determination of Poisson's ratio by means of an interference apparatus, Phys. Rev. **12**, 36 (1901).

[11] Benton, J. R., Elasticity of copper and steel at −186 °C, Phys. Rev. **16**, 17 (1903).

[12] Bez-Bardili, W., Über ein Ultraschall-Totalreflektometer zur Messung von Schallgeschwindigkeiten sowie der elastischen Konstanten fester Körper, Z. Physik **96**, 761 (1935).

[13] Birch, F., Finite elastic strain of cubic crystals, Phys. Rev. **71**, 809 (1947).

[14] Bower, D. I., Claridge, E., and Tsong, I. S. T., Low-temperature elastic constants and specific heats of f.c.c. nickel-iron alloys, Phys. Status Solidi **29**, 617 (1968).

[15] Bozorth, R. M., Mason, W. P., and McSkimin, H. J., Frequency dependence of elastic constants and losses in nickel, Bell. Syst. Tech. J. **30**, 970 (1951).

[16] Bozorth, R. M., Mason, W. P., McSkimin, H. J., and Walker, J. G., Elastic constants and internal loss of single nickel crystals, Phys. Rev. **75**, 1954 (1949).

[17] Bridgman, P. W., The compressibility of thirty metals as a function of pressure and temperature, Proc. Amer. Acad. Arts Sci. **58**, 165 (1923).

[18] Bridgman, P. W., The linear compression of iron to 30,000 kg/cm^2, Proc. Amer. Acad. Arts Sci. **74**, 11 (1940a).

[19] Bridgman, P. W., Absolute measurements in the pressure range up to 30,000 kg/cm^2, Phys. Rev. **57**, 235 (1940b).

[20] Bridgman, P. W., Linear compressions to 30,000 kg/cm^2 including relatively incompressible substances, Proc. Amer. Acad. Arts Sci. **77**, 189 (1949).

[21] Brown, W. F., Jr., The variation of the internal friction and elastic constants with magnetization in iron. Part II, Phys. Rev. **50**, 1165 (1936).

[22] Bungardt, K., Preisendanz, H., and Brandis, H., Beitrag zum elastomechanischen Verhalten von irreversiblen Eisen-Nickel-Legierungen, DEW-Tech. Ber. **2**, 59 (1962).

[23] Burnett, H. C., Unpublished data, National Bureau of Standards, Washington, D.C. (1956).

[24] Carpenter, H. C. H., Hadfield, R. A., and Longmuir, P., Seventh report to the alloys research committee: On the properties of a series of iron-nickel-magnanese-carbon alloys, Proc. Inst. Mech. Eng. London, pts. 3–4, 857 (1905).

[25] Carrington, H., The strength properties of wrought iron, mild steel and nickel steel at high temperatures, Engineering (London) **117**, 69 (1924).

[26] Chevenard, P., Changement thermique des propriétés élastiques des aciers au nickel, C. R. Acad. Sci. **170**, 1499 (1920).

[27] Chevenard, P., Recherches experimentales sur les alliages de fer, de nickel et de chrome, Trav. Mem. Bur. Int. Poids Mes. **27**, 142 (1927).

[28] Chevenard, P., Les propriétés mécaniques dites secondaires, Rev. Met. (PARIS) **40**, 289 (1943).

[29] Chevenard, P., and Crussard, C., Influence de la température sur le coefficient de Poisson des alliages sidérurgiques. Anomalie de ce coefficient liée à la transformation magnétique des ferronickels rèversibles, C. R. Acad. Sci. **215**, 58 (1942).

[30] Chevenard, P., and Crussard, C., Influence des traitements thermiques et mécaniques sur le coefficient de Poisson des métaux et des alliages, C. R. Acad. Sci. **216**, 685 (1943).

[31] Chevenard, P., and Portevin, A., Propriétés élastiques des alliages: Variation en fonction de la composition chimique, C. R. Acad. Sci. **181**, 780 (1926).

[32] Cooke, W. T., The variation of the internal friction and elastic constants with magnetization in iron. Part I., Phys. Rev. **50**, 1158 (1936).

[33] Davies, R. M.. and Thomas, I. H., A dynamical method for the measurement of Young's modulus for imperfectly elastic metals, and the application of the method to nickel and some of its alloys, Phil. Mag. **23**, 361 (1937).

[34] DeKlerk, J., Ultrasonic wave propagation in a nickel single crystal, Proc. Phys. Soc. London **73**, 337 (1959).

[35] DeKlerk, J., and Musgrave, M. J. P., Internal conical refraction of transverse elastic waves in a cubic crystal, Proc. Phys. Soc. London **B68**, 81 (1955).

[36] Dever, D. J., Temperature dependence of the elastic constants in α-iron single crystals: relationship to spin order and diffusion anomalies, J. Appl. Phys. **43**, 3293 (1972).

[37] Diesburg, D. E., Elastic constants of Fe-Ni-C alloys, thesis, Iowa State Univ. (1971).

[38] Döring, W., Über die Temperaturabhangigkeit des Elastizitätsmoduls ferromagnetischer Substanzen, Ann. Phys. (Leipzig) **32**, 465 (1938).

[39] Doroshek, S. I., Influence of a third element and the structure on the ΔE effect and the physical anomalies of ferro-nickel alloys of the invar type, Phys. Metals Metallogr. (USSR) **17**, 168 (1964).

[40] Durham, T. F., McClintock, R. M., Reed, R. P., Guntner, C. J., and Warren, K. A., Cryogenic Materials Data Handbook, PB 171809 (Clearinghouse for Federal Scientific and Technical Information, 5285 Port Royal Road, Springfield, Virginia, 1963).

[41] Ebert, H., Versuche bis zu Drucken von 5000 kg/cm^2, I. Fundamentalbestimmungen des wirksamen Querschnittes der Druckwaagen Z. Physik **36**, 385 (1935).

[42] Ebert, H., and Kussmann, A., Änderung der Sättigungsmagnetisierung druch allseitigen Druck, Z. Physik **38**, 437 (1937).

[43] Eganyan, I. L., and Selisskiy, Ya. P., Young's modulus and magnetic saturation of ordering Ni$_3$Fe-Ni$_3$Mn alloys at elevated temperatures, Russ. Met. **4**, 94 (1967).

[44] Einspruch, N. G., and Claiborne, L. T., Elastic constants of a (73.8% Ni-26.2% Fe) ferromagnetic alloy, J. Appl. Phys. **35**, 175 (1964).

[45] Engler, O., Der Elastizitätsmodul ferromagnetischer Stoffe in Abhängigkeit von der Temperatur und vom Magnetfeld, Ann. Phys. (Leipzig) **31**, 145 (1938).

[46] Epstein, S. G., and Carlson, O. N., The elastic constants of nickel-copper alloy single crystals, Acta Met. **13**, 487 (1965).

[47] Everett, F. L., Strength of materials subjected to shear at high temperatures, Trans. ASME **53**, 117 (1931).

[48] Everett, F. L., and Miklowitz, H., Poisson's ratio at high temperatures, J. Appl. Phys. **15**, 592 (1944).

[49] Faninger, G., Die elastischen Konstanten von Kupfer-Nickel-Vielkristallen, Z. Metallk. **60**, 601 (1969).

[50] Fine, M. E., and Ellis, W. C., Young's modulus and its temperature dependence in 36 to 52 pct nickel-iron alloys, Trans. AIME **188**, 1120 (1950).

[51] Fontana, M. G., Investigation of mechanical properties and physical metallurgy of aircraft alloys at very low temperatures, Pt. II—Strength properties and hardness, Air Force Tech. Rept. 5662, Wright-Patterson AFB, Ohio (1948).

[52] Förster, F., and Köster, W., Elastizitätsmodul und Dämpfung in Abhängigkeit vom Werkstoffzustand, Z. Metallk. **29**, 116 (1937a).

[53] Förster, F., and Köster, W., Über die Abhängigkeit des Elastizitätsmoduls und der Dämpfung transversal schwingender Metallstäbe von der Amplitude, Naturwissenschaften **25**, 436 (1937b).

[54] Förster, F., and Köster, W., Elasticity and damping in relation to the state of the material, Engineer **166**, 626 (1938).

[55] Frederick, J. R., A study of the elastic properties of various solids by means of ultrasonic pulse techniques, Thesis, Univ. of Michigan, Ann Arbor (1947).

[56] Fukuroi, T., and Shibuya, Y., The measurement of the Young's modulus of metals and alloys by an interferomentric method. I. The Young's modulus of Ni-Cu alloys, Sci. Rep. Res. Inst. Tohoku Univ. **A2**, 748 (1950).

[57] Garofalo, F., Malenock, P. R., and Smith, G. V., The influence of temperature on the elastic constants of some commercial steels, in Symposium on Determination of Elastic Constants, 10 (ASTM STP No. 129, Philadelphia, Pa., 1952).

[58] Giebe, E., and Blechschmidt, E., Über den Einfluss der Magnetisierung auf den Elastizitätsmodul bei Dehnungsschwingungen ferromagnetischer Stäbe, Ann. Phys. (Leipzig) **11**, 905 (1931).

[59] Girifalco, L. A., and Weizer, V. G., Application of the Morse potential function to cubic metals, Phys. Rev. **114**, 687 (1959).

[60] Glocker, R., and Schaaber, O., Mechanische und röntgenographische Messung des Torsionsmoduls von Eisen, Ergeb. Tech. Roentgenk. **6**, 34 (1938).

[61] Goens, E., Über eine dynamische Methode zur Bestimmung der Temperaturabhangigkeit der elastischen Konstanten stab formiger Proben bei teifen Temperaturen, Ann. Phys. (Leipzig) **4**, 733 (1930).

[62] Goens, E., and Schmid, E., Über die elastische Anisotropie des Eisens, Naturwissenschaften **19**, 520 (1931).

[63] Goldman, A. J., and Robertson, W. D., Elastic properties of austenite and martensite in iron-nickel alloys, Acta Met. **12**, 1265 (1964).

[64] Grüneisen, E., Die elastischen Konstanten der Metalle bei kleinen Deformationen. I. Der dynamisch und statisch gemessene Elastizitätsmodul, Ann. Phys. (Leipzig) **22**, 801 (1907).

[65] Grüneisen, E., Die elastischen Konstanten der Metalle bei kleinen Deformationen. II. Torsion modul, verhaltnis von Querkontraktion zu Langsdilatation and kubische Kompressibilität, Ann. Phys. (Leipzig) **25**, 825 (1908).

[66] Grüneisen, E., Einfluss der Temperatur auf die Kompresssibilität der Metalle, Ann. Phys. (Leipzig) **33**, 1239 (1910).

[67] Guillaume, C. E., Recherches sur les aciers au nickel. Propriétés métrologiques, C. R. Acad. Sci. **124**, 752 (1897).

[68] Guillaume, C. E., Recherches sur les aciers au nickel, J. Phys. (Paris) 7, 262 (1898).

[69] Guillaume, C. E., L'anomalie d'élasticité des aciers au nickel; réalisation d'un élinvar et son application à la chronométrie, C. R. Acad. Sci. **171**, 83 (1920).

[70] Guillaume, C. E., Recherches metrologiques sur les aciers au nickel, Trav. Mem. Bur. Int. Poids Mes. **27**, 5 (1927).

[71] Guinan, M. W., and Beshers, D. N., Pressure derivatives of the elastic constants of α-iron to 10 KBS, J. Phys. Chem. Solids **29**, 541 (1968).

[72] Gutenberg, B., and Schlechtweg, H., Viskosität und innere Reibung fester Körper, Z. Physik **31**, 745 (1930).

[73] Guye, C.-E., and Freedericksz, V., Sur le frottement intérieur des solides aux basses températures, C. R. Acad. Sci. **149**, 1066 (1909).

[74] Guye, C.-E., and Schapper, H., Sur le frottement intérieur de quelques métaux aux basses températures, Arch. Sci. **30**, 133 (1910).

[75] Guye, C.-E., and Woelfle, H., Étude sur les variations due II^e module d'élasticité de l' "invar" en fonction de la température, Arch. Sci. Phys. Natur. **24**, 62, 159 (1907).

[76] Harrison, E. P., On the measurement of the temperature coefficient of Young's modulus for metallic wires, with special application to nickel, Proc. Phys. Soc. London **27**, 8 (1915).

[77] Hausch, G. and Warlimont, H., Single crystalline elastic constants of ferromagnetic face centered cubic Fe-Ni invar alloys, Acta Met., **21**, 401 (1973).

[78] Hausch, G. and Warlimont, H., Polycrystalline elastic constants of Fe-Ni invar alloys, Z. Metallk., **63**, 547 (1972).

[79] Hill, W. H., Shimmin, K. D., and Wilcox, B. A., Elevated-temperature dynamic moduli of metallic materials, Amer. Soc. Test. Mater. Proc. **61**, 890 (1961).

[80] Honda, K., On some physical constants of iron-cobalt alloys, Sci. Rep. Res. Inst. Tohoku Univ. **8**, 51 (1919a).

[81] Honda, K., On the moduli of elasticity and rigidity of nickel steels, Sci. Rep. Res. Inst. Tohoku Univ. **8**, 59 (1919b).

[82] Honda, K., and Hasimoto, H., On the change of the moduli of elasticity and rigidity in carbon steels by quenching, Sci. Rep. Res. Inst. Tohoku Univ. **10**, 75 (1921).

[83] Honda, K., and Shirakawa, Y., On Young's modulus of elasticity of single crystals of nickel and cobalt, Sci. Rep. Res. Inst. Tohoku Univ. **A1**, 9 (1949); also Nippon Kinzoku Gakkaishi **1**, 217 (1937), in Japanese.

[84] Honda, K., and Tanaka, T., On the moduli of elasticity and rigidity, and their change caused by magnetisation, in different kinds of steel, Sci. Rep. Res. Inst. Tohoku Univ. **15**, 1 (1926).

[85] Honda, K., and Terada, T., On the change of elastic constants of ferromagnetic substances by magnetization, Phil. Mag. **13**, 36 (1907); Proc. Fac. Sci. Imperial Univ. Tokyo **21**, Art. 4 (1906–1907).

[86] Honegger, E., Le module d'elasticité de l'acier a temperature elevée, Brown Boveri Rev. **19**, 143 (1932).

[87] Horton, F., The effects of changes of temperature on the modulus of torsional rigidity of metal wires, Trans. Roy. Soc. London **A204**, 1 (1905).

[88] Hughes, D. S., and Kelly, J. L., Second-order elastic deformation of solids, Phys. Rev. **92**, 1145 (1953).

[89] Hughes, D. S., and Maurette, C., Dynamic elastic moduli of iron, aluminum, and fused quartz, J. Appl. Phys. **27**, 1184 (1956).

[90] Iokibe, K., and Sakai, S., The effect of temperature on the modulus of rigidity, and on the viscosity of solid metals, Phil. Mag. **42**, 397 (1921).

[91] Jacquerod, A., Mügeli, H., Etude sur l'élasticité de flexion: Fer-cuivre-or-argent-platine-verre de silice-nickel, Helv. Phys. Acta **4**, 3 (1931).

[92] Kamber, K., The effect of ferromagnetism on the elastic and plastic properties of metals at elevated temperatures, thesis, Stanford Univ., Palo Alto, Calif. (1963), DMS Rept. No. 63–1. Data also given in ASTIA Repts. AD615561, AD292798, AD245409, and AD235298.

[93] Kawai, T., The effect of cold-working on Young's modulus of elasticity, Sci. Rep. Res. Inst. Tohoku Univ. **19**, 209 (1930).

[94] Kawai, T., On the change of the modulus of rigidity in different metals caused by cold-working, Sci. Rep. Res. Inst. Tohoku Univ. **20**, 681 (1931).

[95] Keulegan, G. H., and Houseman, M. R., Temperature coefficients of the moduli of metals and alloys used as elastic elements, J. Res. Nat. Bur. Stand. **10**, 289 (1933).

[96] Khomenko, O. A. and Tseytlin, A. M., Young's modulus anomaly in alloyed iron-nickel invars, Fiz. Metal. Metalloved. **28**, 246 (1969).

[97] Kikuchi, R., Measurements of the torsion modulus of Ni-Cu alloys, Kinzoku-No-Kenkyu **13**, 41 (1936). In Japanese. Kikuta, T., On the change of rigidity and logarithmic decrement in different metals and alloys at high temperatures, Sci. Rep. Res. Inst. Tohoku Univ. **10**, 139 (1921).

[98] Kimball, A. L., and Lovell, D. E., Variation of Young's modulus with temperature from vibration measurements, Phys. Rev. **26**, 121 (1925).

[99] Kimura, R., On the elastic moduli of ferromagnetic materials. Part I. Dynamical measurements of the elastic moduli of iron crystals, Proc. Phys. Math. Soc. Jap. **21**, 686 (1939a).

[100] Kimura, R., On the elastic moduli of ferromagnetic materials. Part II. The change in Young's modulus due to magnetization and temperature, Proc. Phys. Soc. Jap. **21**, 786 (1939b) Part III. ΔE-effect of iron single crystals, Proc. Phys. Soc. Jap. **22**, 45 (1940a) Part IV. ΔE-effect of iron single crystals at high temperatures, Proc. Phys. Soc. Jap. **22**, 219 (1940b).

[101] Kimura, R., and Ohno, K., On the elastic constants of single crystals of iron, Sci. Rep. Res. Inst. Tohoku Univ. **23**, 359 (1934).

[102] Koch, K. R., and Dannecker, C., Die Elastizität einiger Metalle und Legierungen bis zu Temperaturen, die ihrem Schmelzpunkt naheliegen, Ann. Phys. (Leipzig) **47**, 197 (1915).

[103] Koch, K. R., and Dieterle, R., Die Elastizität einiger Metalle und Legierungen bis zu Temperaturen, die ihrem Schmelzpunkt naheliegen; B. Elastizitätsmodul, Ann. Phys. (Leipzig) **68**, 441 (1922).

[104] Köster, W., Elastizitätsmodul und Dämpfung von Eisen und Eisenlegierungen, Arch. Eisenhuttenw. **14**, 271 (1940).

[105] Köster, W., Beitrag zur Kenntnis der Grösse σ_1 auf Grund der Messung des ΔE-Effektes von Nickel, Z. Metallk. **35**, 57 (1943a).

[106] Köster, W., Elastizitätsmodul und ΔE-Effekt der Eisen-Nickel-Legierungen, Z. Metallk. **35**, 194 (1943b).

[107] Köster, W., Die Temperaturabhangigkeit des Elastizitätsmoduls reiner Metalle, Z. Metallk. **39**, 1 (1948).

[108] Köster, W., and Rauscher, W., Beziehungen zwischen dem Elastizitätsmodul von Zweistofflegierungen und ihrem Aufbau, Z. Metallk, **39**, 111 (1948).

[109] Kototayev, A. D., and Koneva, N. A., Study of deformation strength and elastic character in the process of isothermal ordering in alloys based on Ni_3Fe, Izv. Vyssh. Ucheb. Zaved., Fiz. **74**, 40 (1968). In Russian.

[110] Kouvelites, J. S., McKeehan, L. W., Magnetostrictive vibration of prolate spheroids. Ni-Fe and Ni-Cu alloys, Phys. Rev. **86**, 898 (1952).

[111] Kurnakow, N., and Rapke, J., Härte und Elastizitätsmodul isomorpher Gemische von Kupfer mit Nickel, Z. Anorg. Chem. **87**, 269 (1914).

[112] Landon, D. H., and Davies, R. M., The determination of the rigidity modulus of nickel and some of its alloys in the annealed and unannealed states, Phil. Mag. **26**, 816 (1930).

[113] Lea, F. C., The effect of temperature on some of the properties of metals, Engineer **113**, 829 (1922).

[114] Leamy, H. S., Gibson, E. D., and Kayser, F. X., The elastic stiffness coefficients of iron-aluminum alloys—I Experimental results and thermodynamic analysis, Acta Met. **15**, 1827 (1967).

[115] Leese, J., and Lord, A. E., Elastic stiffness coefficients of single-crystal iron from room temperature to 500 °C, J. Appl. Phys. **39**, 3986 (1968).

[116] Levy, S., and Truell, R., Ultrasonic attenuation in magnetic single crystals, Rev. Mod. Phys. **25**, 140 (1953).

[117] Lord, A. E., and Beshers, D. N., Elastic stiffness coefficients of iron from 77° to 673 °K, J. Appl. Phys. **36**, 1620 (1965).

[118] Maeda, T., Unusual elastic properties of gadolinium and invar, J. Phys. Soc. Jap. **30**, 375 (1971).

[119] Markham, M. F., Measurement of elastic constants by the ultrasonic pulse method, Brit. J. Appl. Phys. Suppl. No. 6, S56 (1957).

[120] Masumoto, H., and Saito, H., On elasticity, its temperature coefficient, and heat expansion coefficient of the nickel-copper alloy system, Nippon Kinzoku Gakkaishi **8**, 49 (1944). In Japanese.

[121] Masumoto, H., Saito, H., and Kobayashi, T., The thermal expansion coefficients and the temperature coefficients of Young's modulus of the alloys of iron and palladium, Trans. Jap. Inst. Metals **4**, 114 (1963).

[122] Masumoto, H., Saito, H., Murakami, Y., and Kikuchi, M., Crystal anisotropy and temperature dependence of Young's modulus of nickel single crystals, Nippon Kinzoku Gakkaishi **32**, 525 (1968). In Japanese.

[123] Masumoto, H., Saito, H., and Sawaya, S., Thermal expansion and temperature dependence of Young's modulus of nickel-copper alloys, Trans. Jap. Inst. Met. **11**, 88 (1970).

[124] Masumoto, H., Sawaya, S., and Kikuchi, M., Thermal expansion and temperature dependence of Young's modulus in Fe-Cr alloys, Trans. Jap. Inst. Met. **12**, 86 (1971).

[125] Mathur, S. S., and Sharma, Y. P., Third order elastic constants of body centered cubic crystals, Phys. Status Solidi **39**, K 39 (1970).

[126] McCain, W. S., and Maringer, R. E., Mechanical and physical properties of invar and invar-type alloys, DMIC Memo. 207, Battelle Memorial Instit., Columbus, Ohio (1965).

[127] Meincke, P. P. M., and Litva, J., Velocity of sound in invar at low temperatures, Phys. Lett. **29A**, 390 (1969).

[128] M'Farlane, D., as quoted in Kawai (1931).

[129] Möbius, W., Der Torsionsmodul des Nickels bei hoheren Temperaturen unter gleichzeitiger Magnetisierung, Z. Physik **33**, 411 (1932).

[130] Möbius, W., Der Torsionsmodul des Nickels bei hoheren Temperaturen unter gleichzeitiger Magnetisierung. II., Z. Physik **35**, 806 (1934).

[131] Möller, H., and Barbers, J., Röntgenographische Untersuchung über Spannungsverteilung und Ueberspannungen in Flusstahl, Mitt. Kaiser-Wilhelm-Inst. Eisenforsch. Duesseldorf **17**, 157 (1935).

[132] Möller, H., and Brasse, F., Spannungs-und Verzerrungszustand an der Grenzflache zweier Kristalle, Arch. Eisenhuttenw. **26**, 231 (1935).

[133] Müller, W., Schlagbeigefestigkeit und schlaghärte legierter konstruktionsstähle, Part 247 in Forschungsarbeiten auf dem gebeite des Ingenieurwesens (J. Springer, Berlin, 1922).

[134] Morrow, J., On an instrument for measuring the lateral construction of tie-bars, and on the determination of Poisson's ratio, Phil. Mag. **6**, 417 (1903).

[135] Mudge, W. A., and Luff, L. W., Some mechanical properties of nickel, manganese-nickel and copper-nickel alloys, Amer. Soc. Test Mater. Proc. **28**, 278 (1928).

[136] Nakamura, K., The effect of magnetization on Young's modulus of elasticity of some ferromagnetic substances, Sci. Repts. Tohoku Univ. **24**, 303 (1935); also Unterschung der Variationen des Elastizitätskoeffizienten der Metallegierung Ni-Fe durch Magnetisierung, Z. Physik **94**, 707 (1935).

[137] Nakamura, K., Effect of temperature on Young's modulus of elasticity in nickel-copper alloys, Sci. Rep. Res. Inst. Tohoku Univ. **25**, 415 (1936).

[138] Neighbours, J. R., Bratten, F. W., and Smith, C. S., The elastic constants of nickel, J. Appl. Phys. **23**, 389 (1952).

[139] Nishiyama, Z., On the measurement of the elastic constant, lattice constant, and density of binary alloys in the range of solid solution, Sci. Rep. Res. Inst. Tohoku Univ. **18**, 359 (1929).

[140] Ochsenfeld, R., Über die magneto-elastischen Eigenschaften

einiger ferromagnetischer Eisen-Nickel-Legierungen, Z. Physik **143**, 375 (1955).

[141] Orlov, A. F., and Fedotov, S. G., Temperature dependence of the Young's and shear moduli of Ni-Cu alloys, Phys. Metals Metallogr. (USSR) **22**, 146 (1966).

[142] Pavlov, V. A., Kriutchkov, N. F., and Fedotov, I. D., Relationship of temperature to elastic modulus in nickel-copper alloys, Phys. Metals Metallogr. (USSR) **5**, 160 (1957).

[143] Powell, B. E., and Skove, M. J., Measurement of higher-order elastic constants, using finite deformations, Phys. Rev. **174**, 977 (1968).

[144] Rayne, J. A., and Chandrasekhar, B. S., Elastic constants of iron from 4.2 to 300 °K, Phys. Rev. **122**, 1714 (1961).

[145] Richards, T. W., Die Zusammendrückbarkeit der Elemente, Z. Elektrochem. **13**, 519 (1907).

[146] Richards, T. W., and Brink, F. N., Die Zusammendrückbarkeit der Elemente und ihre periodischen Beziehungen. III. Die lineare Kompressibilität von Kupfer und Eisen und die kubische Kompressibilität von Quecksilber, Z. Phys. Chem. (Leipzig) **61**, 171 (1907).

[147] Richards, T. W., and Bartlett, E. P., Compressibilities of mercury, copper, lead, molybdenum, tantalum, tungsten, and silver bromide, J. Amer. Chem. Soc. **37**, 470 (1915).

[148] Roberts, M. H., and Mortcliffe, J., Measurement of Young's modulus at high temperatures, J. Iron Steel Inst. **157**, 345 (1947).

[149] Roberts, M. J., and Owen, W. S., The strength of martensitic iron-nickel alloys, Trans. Amer. Soc. Metals **60**, 687 (1967).

[150] Rose, M. F., Pressure dependence of the second order elastic constants, Phys. Status Solidi **17**, K199 (1966).

[151] Rotter, C. A., and Smith, C. S., Ultrasonic equation of state of iron I. Low pressure, room temperature, J. Phys. Chem. Solids **27**, 267 (1966).

[152] Sakurai, J., Ultrasonic propagation in nickel and Mn-ferrite at high magnetic fields, J. Phys. Soc. Jap. **19a**, 311 (1964).

[153] Sakurai, J., Fujii, M., Nakamura, Y., and Takaki, H., Elastic constants of Ni-Fe and Ni-Cu alloys, J. Phys. Soc. Jap. **19**, 308 (1964).

[154] Salama, K., and Alers, G. A., Elastic moduli variations at the martensitic transformation of a Fe-Ni alloy, J. Appl. Phys. **39**, 4857 (1968).

[155] Salama, K., and Alers, G. A., unpublished data (1969). Sarma, V. P. N., and Reddy, P. J., Measurement of third-order elastic elastic constants of single crystal nickel at 298° K, Phil. Mag. **27**, 769 (1973).

[155a] Sarma, V. P. N., and Reddy, P. J., Third-order elastic constants of single crystal nickel at 80 °K, Phys. Status Solidi (a)16, 413 (1973).

[156] Schaefer, C., Über den Einfluss der temperatur auf die Elasticität der Metalle, Ann. Phys. (Leipzig) **5**, 220 (1901).

[157] Scheil, E., and Reinacher, G., Elastizitätsmodul und Dämpfung irreversibler Eisen-Nickel-Legierungen, Z. Metallk. **36**, 63 (1944).

[158] Scheil, E., and Thiele, W., Änderung von Elastizitätsmodul und Dämpfung einer Eisen-Nickel-Legierung bei der γ-α-Umwandlung, Arch. Eisenhuttenw. **12**, 103 (1938).

[159] Seager, G. C., and Thompson, F. C., The influence of temperature on the modulus of elasticity of some plain carbon and alloy steels, J. Iron Steel Inst. **147**, 103 (1943).

[160] Seeger, A., and Buck, O., Die experimentelle ermittlung der elastischen konstanten höherer ordnung, Z. Naturforsch. **15**, 1056 (1960).

[161] Sharma, Y. P., and Mathur, S. S., Higher order elastic constants of some face-centered cubic metals, Can. J. Phys. **47**, 1995 (1969).

[162] Shirakawa, Y., and Numakura, K., Elasticity constants of single crystals of nickel-copper alloys, Sci. Rep. Res. Inst. Tohoku Univ. **A10**, 51 (1957).

[163] Shirakawa, Y., and Numanakura, K., On Young's modulus and grain size in nickel-copper alloys, Sci. Rep. Res. Inst. Tohoku Univ. **A10**, 110 (1958).

[164] Shirakawa, Y., Tanji, Y., Moriya, H. and Oguma, I., The elastic constants of Ni and Ni-Fe (fcc) alloys, J. Jap. Inst. Metals Sendai **33**, 1196 (1969), in Japanese.

[165] Shved, M. M., X-ray determination of elastic constants E and ν, in An UkSSR, Institut Mashinovedeniya i Avtomatiki, Voprosy Mekhaniki Real'nogo Tverdogo Tela (Izd-vo Naukova Dumka, Kiev, 1964) p. 128, Available in English translation as FTIS Rep. No. AD685028.

[166] Siegel, S., Quimby, S. L., The variation of Young's modulus with magnetization and temperature in nickel, Phys. Rev. **49**, 663 (1936).

[167] Slater, J. C., Note on Grüneisen's constant for the incompressible metals, Phys. Rev. **57**, 744 (1940).

[168] Smith, R. T., Stress-induced anisotropy in solids—the acousto-elastic effect, Ultrasonics **1**, 135 (1963).

[169] Smith, R. T., Stern, R., and Stephens, R. W. B., Third-order elastic moduli of polycrystalline metals from ultrasonic velocity measurements, J. Acoust. Soc. Amer. **40**, 1002 (1966).

[170] Smith, S. L., and Wood, W. A., A stress-strain curve for the atomic lattice of iron, Proc. Roy. Soc. London **178**, 93 (1941).

[171] Speich, G. R., Schwoeble, A. J., and Leslie, W. C., Elastic constants of binary iron-base alloys, Met. Trans. **3**, 2031 (1972).

[172] Subrahmanyam, B., and Krishnamurty, B., Elastic moduli of high nickel alloys, Indian J. Pure Appl. Phys. **1**, 193 (1963).

[173] Susse, C., Mesure du module de rigidité du nickel jusqu'a 1000 °C. J. Phys. Radium **17**, 910 (1956).

[174] Takahashi, T., Bassett, W. A., and Mao, H.-K., Isothermal compression of the alloys of iron up to 300 kilobars at room temperature: Iron-nickel alloys, J. Geophys. Res. **73**, 4717 (1968).

[175] Tanji, Y., Shirakawa, Y., and Moriya, H., Young's modulus, shear modulus and compressibility of Fe-Ni (fcc) alloys, Report 1462 of Res. Inst. for Iron, Steel and Other Metals (1970) p. 84. Also in J. Jap. Inst. Metals Sendai **34**, 417 (1970), in Japanese.

[176] Tietz, D., Ultrasonic determination of high-order elastic constants in elastically deformed metal rods, Fifth Intl. Conf. on Nondestruct. Testing, Montreal (1969) p. 164.

[177] Tino, Y., and Maeda, T., On the anomalous thermoelastic variation in the invar-type iron-nickel alloys, J. Phys. Soc. Jap **18**, 955 (1963).

[178] Truell, R., reported in Lord, A. E., and Beshers, D. N. (1965).

[179] Umekawa, S., On Young's modulus of nickel-copper and nickel-cobalt alloys, Nippon Kinzoku Gakkaishi **18**, 387 (1954). In Japanese.

[180] Versé, G., The elastic properties of steel at high temperatures, Trans. ASME **57**, 1 (1935).

[181] Vintaikin, E. Z., X-ray determination of the elastic constants of pure nickel and its alloy with aluminum, Sov. Phys.-Dokl. **11**, 91 (1966).

[182] Voronov, F. F., and Vereshchagin, L. F., The influence of hydrostatic pressure on the elastic properties of metals I. Experimental data, Phys. Metals Metallogr. (USSR) **11**, 111 (1961).

[183] Williams, H. J., Bozorth, R. M., and Christensen, H., The magnetostriction, Young's modulus and damping of 68 Permalloy as dependent on magnetization and heat treatment, Phys. Rev. **59**, 1005 (1941).

[184] Yamamoto, M., The change of Young's modulus of elasticity by magnetization in iron and carbon steels, Sci. Rep. Res. Inst. Tohoku. Univ. **27**, 115 (1938).

[185] Yamamoto, M., Young's modulus of elasticity and its variation with magnetization in ferromagnetic nickel-copper alloys, Nippon Kinzoku Gakkaishi **6**, 249 (1942), in Japanese; also Sci. Rep. Res. Inst. Tohoku Univ. **A6**, 446 (1954).

[186] Yamamoto, M., On the elastic constants of iron single crystals, Nippon Kinzoku Gakkaishi **7**, 346 (1943a). In Japanese.

[187] Yamamoto, M., On the ΔE-effect of iron, nickel and cobalt,

Nippon Kinzoku Gakkaishi **5**, 167 (1941), in Japanese; also Sci. Rep. Res. Inst. Tohoku Univ. **31**, 101 (1943b).

[188] Yamamoto, M., On elastic constants of nickel crystals, Phys. Rev. **77**, 566 (1950); also Sci. Rep. Res. Inst. Tohoku Univ. **A3**, 308 (1951) and Nippon Kinzoku Gakkaishi **6**, 331 (1942), in Japanese.

[189] Yamamoto, M., The ΔE-effect in iron-nickel alloys, Sci. Rep. Res. Inst. Tohoku Univ. **A11**, 102 (1959).

[190] Yamamoto, M., and Taniguchi, S., The ΔE-effect, Young's modulus, and their change due to quenching in iron-aluminum alloys, Nippon Kinzoku Gakkaishi **11**, 584 (1954). In Japanese.

[191] Yamamoto, M., and Taniguchi, S., The ΔE-effect and Young's modulus in nickel-cobalt alloys, Sci. Rep. Res. Inst. Tohoku Univ. 35 (1955); also Nippon Kinzoku Gakkaishi **B15**, 337 (1951), in Japanese.

[192] Zacharias, J., The temperature dependence of Young's modulus for nickel, Phys. Rev. **44**, 116 (1933).